UNIVERSIDADE FEDERAL DE UBERLÂNDIA

FACULDADE DE ENGENHARIA ELÉTRICA

Rhaíra Helena Caetano e Souza

EXAMINING BRAIN AND EYE-TRACKING SIGNALS INTEGRATION DURING EXERGAME SESSION: A CASE STUDY WITH A POST-STROKE PATIENT

Uberlândia, MG

2023

UNIVERSIDADE FEDERAL DE UBERLÂNDIA

FACULDADE DE ENGENHARIA ELÉTRICA

Rhaíra Helena Caetano e Souza

EXAMINING BRAIN AND EYE-TRACKING SIGNALS INTEGRATION DURING EXERGAME SESSION: A CASE STUDY WITH A POST-STROKE PATIENT

Tese de doutorado apresentada ao Programa de Pós-graduação em Engenharia Elétrica da Universidade Federal de Uberlândia, como parte dos requisitos para obtenção do título de Doutor em Engenharia Elétrica.

Orientador: Prof. Eduardo Lázaro Martins Naves, PhD

Uberlândia, MG

2023

Ficha Catalográfica Online do Sistema de Bibliotecas da UFU
com dados informados pelo(a) próprio(a) autor(a).

S729 Souza, Rhaíra Helena Caetano e, 1991-
2023 Examining brain and eye-tracking signals integration during exergame session: a case study with a post-stroke patient [recurso eletrônico] / Rhaíra Helena Caetano e Souza. - 2023.

Orientador: Eduardo Lázaro Martins Naves.
Tese (Doutorado) - Universidade Federal de Uberlândia, Pós-graduação em Engenharia Elétrica.
Modo de acesso: Internet.
Disponível em: http://doi.org/10.14393/ufu.te.2023.461
Inclui bibliografia.

1. Engenharia elétrica. I. Naves, Eduardo Lázaro Martins,1970-, (Orient.). II. Universidade Federal de Uberlândia. Pós-graduação em Engenharia Elétrica. III. Título.

CDU: 621.3

Bibliotecários responsáveis pela estrutura de acordo com o AACR2:
Gizele Cristine Nunes do Couto - CRB6/2091
Nelson Marcos Ferreira - CRB6/3074

RHAÍRA HELENA CAETANO E SOUZA

EXAMINING BRAIN AND EYE-TRACKING SIGNALS INTEGRATION DURING EXERGAME SESSION: A CASE STUDY WITH A POST-STROKE PATIENT

Tese de doutorado apresentada à Faculdade de Engenharia Elétrica da Universidade Federal de Uberlândia como parte dos requisitos necessários para a obtenção do título de Doutor em Engenharia Elétrica.

Comissão examinadora:

Prof. Dr. Eduardo Lázaro Martins Naves
(Orientador – UFU)

Prof. Dr. Adriano de Oliveira Andrade
(Examinador – UFU)

Profa. Dra. Angela Abreu Rosa de Sá
(Examinadora – UFU)

Prof. Dr. Ramón Hypolito Lima
(Examinador – IIN-ELS)

Profa. Dra. Isabela Marques Miziara
(Examinadora – UFPA)

Uberlândia, 10 de agosto de 2023

UNIVERSIDADE FEDERAL DE UBERLÂNDIA
Coordenação do Programa de Pós-Graduação em Engenharia Elétrica
Av. João Naves de Ávila, 2121, Bloco 3N - Bairro Santa Mônica, Uberlândia-MG, CEP 38400-902
Telefone: (34) 3239-4707 - www.posgrad.feelt.ufu.br - copel@ufu.br

ATA DE DEFESA - PÓS-GRADUAÇÃO

Programa de Pós-Graduação em:	Engenharia Elétrica				
Defesa de:	Tese de Doutorado, 323, PPGEELT				
Data:	Dez de agosto de dois mil e vinte e três	Hora de início:	8:30	Hora de encerramento:	13:00
Matrícula do Discente:	11713EEL013				
Nome do Discente:	Rhaíra Helena Caetano e Souza				
Título do Trabalho:	Examining brain and eye-tracking signals integration during exergame session: a case study with a post-stroke patient				
Área de concentração:	Processamento da Informação				
Linha de pesquisa:	Processamento Digital de Sinais e Redes de Computadores				
Projeto de Pesquisa de vinculação:	Coordenador do projeto: Eduardo Lázaro Martins Naves Título do projeto: Reabnet – Rede de Telerreabilitação por meio de Realidade Virtual e Aumentada Agência financiadora: CNPq Número do processo na agência financiadora: 307754/2020-0 Vigência do projeto: 01/03/2021 a 29/02/2024				

Reuniu-se por meio de videoconferência, a Banca Examinadora, designada pelo Colegiado do Programa de Pós-graduação em Engenharia Elétrica, assim composta:

Professores Doutores: Adriano de Oliveira Andrade - FEELT/UFU; Angela Abreu Rosa de Sá - FEELT/UFU; Ramón Hypolito Lima - IIN-ELS; Isabela Marques Miziara - UFPA; Eduardo Lázaro Martins Naves - FEELT/UFU, orientador(a) do(a) candidato(a).

Iniciando os trabalhos o(a) presidente da mesa, Dr(a). Eduardo Lázaro Martins Naves, apresentou a Comissão Examinadora e o candidato(a), agradeceu a presença do público, e concedeu ao Discente a palavra para a exposição do seu trabalho. A duração da apresentação do Discente e o tempo de arguição e resposta foram conforme as normas do Programa.

A seguir o senhor(a) presidente concedeu a palavra, pela ordem sucessivamente, aos(às) examinadores(as), que passaram a arguir o(a) candidato(a). Ultimada a arguição, que se desenvolveu dentro dos termos regimentais, a Banca, em sessão secreta, atribuiu o resultado final, considerando o(a) candidato(a):

Aprovada

Esta defesa faz parte dos requisitos necessários à obtenção do título de Doutor.

O competente diploma será expedido após cumprimento dos demais requisitos, conforme as normas do Programa, a legislação pertinente e a regulamentação interna da UFU.

Nada mais havendo a tratar foram encerrados os trabalhos. Foi lavrada a presente ata que após lida e achada conforme, foi assinada pela Banca Examinadora.

Documento assinado eletronicamente por **Angela Abreu Rosa de Sá**, **Usuário Externo**, em 10/08/2023, às 13:01, conforme horário oficial de Brasília, com fundamento no art. 6º, § 1º, do Decreto nº 8.539, de 8 de outubro de 2015.

Documento assinado eletronicamente por **Eduardo Lazaro Martins Naves**, **Professor(a) do Magistério Superior**, em 10/08/2023, às 13:02, conforme horário oficial de Brasília, com fundamento no art. 6º, § 1º, do Decreto nº 8.539, de 8 de outubro de 2015.

Documento assinado eletronicamente por **Isabela Marques Miziara**, **Usuário Externo**, em 10/08/2023, às 13:02, conforme horário oficial de Brasília, com fundamento no art. 6º, § 1º, do Decreto nº 8.539, de 8 de outubro de 2015.

Documento assinado eletronicamente por **Ramon Hypolito Lima**, **Usuário Externo**, em 10/08/2023, às 13:07, conforme horário oficial de Brasília, com fundamento no art. 6º, § 1º, do Decreto nº 8.539, de 8 de outubro de 2015.

Documento assinado eletronicamente por **Adriano de Oliveira Andrade**, **Professor(a) do Magistério Superior**, em 10/08/2023, às 14:54, conforme horário oficial de Brasília, com fundamento no art. 6º, § 1º, do Decreto nº 8.539, de 8 de outubro de 2015.

A autenticidade deste documento pode ser conferida no site https://www.sei.ufu.br/sei/controlador_externo.php?acao=documento_conferir&id_orgao_acesso_externo=0, informando o código verificador **4672419** e o código CRC **B49C2B44**.

Referência: Processo nº 23117.052282/2023-13 SEI nº 4672419

Por vezes sentimos que aquilo que fazemos não é senão uma gota de água no mar. Mas o mar seria menor se lhe faltasse uma gota.

Madre Teresa de Calcutá

Pensava que quando se sonha tão grande a realidade aprende.

O filho de mil homens – Valter Hugo Mãe

Agradecimentos

À Deus, pelo dom da vida, por me guiar e mostrar propósito, sempre me erguendo nas adversidades, me dando sabedoria;

À minha mãe Iraci, por não medir esforços, por se dedicar à família, por ser um exemplo de ser humano para mim. Pela sua bondade, fé, sabedoria e apoio incondicional, tenho eterna gratidão. Ao meu pai Luiz e irmão Ryhã, por sempre torcerem por mim e me apoiarem nos meus desafios;

Ao meu marido Vinicius, exemplo de dedicação, caráter e sabedoria. Não tenho palavras suficientes para lhe agradecer. Sou grata pelo apoio incondicional, pela parceria em todos os momentos e por acreditar em nós, em nossa família. Obrigada pelos nossos filhos, Cássio e Clara (ainda no ventre). Te amo hoje, mais que ontem e menos que amanhã...

Às minhas amigas, que entendem a minha ausência, acolheram meus desafios, me incentivaram e torceram para meu sucesso;

Ao Prof. orientador Eduardo, pela sua orientação ao longo de tantos anos. Obrigada pela sua prontidão, confiança e incentivo diante dos meus desafios profissionais e pessoais nesses anos. Sem a sua orientação, eu não seria capaz de chegar até aqui. Muito obrigada!

Às instituições, com suas instalações e oportunidades: Núcleo de Tecnologia Assistiva da UFU e Instituto Federal de Brasília – Campus Ceilândia pelo apoio, sem o qual, este estudo não seria concretizado. Aos colegas do NTA, em especial à Júlia, pela contribuição tão necessária nesse trabalho;

Aos servidores da UFU, professores e técnicos, pela dedicação e apoio constante. Sou muito grata a essa instituição e pessoas que fazem tudo acontecer, onde estive nos últimos 13 anos. De fato, foram anos memoráveis que mudaram a minha história. Tenho enorme gratidão por ter feito parte dessa comunidade;

Às instituições de apoio financeiro, PROAE, CAPES (bolsista 2017 e 2018 pelo PROGRAMA APOIO DE TECNOLOGIA ASSISTIVA – PGPTA), CNPq, FAPEMIG, não só pelo apoio neste trabalho, mas pelo apoio decisivo em toda minha trajetória acadêmica;

Ao Programa de Pós-Graduação em Engenharia Elétrica (PPGEELT) da Faculdade de Engenharia Elétrica (FEELT) - UFU pela oportunidade;

E, por fim, aos membros da banca de avaliação deste trabalho, pelas suas inestimáveis contribuições.

Muito obrigada!

Resumo

Considerando os efeitos do AVC no tecido cerebral e o comprometimento motor correlato, o emprego da reabilitação com realidade virtual (RV) pode ser um aliado na ativação neuroplástica. Uma nova abordagem RV para a detecção de atenção e imersão, através de biopotenciais é apresentada com base nas características dos sinais elétricos cerebrais e sinais eye-tracking neste estudo. Com vista à demanda competitiva de atenção em nosso cotidiano e a identificação de processos neurais nos sinais de EEG associados a ela, além da disponibilidade de dispositivos portáteis baseados em biopotenciais, torna-se possível interpretações por métricas na caracterização da atenção, imersão e concentração do usuário baseadas em parâmetros extraídos do sinal de EEG e monitoramento eye-tracking (ET). Dados de ET foram monitorados como potenciais relacionados à fixação do olhar. Em relação às bandas de frequência do EEG relacionadas com a atenção nas formas de imersão e concentração, como métricas da rede cerebral por meio de densidade espectral de potência, as áreas frontal e parieto-occipital foram ativadas nas bandas θ, α e β. A assimetria frontal alfa foi investigada, resultando em mudanças significativas nos estados de imersão, em comparação com o estado de relaxamento. Áreas específicas do cérebro e bandas de frequência foram analisadas: análise frontal de EEG, bem como índices relacionando razão entre bandas de frequência de muitos canais de EEG foram usados para investigação de concentração em duas tarefas de atenção diferentes. Um maior nível de atenção reflete um aumento no potencial teta (θ) nos eletrodos frontais e, nos eletrodos parietais, um aumento no potencial em relação ao ritmo alfa (α). Como direções futuras, indicamos um maior número de pacientes na investigação, uso de novas características de resposta do sinal cerebral, como tempo de reação e investigações em tempo real através das métricas estabelecidas neste trabalho.

Abstract

Considering the effects of stroke on brain tissue and related motor impairment, the use of rehabilitation with virtual reality (VR) can be an ally in neuroplastic activation. A new VR approach for detecting attention and emotion through biopotentials is presented based on the characteristics of brain electrical signals and eye-tracking signals in this study. With a view to the competitive demand for attention in our daily lives and the identification of neural processes in the EEG signals associated with it, in addition to the availability of portable devices based on biopotentials, it becomes possible to capture by attraction in the characterization of attention, immersion, and concentration of the User tracked on parameters extracted from the EEG signal and eye-tracking (ET) monitoring. ET data were monitored as potentially related to gaze fixation. Regarding the EEG frequency bands related to attention in the forms of effort and concentration, as metrics of the brain network through power spectral density, the frontal and parieto-occipital areas were activated in the θ, α, and β bands. The alpha frontal asymmetry was investigated, it had significant changes in the immersion states, compared to the relaxed state. Specific brain areas and frequency bands were surveyed: frontal analysis of EEG as well as indices relating ratios between frequency bands of many EEG channels were used to investigate concentration in two different attentional tasks. A higher level of attention reflects an increase in theta potential (θ) in the frontal electrodes and, in the parietal electrodes, an increase in potential relative to the alpha rhythm (α). As future considerations, we indicate a greater number of patients in the investigation, and use of new brain signal response characteristics, such as reaction time and real-time thinking through resistances in this work.

DERIVATIVE WORK

Souza, RHC and Naves, ELM. (2021) Attention Detection in Virtual Environments Using EEG Signals: A Scoping Review. Front. Physiol., 23 November 2021. Sec. Computational Physiology and Medicine. Volume 12 - 2021 | https://doi.org/10.3389/fphys.2021.727840

FIGURE INDEX

TABLE INDEX

ABBREVIATIONS INDEX

AOI – Area of Interest

CVA – Cerebrovascular Accident

EEG – Electroencephalographic

EM – Eye movements

ERD – Event-related desynchronization

ERP – Event-related potential

ERS – Event-related Synchronization

ET – Eye-tracking

FRP – Fixed-related potential

SNR – Signal to noise ratio

VR – Virtual reality

TABLE OF CONTENTS

Chapter 1

INTRODUCTION

The attention assessment is of great importance as one of the cognitive human processes. The distinction between states of concentration and immersion can be identified by neural processes, extracted from electroencephalographic signals (EEG) (LIM; YEO; YOON, 2019). Electroencephalographic (EEG) signals have been used for two purposes for assessing attention. The first is in separation between groups of individuals with and without attention deficit disorder and the second is in a way of estimating many different types of attention during specific activities (BAGHDADI; TOWHIDKHAH; RAJABI, 2021).

Identifying adequate process measures to study and better understand cognitive effects of attention processes has become a central focus in instructional psychology and neuroscience (HARTEIS; KOK; JARODZKA, 2018). Especially, combining eye-tracking has become increasingly popular for analyzing instructional materials (SCHARINGER; SCHÜLER; GERJETS, 2020).

By means of EEG frequency band powers, alpha waves have been widely reported in concentration states (RAY; COLE, 1985). Beta bands increase in states of more attention (LEE, 2009). Ratios, beta/alpha, theta/alpha were reported as indicators of an increase in concentration states. Nevertheless, there are many limitations in neurophysiological testing and the usage of EEG signals: few specific criteria limitations, low convergence in the methodologies for identifying the variation of attention over time, cultural limitations, lack of validation of prediction of local tests (DEMECO *et al.*, 2023).

In that context, virtual reality (VR) systems appear as one alternative to standardizing the exposure of individuals to objective and generalized stimuli. The use of VR presents itself as a free field for creating environments, combining elevated security and limited prediction. These characteristics are relevant at the standardization of the visual stimulus to be evaluated, reflected in the EEG signal. With the growing popularization of VR wearable and EEG recording wearable, this alternative is of interest to deal with a system of attention evaluation.

VR systems are helpful in exposing the user, or patient, in case of an exergame/serious game, to punctual and constant stimuli, varying its intensity. Thus, the increase in attention can change and when monitored, can supply individual 's information modulated per those stimuli. The combination of EEG signals monitoring and eye-tracking signals have been alternative as non-invasive, portable solution in monitoring processes in neuroscience. Growing equipment popularization and low-cost ones (compared to lab solutions) is a strategy applied in situations that mimic daily conditions in use of therapy (KHOKALE *et al.*, 2023).

The VR system that is developed for therapy/physiotherapy purposes, with ludic features, manipulated by a patient with specific protocol, can be agreed as a serious game. A patient stricken per cerebrovascular accident (CVA), can enjoy serious game features in search for a quality-of-life improvement, associating a more pleasurable one activity practice of regular physiotherapy (KHOKALE *et al.*, 2023). Serious game use in the context of therapy and rehabilitation was recently quite explored at lab practice, each turn more into clinical practice.

Cerebrovascular Accident (CVA), or Stroke, is the second biggest cause of death today in the world (11.8%), ahead only is ischemic heart disease (FEIGIN; NORRVING; MENSAH, 2017). Together with the advances in the quick and careful interventions, deaths relative to stroke have decreased. However, the post-stroke outcomes are diverse, for example elevated individuals' disability, depression, anxiety, vascular cognitive impairment (VCI) and severe fatigue, generating challenges that prevent the full recovery of the individual, generating low functional rehabilitation and compromising quality of life. Associated with this, only 19% of those affected have access to a rehabilitation program (KATAN; LUFT, 2018).

Therefore, this study goal is to characterize EEG and eye-tracking signals patients affected per cerebrovascular accident (CVA), inducing upper limb commitment, that also complain of difficulty in paying attention in daily activities. The present study relates current research and band ratios assessment methodologies through the EEG signal in the context of a VR system - serious game/exergame aimed to treat at the therapy level of stroke survivors - and eye-tracking signals.

1.1 THESIS RELEVANCE

Identifying adequate process measures to study and better understand cognitive processes is a central point of research in neuroscience. Especially non-invasive solutions, and low-cost

ones, have increased the capability of doing research outside laboratory conditions, mimicking daily activities, and finding new perspectives for improving people's quality of life.

Using EEG wearable with 8 channels, for analyzing EEG frequency band power, and eye-tracking device, this thesis uses recent lean technologies (customer-value focused approach) and strategies, working with physiological measures, in a state of art proposal, regarding the recent literature, in a VR context.

Analyzing eye-tracking data and EEG data simultaneously in one study is due to provide further insights into the sensitivity of these measures to assess mental processing demands in the context of a free-viewing task, in different demands of attention. Finally, the combined recording of eye-tracking and EEG data allows to additionally analyze the EEG data fixation-related in certain areas of interest (AOIs), which might be in general a promising methodology for studying the EEG in complex, multimedia task materials (SCHARINGER, 2018).

In this thesis we wanted to describe the outcomes of metrics in fixation-related EEG frequency power analysis in different attention states, and present reproducibility of the methodology in the context of VR systems, showing statistical relevance and comparison. Our focus is on collaborating with the immersive virtual reality approach to post-stroke rehabilitation therapies. As (SCHARINGER; SCHÜLER; GERJETS, 2020) describes, fixation-related EEG data analysis has been proposed as a promising methodology to study the EEG in free-viewing situations, yet most studies so far focused on the time-domain, that is on fixation-related potentials and not on the frequency domain. As this, fixation-related frequency band power analysis may be more explored.

This thesis is divided in 6 sections/chapters. Chapter 1 presents the general idea of this thesis work, introducing terminologies that will be defined in Chapters 2 and 3. Chapter 2 gives the idea of how EEG signals are formed and recorded in a non-invasive approach. Chapter 3 is based on a published work by the author of this Thesis, https://doi.org/10.3389/fphys.2021.727840. Chapter 4 shows each step used to investigate attention, through EEG and eye-tracking, in the context of a specific VR system. Chapter 5 presents the results found. Chapter 6 discusses and make final considerations. References are added at the end of each Chapter.

Chapter 2

ELECTROENCEPHALOGRAPHY

The first records of electrical brain activity in humans were systematically made by the German psychiatrist Hans Berger, in mid-1928, who introduced the term electroencephalogram (EEG) to denote the recorded fluctuating potentials of the brain, being the founder of clinical neurophysiology (WEBSTER; NIMUNKAR; CLARK, 2010). The fluctuating scalp potentials represent the positioning of field potentials produced by a variety of neuronal active ionic currents found in the mean conducting volume. To understand how ionic currents are registered by the electrodes and how the mean conductive volume influences, the following sections are presented: (2.1) brain function and its general anatomy, (2.2) the field potentials of unit neurons, and (2.3) the cortical potential recorded and (2.4) the typical brain waves recorded on the EEG by electrodes on the scalp.

2.1 CENTRAL NERVOUS SYSTEM (CNS)

The CNS consists of a spinal cord, covered with a vertebral column and its extension, the brain, protected by the skull. The cerebrum is a large, modified portion of the CNS, covered by three meninges and the skull. The brain is divided into three main parts – cerebrum, cerebellum, and brainstem, see Fig. 2.1.1. The olfactory bulb can also be seen in the image.

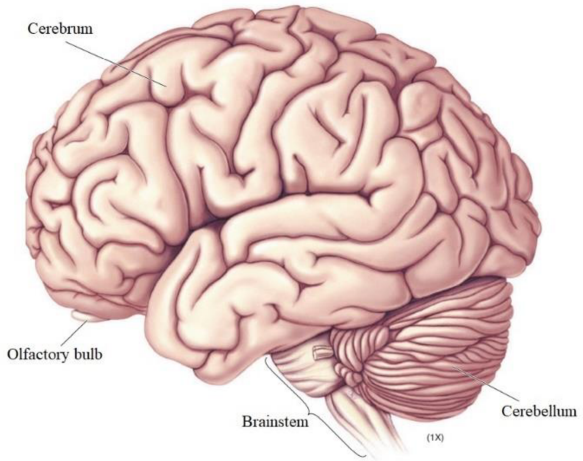

Fig. 2.1.1 Three main brain parts. [Source]: translated from (BEAR, 2013)

The brain is a paired structure, which corresponds to the right and left hemispheres, each relating to the opposite side of the body. The surface of the hemisphere (most superficial layer) is called cortex, which receives information from the skin, eyes, ears, and other receptors located generally on the opposite side of the body and is divided into six layers, which add up to 1 cm thick, called neocortex (Figure 2). Each hemisphere consists of several layers, where the outermost layer is a dense collection of nerve cells called gray matter, 1.5 to 4 mm thick, formed by neuron cups, neuroglial cells, and unmyelinated nerve fibers (WEBSTER; NIMUNKAR; CLARK, 2010).

The brain and its main functions can be divided by regions, which are called cerebral lobes, see Fig. 2.2. There are four lobes located in the cerebral cortex: frontal, parietal, occipital and temporal lobes, named after the corresponding skull bones. There is also the insula lobe, internal to the parietal, frontal and temporal lobes. The insula/insular lobe is a hidden portion of the cerebral cortex that can be visualized by delicately pulling apart the margins of the lateral fissure (BEAR, 2013).

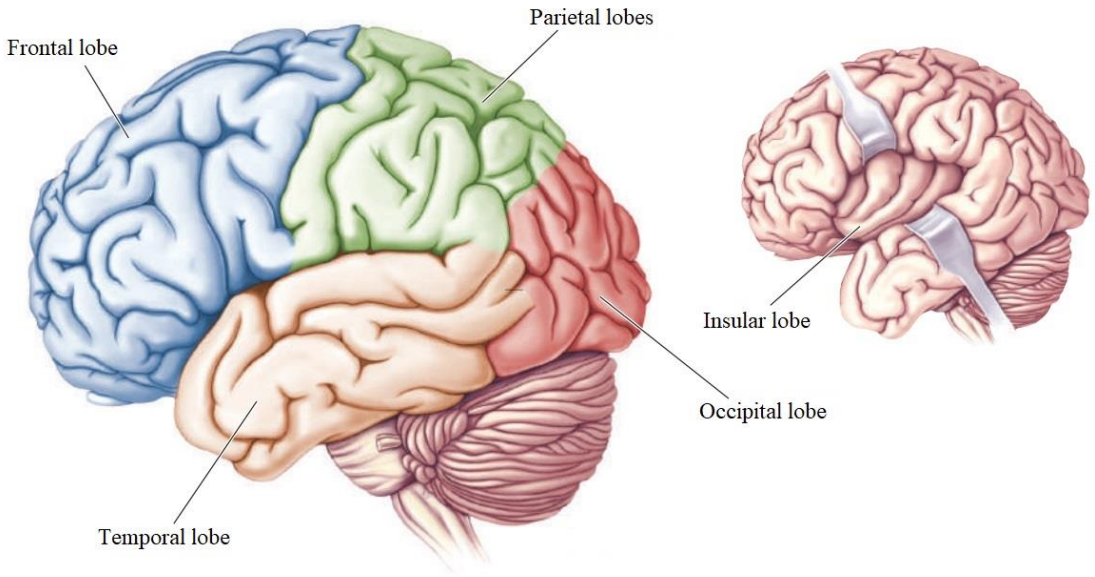

Fig. 2.1.2. Lobes of the brain. [Source]: translated from (BEAR, 2013)

Another way of dividing the cerebral cortex is into three types of functional areas, the primary, secondary, and association areas. The cortical areas responsible for basic functions are called primary motor or sensory areas. Secondary areas are located next to each primary area and receive afferent projections from the corresponding primary areas and the thalamus. They are responsible for integrating the original signal from the primary areas with the information received from the thalamus, to refine the input from the primary area.

The association areas, on the other hand, are cortical areas that integrate, process, and analyze different types of stimuli that reach the brain, and are involved in mediating higher cognitive functions, one of the most important being the prefrontal cortex area.

The various areas, called Brodmann areas, differ in microscopic structure and function.

Visual areas are found in the occipital lobe, somatosensory areas in the parietal lobe, auditory areas in the temporal lobe. The sensory information analysis areas, motor control areas, are in the frontal lobe. Associative areas of the cortex being those that are not directly involved with motor or sensory functions, see Fig. 2.1.3.

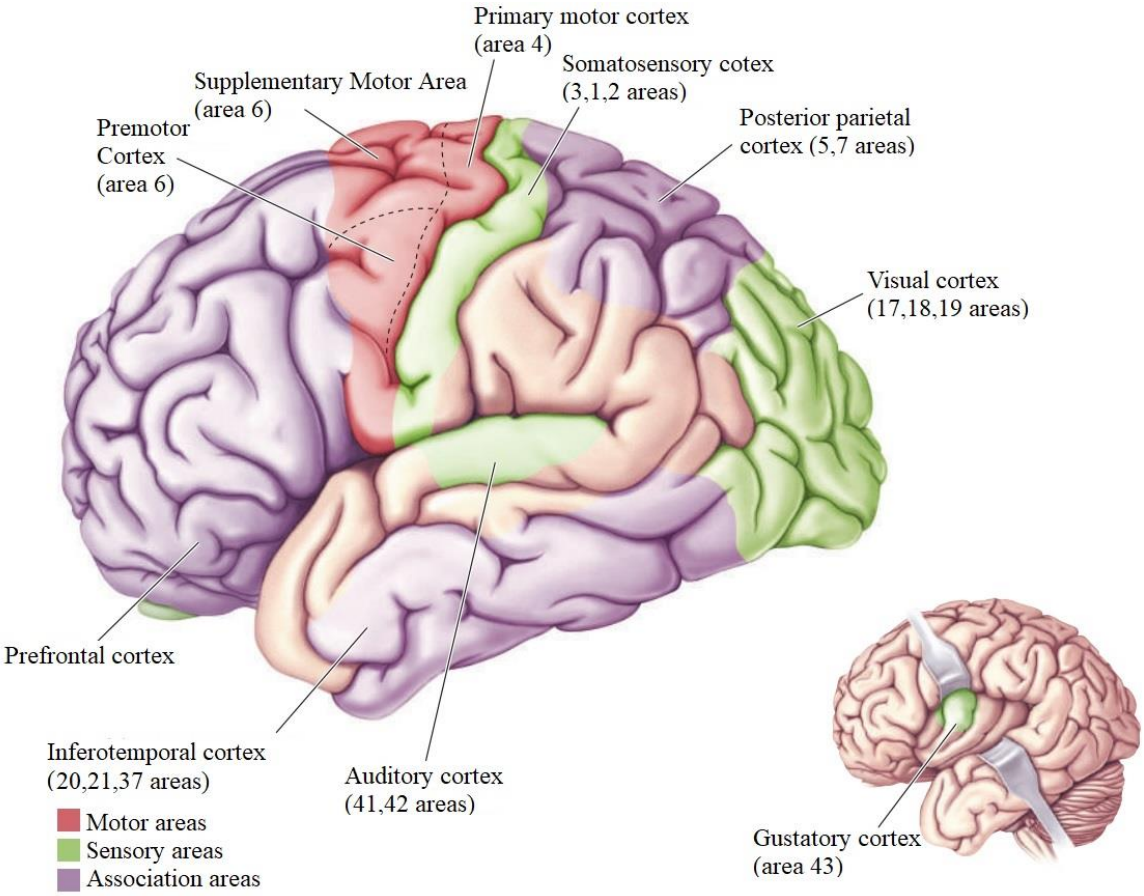

Fig. 2.1.1 Major sensory, motor, and associative cortical areas. [Source]: translated from (BEAR, 2013).

2.2 Basic Functional Unit

Two major categories of cells in the nervous system are: neurons and glia, among which there are many types of cells that differ in structure, chemistry, and functionality. Although there are approximately equal numbers of neurons and glial cells in the adult human brain (about 85 billion each), neurons are responsible for most functions unique to the nervous system. It is the neurons that sense changes in the environment, communicate these changes to other neurons, and direct the body's responses to these sensations. Glia, or glial cells, contribute to neural functions primarily through their insulating, supportive, and nurturing effect on neighboring neurons (BEAR, 2013).

Most cells are 0.01 to 0.05 mm in size. The neuron has distinct regions, a central region contains the nucleus of the cell and is called the soma. The thin tubes radiating from the soma (cell body) are the neurites, subdivided into dendrites and axons. Dendrites can reach up to 2 mm in length, while axons can travel great distances in the body, reaching more than one meter in length (BEAR, 2013).

Neurons can be classified according to the number of neurites or the aspect of the dendrites, among other classifications (types of connections and length of the axon). Two large classes are differentiated in the cerebral cortex, stellate cells – star-shaped – and pyramidal cells – pyramidal in shape (Fig. 2.2.1) and uniformly positioned perpendicular to the cortical surface. This characteristic is differential so that the postsynaptic potential, to be seen in the next topic, can be added, and recorded by EEG electrodes on the scalp.

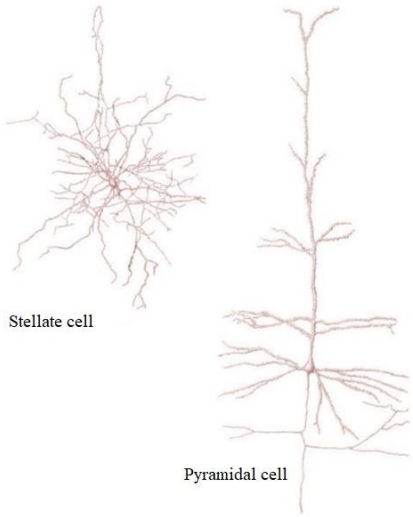

Fig. 2.2.1 Classification of neurons based on the structure of the dendritic tree. [Source]: translated from (BEAR, 2013)

Fig. 2.2.2 presents a schematic drawing of a typical pyramidal cortical neuron. Bodies of this cell type are commonly triangular, with the base downward and the apex toward the cortical surface. The pyramidal neuron usually has a unitary axon, which emerges from the inner surface of the cortex with the projection of its fibers to other areas of the cortex, or other structures of the brain. Often their axons send branches back, as feedback, to the cellular region where they first originated (WEBSTER, NIMUNKAR AND CLARK, 2010).

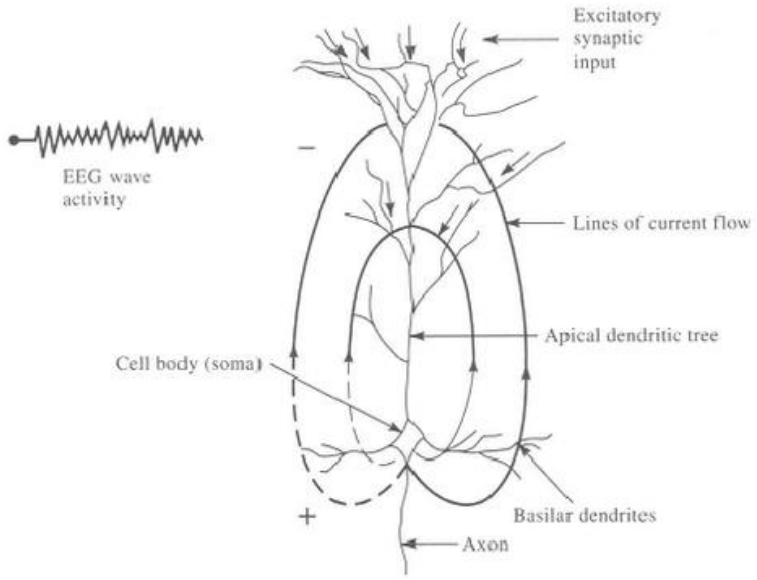

Fig. 2.2.2 Electrogenesis from the field of cortical potentials to a network of excitatory inputs in the apical dendritic tree of a typical pyramidal cell. The resulting current flow moves like waves between synaptic buttons. [Source]: (WEBSTER; NIMUNKAR; CLARK, 2010)

2.3 ACTION POTENTIAL

The signal that carries information along the nervous system is called an action potential. From the cellular and resting point of view (resting potential condition), the interior of the neuronal membrane is negative in relation to the external environment. In the action potential, there is a rapid inversion of this state, with the internal environment becoming more positive in relation to the external environment. The action potential is also called a spike potential, nerve impulse or discharge (BEAR, 2013).

The action potential generated in a portion of the membrane is constant in size and duration and does not decrease as it propagates down the axon. It is the frequency and pattern of action potentials that constitute information to be transferred from one location to another.

Its properties and characteristics are universal to the animal kingdom, as can be seen in Fig. 2.3.1.

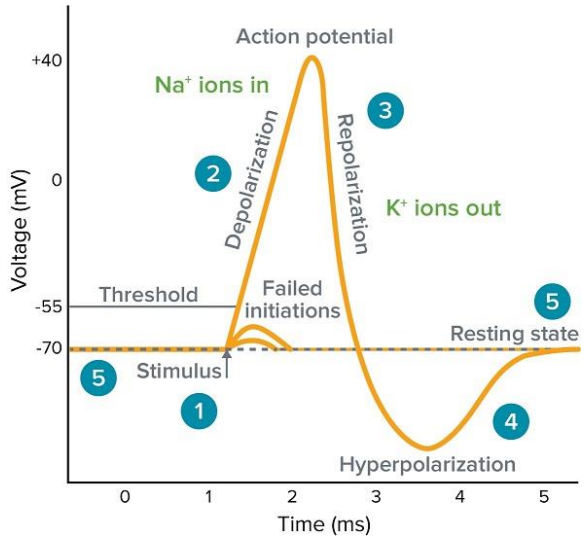

Fig. 2.3.1 Action potential phases and characteristics. [Source]: [https://www.moleculardevices.com/applications/patch-clamp-electrophysiology/what-action-potential], access on June 28, 2023.

Fig. 2.3.1 represents a graph of the membrane potential against time. There are identifiable parts, shown in Figure 6: 1. The onset phase, 2. the ascending phase – rapid membrane depolarization – which allows the internal membrane potential to reach the maximum peak value of 40 mV, with influx of Na^+. Failed depolarizations happen due to not reaching the threshold level. When there is the overdrive spike, the interior of the neuron is positively charged relative to the outside. 3. In the descending phase – rapid repolarization of the inner medium of the membrane – the inner medium becomes more negative than the resting potential, when K^+ ions come outside. 4. In the next phase – post potential hyperpolarization or undershoot – there is a gradual restoration of the 5. resting potential. From start to finish, this event lasts about 2 milliseconds (*ms*), and the stimulus generating the action potential must overcome a threshold for the onset of depolarization (BEAR, 2013).

Under normal conditions, the action potentials conducted by axons in the cortex contribute very little to the integrated surface potential because there are many axons in the cortex that are going in different directions and that depolarize asynchronously. Consequently, the temporal and spatial influence on the field potential at the cortical surface is neglected. When there is a synchronous response to cortical inputs/stimuli, it is called an evoked potential, and it has a relatively large amplitude. Synchronicity of adjacent fiber and cortical neuronal activity is the biggest factor influencing the magnitude of the surface potential that can be recorded with scalp electrodes (WEBSTER, NIMUNKAR AND CLARK, 2010).

Unipolar field potentials recorded in cortical layers reveal that surface cortical potential is increased by the 'network' effect of postsynaptic potentials from cortical cells, as shown in the pyramidal cell polarization in Fig. 2.2.2. This network of potentials can be excitatory or inhibitory - changing only the polarity of the dipole shown in Fig. 2.2.2 - and recorded directly below the electrode or at some distance from it. The potential change recorded at the surface is measured by this network of falling potentials between the surface location and the distance from the reference electrode. This network could have a resultant of zero, nullified by a closed field effect (WEBSTER; NIMUNKAR; CLARK, 2010).

Since this is an ordered and symmetrically fitted cortical surface with specific types of cortical cells, the recorded cortical electrical change may create a situation of open field potentials, which is favorable for detecting postsynaptic depolarizations. Pyramidal cells make this situation possible, as they are oriented vertically, with their long apical dendrites arranged parallel to each other. Thus, potential changes in one part of the cell relative to another part create a measurable current movement on the cortical surface, which is illustrated in Fig. 2.2.2 (WEBSTER, NIMUNKAR AND CLARK, 2010).

On the other hand, the non-pyramidal cells of the neocortex do not contribute substantially to surface recordings. This dipole relationship in the pyramidal cell, between dendrite and soma, dependent on excitatory or inhibitory stimulus, is what constantly alters the current dipole, where variations in dipole orientation and density produce fluctuations that resemble waves in the surface field potential. The recording of these fluctuating signals is given by electrodes on the scalp and originate the electrocardiogram, a signal that will be discussed in the next topic. The sum of negative dendritic activity, relative to the cell, it becomes excitable and depolarized. When positive, the cell is hyperpolarized and less excitable (WEBSTER, NIMUNKAR AND CLARK, 2010).

2.4 ELECTROENCEPHALOGRAM

The electroencephalogram is used to non-invasively diagnose brain injuries and tumors, just as it is used in neuropsychological research. Electroencephalograms are usually recorded from the scalp, which means that underlying brain cortical electrical activity must pass through the meninges, pia and dura mater, cerebrospinal fluid, skull, and scalp. When the ion waves hit the electrodes, the voltage difference between the electrodes can be measured by a voltmeter. Accounting for these voltages over time results in the EEG tracing, which is a 2D representation of the conduction volume, which is 3D. It is estimated that each of the EEG electrodes sees a solid angle adding up the activity of about 6 cm^2 of underlying cortex, with a significant number of thousands of cells in synchrony, indicating the behavior of cortical neurons (OLEJNICZAK, 2006).

Considerable attenuation and spatial averaging of the brain signal occurs due to various structures that electrical activity must travel through. The highest brain potential recorded on the scalp is approximately 150 μV peak. The standard for EEG recording via scalp electrodes is 10-20 – recommended by the *International Federation of Societies for Electroencephalography and Clinical Neurophysiology*, with positioning relative to anatomical landmarks of the skull and 10% or 20% intervals, see (NORTHROP, 2003) and Fig. 2.4.2. Different devices for EEG recording can vary from 1 to 32 electrodes across the scalp, and a total of 128 towards the face. The electrodes are the initial element for recording these biopotentials, as this is where the transduction of the ionic signal into an electrical one takes place. The electrodes must have metallic components and can have two main formats – disk or pins – and provide signal transduction with or without the help of conductive gel. The disc-

shaped electrodes, Fig. 2.4.1 are generally made of AgCl (silver chloride) and positioned with the help of a conductive gel at the electrode-skin interface.

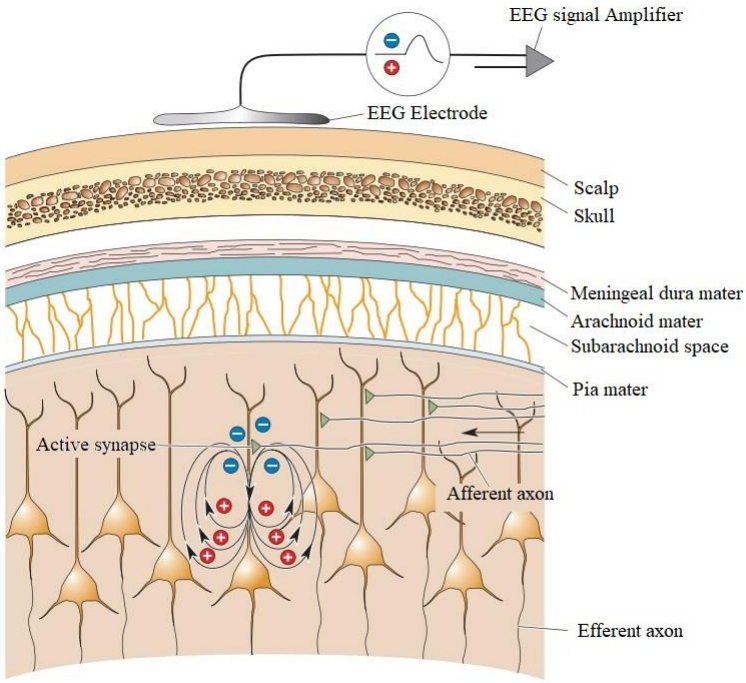

Fig. 2.4.1 Recording of brain electrical activity with an EEG electrode. The small electric fields are produced by electric dipoles in the pyramidal cells, in a postsynaptic depolarization. [Source]: translated from (BEAR, 2013)

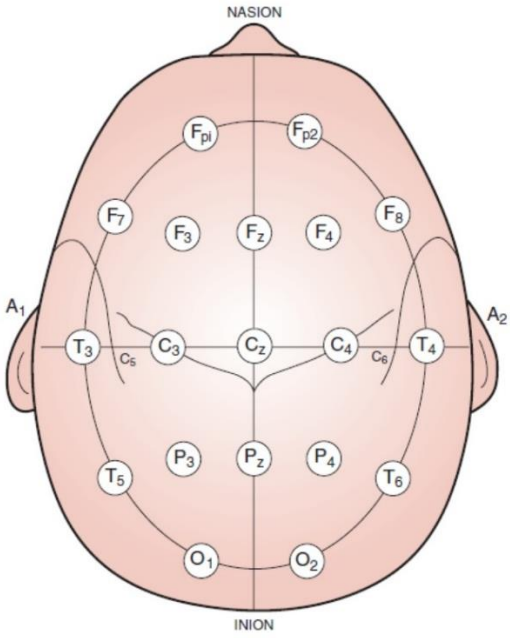

Fig. 2.4.2 International electrode positioning system, 10-20, with its traditional 19 electrodes. For referential (unipolar) recording, atria A1 and A2 are used as reference [Source]: (MARCUSE; FIELDS; YOO, 2015)

Typical EEG signals have frequencies in their spectrum corresponding to specific activities. Its characteristics can be seen in the Fig. 2.4.3 and Fig. 2.4.4, and it is possible to see that they are stochastic signals – they do not repeat themselves as a function of time. A complete EEG signal recording system comprises electrodes positioned on the scalp, connected to the amplification and filtering unit, subsequent analogue-digital conversion, signal processing, and recording or demonstration of the signal in real time. The signal/noise ratio of the EEG signal is relatively low, it is also subject to a strong attenuation at the skin-electrode interface, due to the impedance that characterizes it, in addition to the half-cell potential of the electrodes, which demands that computational algorithms assist in the process extraction of EEG signals and their possible characteristics of interest (WEBB, 2018). The removal of noise from the EEG signal in each channel (electrode) and its correlation with other channels, can generate information on the interactions of different areas of the brain, which can be observed by investigating the EEG rhythms.

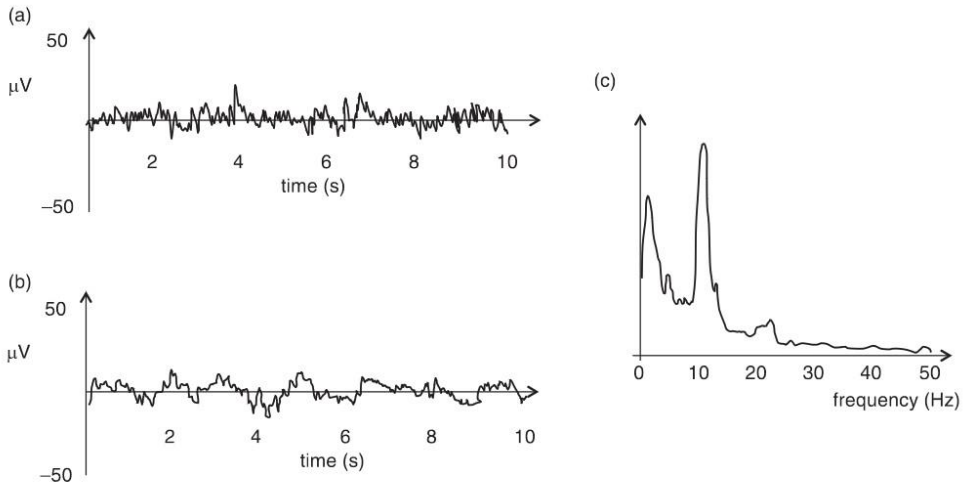

Fig. 2.4.3 (a,b) Characteristic EEG signals from two electrodes positioned at different physical locations on the scalp (c) Summed EEG frequency spectrum of all scalp areas for a typical EEG [Source]: (WEBB, 2018)

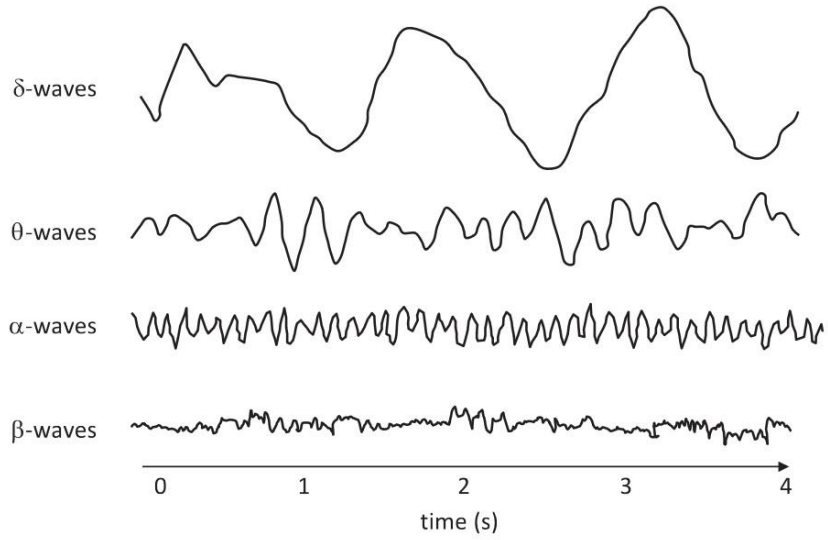

Fig. 2.4.4 Schematic example of EEG waveforms in different frequency bands [Source]: (WEBB, 2018)

EEG signal rhythms are correlated with certain behavioral states and pathologies. Brain rhythms are categorized into five most analyzed bands, depending on their frequencies, they are: the delta (δ), theta (θ), alpha (α), beta and gamma (γ) bands. The gamma band (γ) will not be addressed in this work, as it is a very high frequency range, normally associated with neuroscientific investigations, but which requires high precision from recording devices. Traditionally, the rhythms are described as follows, presenting the main associated behaviors.

Delta (δ) rhythms are slow, with high amplitude and frequencies below 4 Hz, normally only observed in children and adults who are in a state of deep sleep. A large detection of delta activity in awake adults is abnormal and is often associated with neurological disease. Delta waves originate in the thalamus or the cortex (WEBB, 2018).

Theta rhythms (θ) have high amplitude, low frequency, with a defined band of 4.1 to 7.9Hz. It occurs in small amounts in a normal waking adult, in a state of meditation and problem solving, as well as in large amounts it is associated with neurological diseases. A greater amount of these waves is seen in young and older children, and adults in a light sleep state. The theta band is associated with a wide range of cognitive processes (WEBB, 2018).

Alpha (α) rhythms occur at a frequency of 8 to 13 Hz. They are found in almost all normal people when they are in a state of wakefulness, creativity, concentration and in a state of relaxation. It is measured over the occipital region of the brain, primarily reflecting visual processing and memory retrieval. Its amplitude is high when the eyes are closed and body

relaxation, and it is attenuated when the eyes are open and when performing mental tasks (WEBB, 2018).

Beta (β) rhythms are found between 13.1 and 30Hz and are registered by the frontal and contralateral regions of the brain. Beta waves are characterized by a symmetrical distribution at the peaks of their waveform when there is no motor activity, and it becomes asymmetrical – desynchronized – with low amplitude during movement (WEBB, 2018).

Table 2.4 Brain Waves features

Brain Wave	***f* (Hz)**	**A (μV)**	**Description**
Delta	1 – 4	20-200	Predominant in the deep sleep state, loss of bodily awareness, dreamless sleep, unconscious
Theta	4.1 – 8	10	Found in the sleep state and in tasks that do not require concentration, such as automatic tasks. Reduced consciousness, dreams, light sleep
Alpha	8.1 – 13	20-200	Physically and mentally relaxed, state of attention, conscious, super learning. The occipital, parietal and frontal areas have the greatest amplitudes.
Beta	13.1 – 30	5-10	State of alert with attention to an external stimulus or concentrated on a task that requires reasoning, focus. It presents a lower amplitude than alpha oscillations and it is commonly found in the parietal and frontal lobes.
Gama	32 – 100	5-10	Observed in synchrony with visual information, whether consciously or not. Waves are prominent at 40Hz and associated with sensory processes in the visual cortex.

A: amplitude; *f*: frequency.

2.5 CEREBROVASCULAR ACCIDENT / STROKE

Stroke is one of the major causes of death and disabilities in the world and the reason for 116.4 million disability-adjusted life-years (DALYs) (MAROTTA *et al.*, 2020). The *Global Burden of Diseases, Injuries, and Risk Factors Study* reports that, in 2016, stroke was responsible for 5.5 million deaths globally. The great challenge of the survivors of stroke is to address the long-term consequences as sensory, motor, cognitive, and visual impairments. These neurological deficits are the main rehabilitation targets since these reduce the ability of individuals to perform activities of daily living (ADL) (KATAN; LUFT, 2018).

The most common involvement caused by stroke and the most widely reported is motor damage. This may be noted as loss of muscle control function, or limitation in mobility. Therefore, several new models of rehabilitation for motor recovery, such as robotic therapy and non-invasive brain stimulation, have been developed based on clinical studies and science, with

the aim of characterizing brain remodeling, due to the process of neuroplasticity - the brain's ability to adapt to environmental pressure, experiences and challenges, including brain damage (YUAN *et al.*, 2021).

Stroke survivors' manifest deficits in physical functions, e.g., motor impairment in up to 80% of cases, associated with disability in language, sensory, behavioral, and visual functions, dysphagia and cognitive domain (difficulty in intellectual capacity, memory, attention, orientations, awareness). The location of the brain damage, its extent and the amount of the recovery are key-points in the stroke's final outcome (LANGHORNE; BERNHARDT; KWAKKEL, 2011).

The use of brain-computer interfaces (BCI) has been applied for post-stroke rehabilitation. Most studies report patients who actively operated devices, performing robotic movements, for example, with the help of this interface to promote their rehabilitation. The use of BCI implies modifying the patient's neuronal activity, under the effect of progressive practice, with certain feedback or reward. It is estimated that changes in cortical activation patterns remain in the patient, when they perform similar activities, even after cessation of therapy activities (Yuan et al., 2021). In a current review, it was found that the use of short-term therapies with devices, immediately after the end of the intervention, is significantly more effective than the control interventions in post-stroke upper limb rehabilitation (MANSOUR *et al.*, 2022).

Recording the EEG signal in this context has proven to be a prominent tool that offers a more direct measurement of the electroencephalographic signal with greater temporal resolution to explore the dynamics of brain processes. Effective connectivity developed from Granger causality theory can be derived from the EEG signal (YUAN *et al.*, 2021). This type of connectivity theory reveals directed information flowing from one region to another and asserts directed information and correlation between brain areas. EEG can be applied to estimate functional and effective connectivity. Functional connectivity is defined as a statistical interdependence between spatially distant neurophysiological regions, usually measured by correlation, coherence and information theory (CAO *et al.*, 2022).

Generally, EEG data can be used either for evaluating the presence of neural plasticity in stroke patients before and after neurobehavioral treatment or as neurofeedback for brain-computer interface (BCI) systems. Indeed, the most common brain signal activity (EEG rhythms) used with BCI paradigms in stroke patients is related to motor planning and execution. During a motor attempt, the temporal pattern of the Alpha rhythm (8–12 Hz) over the

sensorimotor cortices desynchronizes. This rhythm is considered an indirect indication of the action observation network and reflects the general sensorimotor activity. When these EEG signatures change in the Beta rhythm (12–30 Hz) in the form of event-related desynchronization, they indicate that motor action is executed (ARCURI *et al.*, 2021).

Chapter 3

STATE OF ART

The first derivative work from this Thesis is the paper https://doi.org/10.3389/fphys.2021.727840. In this work, we focused on presenting a scoping review relating EEG signal processing attention detection findings and most used strategies, in a context of immersion in VR systems, with or without the addition of more devices for measuring physiological data, in a non-invasive manner. This chapter, will be presented the main considerations from the paper that are relevant to this work, together with new research findings from the literature.

3.1 VR SYSTEMS

Individual's conscious and unconscious states in reaction to external and internal stimuli can be evaluated by means of physiological signals, such as EEG and eye-tracking. The external stimulus can be a virtual reality system (VR), composed of sound and, mainly, image, being a means of communication that allows the user to feel physically present in the virtual experience. VR systems can present different levels of immersion of the user in the virtual environment, the more immersive, the greater the feeling of belonging of the user, and the brain waves recorded by the EEG may reflect this state (SOUZA; NAVES, 2021).

In VR systems, the user is exposed to punctual and constant stimuli, some with greater intensity than others. Thus, levels of attention can change and when monitored by means of EEG, it is possible to infer the individual's dedicated attention (immersion). Immersion can be a complex concept, as we discuss in the paper (SOUZA; NAVES, 2021), correlating some characteristics, such as lack of awareness of time, loss of awareness of the real world, involvement, and sense of being present in the task environment. In this sense, selective/oriented attention to the virtual environment may denote levels of immersion.

Analogous to immersion, concentration brings the individual into a very similar state of mind, which requires directing attention toward a particular task. However, the authors Lim, Yeo and Yoon (LIM; YEO; YOON, 2019) conducted a study in an attempt to differentiate the

states of concentration and immersion through the EEG signal. In concentration, subjects should focus on a red dot in the center of the screen, while in immersion they should focus on playing a VR game. The beta waves rose in both the concentration and immersion states in the frontal and occipital lobes, increasing further in immersion. The alpha waves showed only decay at rest times, in both concentration and immersion states, between tasks. Factors that call the individual's visual attention, causing fixation-related potentials (FRPs), were not investigated in that work, any intention existed to assess the individual's eye-tracking data during recording of the EEG signals.

To allow more immersion into VR systems, the individual's immersion process in the virtual environment is the individual's presence in the virtual environment. This is possible through an avatar, which is defined as a direct extension of ourselves as they are a close resemblance of what we experience in the real world (WALTEMATE *et al.*, 2018). Games are the main way to explore the individual's presence in the virtual environment. More focused on medical attention, exergames (VR-based exercises) have been a recent investigation into the approach of VR technologies, scientific investigation of physiological signals and therapies, often using avatars.

Virtual reality (VRs) systems can be classified according to its type of interaction with the user, allowing levels of immersion, into desktop-based VR systems, semi-immersive and fully immersed VR systems. These differences are necessary in the classification of immersive VR environments, since the user, when watching a 2D or 3D video, without controlling the virtual environment, in a passive way, is not facing an immersive environment – non-immersive VR, or desktop-based VR systems. Semi immersive VR devices, or distributed VR systems, allow a mixed view of the virtual environment, as with the use of 3D glasses, or controlling a desktop-based system. In the fully immersed VR system, the immersion device must be an HMD or be placed in a cave automatic virtual environment (CAVE), which is a room covered by screens on all walls (LI, Gang; ZHOU; *et al.*, 2020).

As presented at the end of Chapter 2, new technologies, such as virtual reality (VR), have been developed to enhance reorganization of the neuromotor ways and reduction of motor disability. Thanks to the distinctive characteristics of the surroundings created by the VR system and the multiple sensor-based interactions between the subject and the system, a virtual scenario can be perceived as a realistic experience. In a virtual environment, the therapist can build, adjust, and propose exercises that in conventional practice are unsafe, difficult to realize or too expensive. Moreover, due to the possibility of a gamification of the therapy, patients show more

enthusiasm during a virtual experience in comparison to the tasks' repetition of standard care rehabilitation, increasing patient's compliance. The use of multi-sensorial stimuli and challenging levels motivate the patients, which is one of the important elements to continue the treatment and improving rehabilitation outcomes. Another key feature of virtual reality is the "sense of presence" and the degree of integration can be so intense that it could also influence pain reaction, with a pain alleviation during an immersive virtual reality distraction (DEMECO *et al.*, 2023).

3.2 POST-STROKE UPPER LIMB FUNCTION AND REHABILITATION

Strokes and transient ischemic attacks one of the most common causes of hemiparesis, which can develop into hemiplegia as symptoms worsen. Hemiplegia is a condition caused by brain damage and spinal cord injury that leads to paralysis on one side of the body. It causes paralysis of one side of body, with loss of movement control, and muscle tightness (Increase muscle tone), see Fig. 3.2.1 for more detailed hemiplegia aspects.

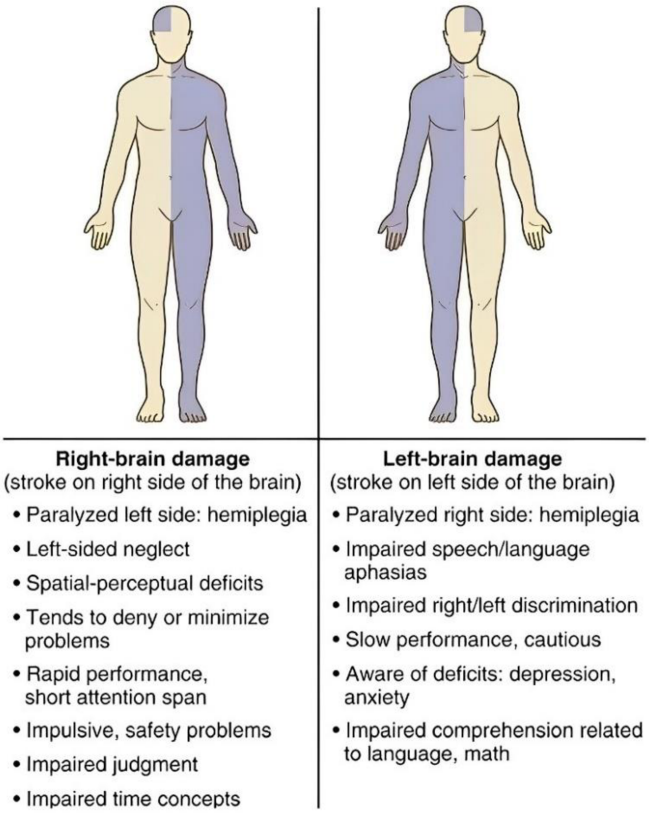

Fig. 3.2.1 Right and Left hemiplegia

(SUBRAMANIAN, 2013) analyzed kinematic data from arm and trunk movements, and the study showed that the virtual reality group had better results than the control group in terms of motor functioning ($p < 0.05$) and smoothness of movements ($p < 0.001$). Furthermore, the

authors demonstrated that these results were also correlated with minor cognitive deficits in memory, attention, visual perception capacity and problem solving.

(LIN *et al.*, 2021) demonstrated an improvement in the VR mirror therapy group regarding total score and hand component. Immersive virtual reality treatment has great potential in motor stroke rehabilitation and can offer additional benefits in comparison with standard therapy. Upper limb deficits are a common consequence of stroke: over 80% of stroke survivors have an upper limb dysfunction, e.g., spasticity, dystonia, muscle contracture, loss of strength and dexterity, decreased active joint range of motion, lack of precision and bi-manual coordination (DEMECO *et al.*, 2023). Five typical arm spasticity patterns are shown in Fig. 3.2.2, as elucidated by (DOUSSOULIN *et al.*, 2020). A global movement is addressed in the *Free to Fly* exergame to rehabilitate the typical spasticity patterns.

	I	II	III	IV	V
		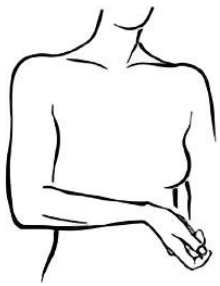			
Shoulder	Internal rotation/ adduction	Internal rotation/ adduction	Internal rotation/ adduction	Internal rotation/ adduction	Internal rotation/ retroversion
Elbow	Flexion	Flexion	Flexion	Flexion	Extension
Forearm	Supination	Supination	Neutral	Pronation	Pronation
Wrist	Flexion	Extension	Neutral	Flexion	Flexion

Fig. 3.2.2 Prevalence of Spasticity and Postural Patterns in the Upper Extremity Post Stroke

3.3 EYE-TRACKING

The use of technologies, such as an eye-tracking device (eye-tracker) can help in the composition of individual behavior metrics and physiological data, so that the researcher learns about cognitive processes and other information processing skills, in different contexts: reading, educational research, level of attention and visual behavior in interaction with a VR system (LEE; ANDERSON, 2001).

Several metrics can be extracted from subject eye-tracking. Natural eye movement tracking called eye-gaze, blinks, smooth eye movement tracking, rapid eye movement tracking

between two fixation points called saccade, pupil dilation data, fixation-related potential signal and time on a particular activity or region, and time data under an area of interest (AOI), when using systems limiting the individual's field of view. In the studies by (LIM; YEO; YOON, 2019; VARELA CASAL *et al.*, 2019), biomarkers are deduced from eye-tracking information. The individual's attention is calculated from measurements of the fixation time on a target in the center of the screen to which he is exposed.

Approaches on eye-tracking metrics date back to the beginning of the 20th century, where the corneal reflex method was created, and it is based on the use of the eyeball as a spherical pattern that rotates like the center of a circle, and the reflex point is always fixed (LI, ZHAOWEI; GUO; SONG, 2021). This was the first eye-tracker to generate data in two dimensions (*x,y*), developed by Stratton and used for studies of illusions, aesthetics and object perception (STRATTON, 1906). Applied to the study of relevant tasks and ocular focus as an attention strategy, the first evidence with an eye-tracking experiment dates back to 1999 by (HAIDER; FRENSCH, 1999).

A very common commercial device for recording eye-tracking is the Tobii® (https://www.tobii.com/) eye-tracker, which has several versions, and nowadays afford many devices options. Its overall technology allows tracking the main variables of interest in eye-tracking: heat map, area of interest, saccade occurrence, fixation time and duration, among others. While the system is quite stable and does not change the measurement variables due to changes in the user's head, wearing specific clothes or glasses, blinking or problems with the user experience.

For processing gaze data, an open-source solution is *OGAMA* (VOSSKÜHLER *et al.*, 2008), which is a gaze data analytic tool to collect a large body of records consisting of fixation points linked by paths. Heatmaps, scan-paths, transition matrices, fixation metrics and charts of AOIs provide useful visualization techniques to support insight discovery from gaze data. However, they always provide a partial information between the visualization of the raw data, often dense and complex, and a given level of abstraction which gives a specific point of view of the data. Because of that, merging eye information and EEG data, may lead to new perspectives.

Specifically, to fixation time and duration data from eye-tracking, the fixation-related potentials on EEG may allow promising combination of EEG and Eye-tracking data, giving an improved overview of the interaction. It has been only recently studied and can be observed through combined analysis of EEG and Eye-tracking recordings. Fixation-related Potentials

(FRPs) are a subcategory of event-related potentials (ERPs) that rely on eye-fixation based events to give context to brain activity. This type of ERP is time-locked to the onset of an eye fixation. This characteristic aligns these events with the underlying cognitive processing which occurs during visual exploration. This subsequently allows to inspect said cognitive processes as they relate to the examined visual information (WOBROCK *et al.*, 2020).

FRPs have been generally studied in very controlled environments, proposing artificial and curated stimuli to the users during interaction. Yet, these potentials lend themselves to an enhanced evaluation of brain activity in a wide variety of more natural scenarios, indicating free-viewing approaches to be successful. Indeed, the additional recording of eye movements allows for the monitoring of where and how the user attention is allocated with respect to the manipulated system (WOBROCK *et al.*, 2020).

Both eye-tracking (ET) and electroencephalography (EEG) have a rich history of experimental paradigms and results that have revealed much about the workings of visual perception. Studies are increasingly combining these two techniques into what we will refer to as ET-EEG experiments. Where eye movements (EMs) offer a close insight into the temporal and spatial allocation of attention, EEG is informative about what happens in the brain before, during, and after the eyes land on a certain region of a stimulus. EEG-only paradigms often require observers to not move their eyes and not blink during trials. Such paradigms without eye movements (static EEG experiments) often aim to infer the workings of perception in everyday life. But eye movements are abundant in everyday tasks. Allowing eye movements in experiments is a natural step towards studying these processes in ways that generalize better to situations outside the lab (CORNELISSEN; SASSENHAGEN; VÕ, 2019).

3.4 EEG FEATURES IN ATTENTION ALLOCATION AND GAMES

In the context of cognitive neuroscience, attention is one of the three cognitive control abilities (the other two are working memory and goal management) (GAZZALEY; ROSEN, 2016). The EEG signal extracted from the scalp surface can be divided into frequency bands, which have stochastic characteristics of similar amplitude and frequency. The different bands of brain frequencies carry information about the states of individuals. For the same individual and between individuals, the amplitudes and occurrence of rhythms activity can vary greatly.

The use of EEG-based devices has become popular with the advancement of EEG wearable devices, as it lowers the cost of capturing EEG signals and allows its use in uncontrolled environments, as well as in non-medical environments, with the most popular

being the Neurosky ®, OPENBCI® and Emotiv ®, which generate measurements of ratios and frequency bands of brain waves. BCIs or BMIs, by definition, are interfaces that use brain signals to control close-loop systems in real time. The variability of the inter- and intrapersonal EEG signal has generated, over several decades, discomfort for scientific purposes. Only in the last decade, with the advancement of technology and the advent of low-cost portable EEG wearable device, it has been possible to popularize the capture of the EEG signal in various non-laboratory contexts and generate comparative patterns between experiments from pre-defined levels and scales by these equipment (SOUZA; NAVES, 2021).

Regarding brainwave bands, the increase in α – alpha waves (low alpha 8–11 Hz and high alpha 11.1–13 Hz) has been the main physiological indicator of low anxiety state, especially high alpha (LI, Gang; HUANG; *et al.*, 2020) which indicates also cognitive idleness, being a marker of external stimuli suppression capable of reorienting the individual's attention (VORTMANN; KROLL; PUTZE, 2019). In this sense, there is an indicator of the alpha wave arousal on the top-down attention direction (external stimulus oriented), a restorative process that reduces anxiety and fatigue. The individual's immersion in environments that encourage contact with nature, with the intention of transmitting tranquility, relaxation, and increased meditation activity, increases the power of alpha waves (GRASSINI *et al.*, 2019).

Event-related potentials (ERPs) are brain electrical potentials, associated with the individual's internal and external stimuli. Therefore, they can be the result of external or internal stimuli attention, in terms of attentional orientation (LINDSAY, 2020). ERPs can be the result of cognitive processes, but are also easily affected by mood and emotion, and are analyzed with a focus on time-domain monitoring of the EEG signal at a specific interval after the source stimulus. Since signal to noise ratio (SNR) of EEG measurements is relatively low, data from a single stimulus presentation usually do not allow inferences about the stimulus related activity of interest. So, ERPs specifies an important role averaging the EEG signal/specific band around a stimulus. The trigger for the primary stimulus is a crucial factor in understanding these potentials, which are validated in terms of their amplitude and latency measures and may be an intra- or inter-individual assessment.

Prominent FRP components might represent in relation to cognitive processing. Each component considers the aspects of processing associated mainly with reading. The earliest effect observed is a positive visually evoked response that originates from the occipital regions of the scalp with a peak at approximately 100 *ms* after fixation onset on a written word. This visually evoked response, once labelled 'lambda wave', is now considered the equivalent of the

P1 component. The P1 component is followed by the N1 component, a negative potential which is largest over left occipital, parietal and temporal areas of the scalp, with a peak approximately 200 ms after fixation onset (DEGNO; LIVERSEDGE, 2020). Fig. 3.4.1 shows waveforms that might (ideally) be revealed if deconvolution processes are applied successfully to an average FRP data stream recorded across two successive fixations regarding reading process. The word "carrot" and then on the word "juice" are targets as the sentence "John made a very tasty carrot juice with fresh carrots yesterday" is read (DEGNO; LIVERSEDGE, 2020).

Following the N1 component, a P2 component has also been observed. This positive potential is observed first over anterior and central areas of the scalp between approximately 140–280 *ms* after fixation onset, being modulated by semantic relatedness and word predictability (DEGNO; LIVERSEDGE, 2020).

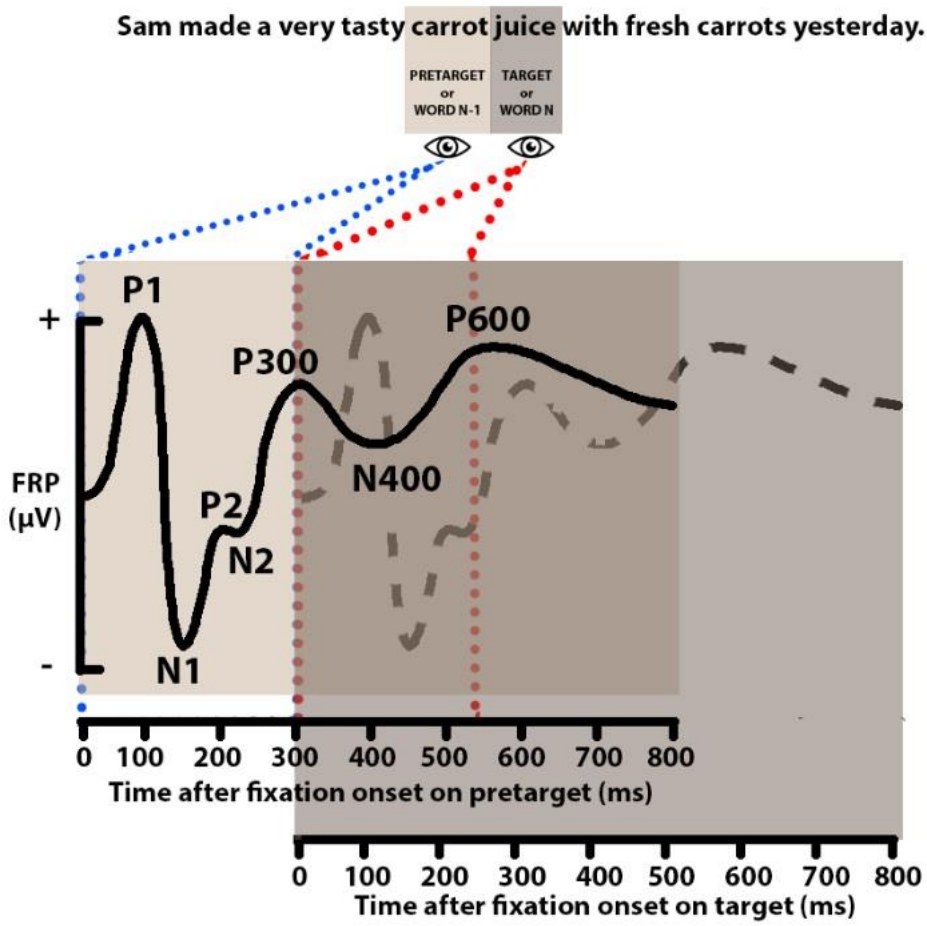

Fig. 3.4.1 The solid black line represents the waveform and components (i.e., P1, N1, P2, N2, P300, N400, P600) that result from processes associated with the fixation on pre-targets. Dashed line continues what should be for targets (DEGNO; LIVERSEDGE, 2020).

A variety of spectral characteristics/dynamic variables can be extracted from the EEG signal as indicative of cognitive variation, which provide satisfactory measures and

classification of cognitive workload. The EEG signal features shows that most investigations of mental load/arousal/attention allocation are by means of the maximum, ratio or averaged power spectral density (PSD) over theta, alpha and beta bands, mainly (BIOULAC *et al.*, 2019; LIM; YEO; YOON, 2019; MAGOSSO *et al.*, 2019; MATTHEWS *et al.*, 2015; YIN; ZHANG, 2014; YU *et al.*, 2015).

The EEG frequency band power, and more specifically the EEG theta (4–6 Hz) frequency band power at frontal electrodes and the EEG upper alpha (10–13 Hz) frequency band power at parietal electrodes have been shown to be sensitive for measuring mental processing demands in a variety of different tasks, so far predominantly in highly controlled task settings of basic research, as described by (SCHARINGER; SCHÜLER; GERJETS, 2020) with examples. Increased mental processing demands typically result in increased EEG theta power at frontal electrodes and decreased (upper) alpha power at parietal electrodes. A (relative) increase in frequency band power is typically termed event-related synchronization (ERS), a (relative) decrease in frequency band power is termed event-related desynchronization (ERD). One prominent way to express changes in EEG frequency band power (with respect to a baseline) is the use of the ERD/ERS%-measure (PFURTSCHELLER; LOPES DA SILVA, 1999). ERD/ERS%-values are calculated using the following formula: ERD/ERS% = 100 * (frequency band power condition -frequency band power baseline) /frequency band power baseline. In principle, three different baseline-selections are possible for calculating ERD/ERS%-values: a) using a pre-stimulus baseline, b) using a separate condition as baseline (e.g., a rest baseline), or c) using a whole trial condition-average baseline (COHEN, 2014). The ERD/ERS%-values are calculated separately for each electrode and each frequency band. Depending on the concrete selection of the baseline for calculating ERD/ERS%-values and ERS (or ERD) might not always be associated with a positive (or negative) sign as originally defined by (NEUPER; PFURTSCHELLER, 2001). ERD and ERS are not explored in results of this study, besides it can be inferred by increasing and decreasing of EEG bands over the scalp.

In the context of VR systems, some findings are pointed out, and compared in this study in the discussion section:

- for different levels of a game, no significant differences were found in α and β waves for the subjects' brainwave power data (COENEN *et al.*, 2020), while (COWLEY; RAVAJA, 2014) identified decreased delta power and relatively balanced fronto-hemispheric alpha power in the five analyzed levels;

- for different cognitive load demands in the game, as learning increases, the best predictors are frontal alpha power and alpha and delta ERSPs, but not P300 (MATHEWSON *et al.*, 2012);
- it is estimated that a higher level of attention reflects an increase in the theta potential (θ) in frontal electrodes and, in parietal electrodes, an increase in the potential relative to the alpha rhythm (α) (TREJO *et al.*, 2015).

Chapter 4

MATERIAL AND METHODS

4.1 EXPERIMENT DESIGN AND DATA ACQUISITION

The study subjects consisted of 5 chronic stroke survivors (1 woman and 4 men) in their adulthood who had no closed diagnosis for psychiatric illnesses, one subject (patient 5 – Table 4.1) was excluded from analysis owing to data error. The recruited subjects were adults who had never played *Free to Fly* game before participating in the experiment. The mean age was 57.6 years with a standard deviation of ±7.83. This is a case study; no sample size was estimated. The experiments in this study were approved by the ethics committee of *Federal University of Uberlandia (UFU)*, register number 39232820.2.0000.5152 v.6 and took place at the *Assistive Technology Lab (NTA-UFU)*.

Inclusion criteria were chronic stroke (>6 months of occurrence), recommendation of a minimum of 8 hours of sleep on the last night, no use of stimulant drinks in the last 2 hours, impairment of motor function in the limb superior, and brain injury/subcortical injury demonstrated by CT/imaging studies. Exclusion criteria were the presence of intracranial metal or being unable to understand procedure instructions. All subjects were right-handed prior to the stroke and had normal or corrected-to-normal vision. The experimental protocol was in accordance with the 1964 Declaration of Helsinki. An informed consent form was obtained from all patients agreeing to participate in the study.

Table 4.1 Patient's clinical data

Patient	Age (years)	Stroke occurrence (months)	Affected side	Complaint of Forgetfulness/Attention Deficit
1	64	74	R	N
2	52	99	L	N
3	47	121	L	Y
4	65	75	L	N
5	60	16	L	Y
Average	57.6	77		
Standard Deviation	7.83	39.22		

Brain waves were measured using an Ultracortex ‘Mark IV’ EEG wearable device, from OpenBCI®. There were 8 channels, and the Fp1, Fp2, F3, Fz, F4, C3, C4, and Pz positions were measured based on the 10–20 system, connected to the *OpenBCI Cyton 8-channel conditioning Board*, with a sample rate of 250 Hz (ADS1299 chip, ~1GΩ input impedance, promoting impedance matching with the skin). The channels of the electrodes were numbered sequentially, starting from 1 for Fp1 to 8 for Pz. Two reference electrodes/ear clips were attached to the ear lobes. Dry pin (spikey) electrodes were used (Fig. 4.1.1 A), made of plastic with a metallic print cover on the pins, installed in Ultracortex nodes with hair, positioned in the 3D laboratory printed cap (Fig. 4.1.1 D), Fig. 4.1.1. To reduce discomfort, 5 comfort units (Fig. 4.1.1 C), that have springs, and 2 flat unit electrodes (Fig. 4.1.1 B) are used in no hair parts, distributed over the wearable, weighting it equally. Then, a battery pack is placed on the head, right upon the Cyton board site.

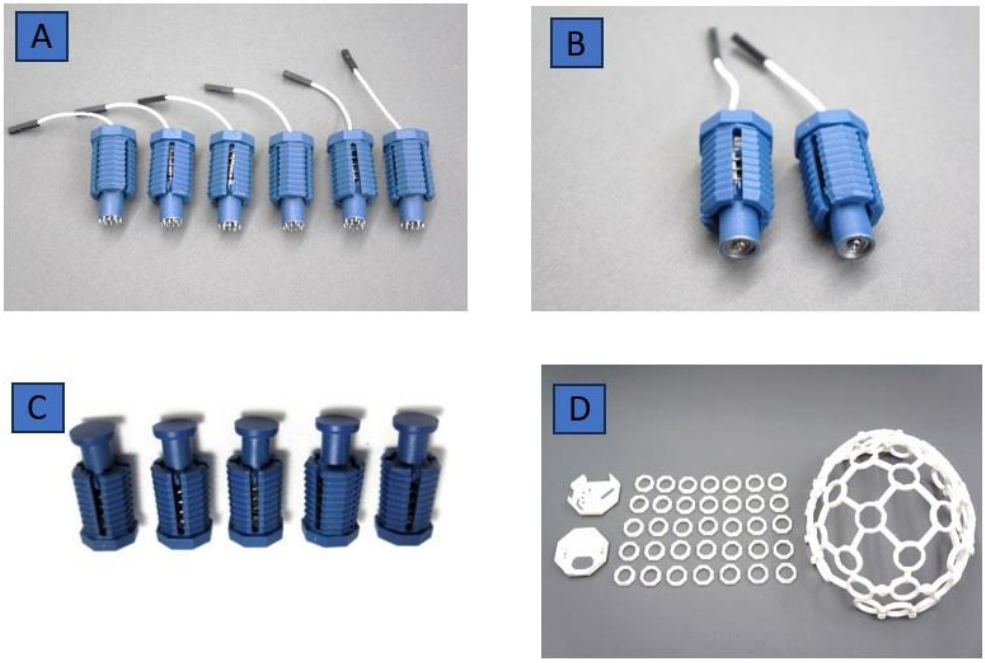

Fig. 4.1.1 Spikey units, Flat units, comfort units, and 3D printed parts of Ultracortex IV Mark wearable device/ “headset”. [Source]: {https://shop.openbci.com/collections/frontpage/products/ultracortex-mark-iv?variant=43568381966}, accessed on June 28, 2023.

Fig. 4.1.2 shows the connection of each component. Tobii® Eye-tracker 4C was used to register ET information, i.e. *x,y* positioning list of the eye on the screen (1600x900

pixels). The role screen was the AOI in this experiment. The physiological signals are recorded one time, synchronized later with the EEG signal by a timestamp log, in an offline fashion. Both signals are recorded in the same machine. ET approaches 1) Constant recording during the three tasks at 60 Hz. The eyes' position in a 2D VR environment and their direction are registered in an *x,y* matrix. 2) The time and timestamp measurements are registered for the attentional tasks for each trial.

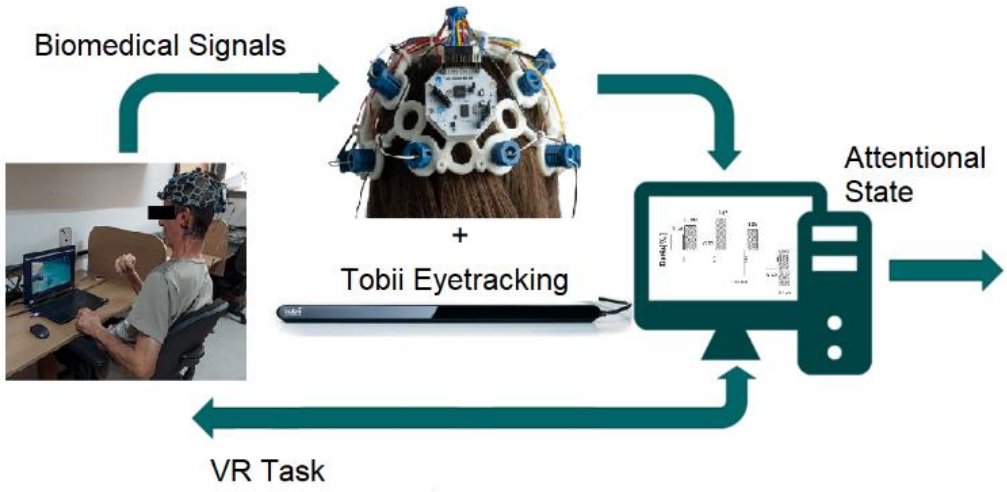

Fig. 4.1.2 Study framework components

A method based on the recording of the resting state eye open and closed has been presented in their study. From the five different frequency bands, we consider only three bands: theta, alpha, and beta. This choice has been motivated by the fact that delta bands are more presented in the deep sleeping state, which is not the case in this study, and that the gamma bands tend to be more affected by noise (e.g. electrical noise having a frequency of 60 Hz) and are also merge with beta band in several studies, their contribution being minors. This methodology merges aspects from (DELVIGNE *et al.*, 2020; LIM; YEO; YOON, 2019) works.

A VR Environment was developed at NTA-UFU, an assistive technology laboratory inside UFU. This VR Environment checked for VR exergame characteristics, developed for upper limb rehabilitation purposes (TANNUS DE SOUZA *et al.*, 2021), achieving good tracking accuracy, simplified use, and practicality to patients and professional assistance, greater accessibility than commercial solutions, in a low-cost tracking system fashion, using the webcam from the laptop. See Fig. 4.1.3 to visualize the colored ball, the tracked part to control the exergame, to maximize the fruits gained by the avatar. Griping the colored ball, the patient practices the claw and hold move, and a global arm

move directs the avatar through the desired path, which is a comfortable VR beach view, where the avatar must catch as many fruits as it can.

The role patient's play was to achieve rehabilitation's movements in a non-conservative fashion. The VR environment was designed as in the (TANNUS DE SOUZA *et al.*, 2021) work, called *FreeToFly*, developed in Unity® 3D platform, with minor modifications to elucidate each part of the stimulation phase. This approach meets some comments from (DEMECO *et al.*, 2023) work, as (ÖGÜN *et al.*, 2019) work. In the experimental protocol consisting of some games, but not targeting specific function of the upper limb: grip function, hand, and forearm movement to handling items and complete complex gesture.

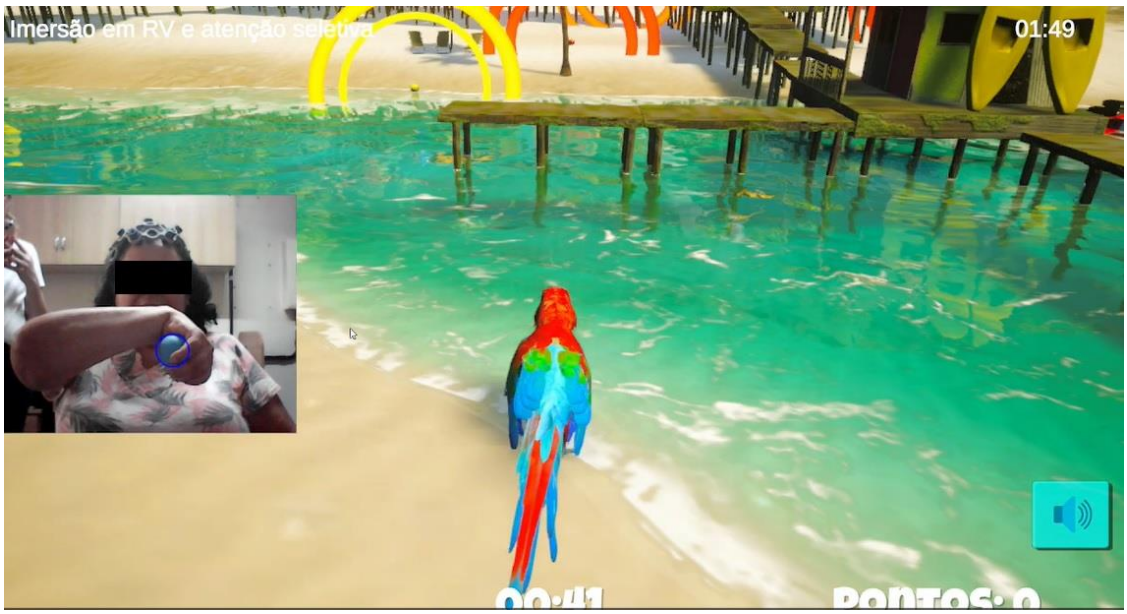

Fig. 4.1.3 Screen view with feedback sight

The experiments were conducted in the order of *Eyes Closed (EC), REST, SelAT,* and *SusAT*, Fig. 4.1.4. *REST* state is a concatenation of Eyes Open rest state and RV Immersion with no command over the avatar. These two moments were summed up after evaluation of ET and EEG signal data, by their similarity. The state' duration was then improved merging those experimental phases.

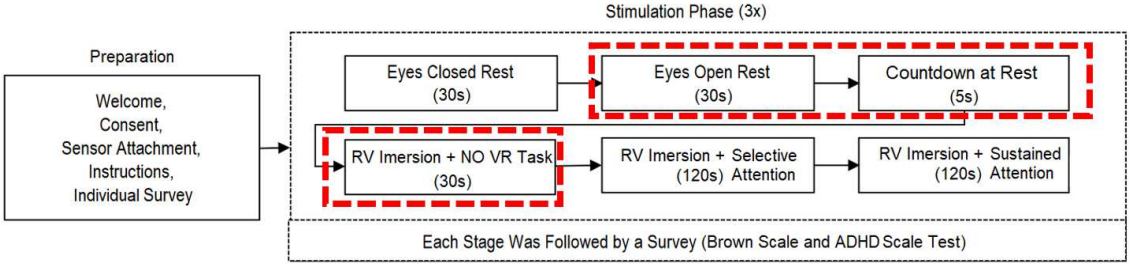

Fig. 4.1.4 Study framework detailing preparation phase and the stimulation phase in each state. Red parts form *REST* state, RV Immersion + Selective Attention constitutes *SelAT* state and RV Immersion + Sustained Attention constitutes *SusAT* state

In this environment, a 1 min task (REST) is performed, as well as, 2 minutes attention tasks duration:

- relaxation (*REST*)
- selective attention (*SelAT*)
- sustained attention (*SusAT*)

The attention states had no longer duration due to reported arm pain/tiredness from patients during pilot studies. The patients were seated 60 cm from the laptop screen, legs should touch the floor at a 90º angle at the knee joint. Each participant performed 3 trials, concluded 3 times the stimulation phase detailed in Fig. 4.1.4. At the end of the trials, the patient answered the translated and validated Brown attention-deficit disorder scale (BADDS) for use in Brazil (KAKUBO *et al.*, 2018).

BADDS is a self-report questionnaire that is used for screening adults with a possible case of ADHD. The questions in BADDS are not driven in terms of inattention-hyperactivity-impulsivity symptoms, but instead assess functional impairment in five areas, through 40 questions. These five areas are as follows (KAKUBO *et al.*, 2018):

1. organizing and prioritizing work and activation for work;
2. focusing on tasks, sustaining this focus and shifting attention to tasks;
3. regulating alertness and sustaining effort, and the ensuing processing speed;
4. managing frustration and modulating emotions; and
5. using working memory and accessing recall.

Each question has a possible score from 1 to 4. The higher the cluster score and overall score are, the higher the risk is that the individual has ADHD. All individuals who complete the BADDS questionnaire are classified into three groups: i) possible, but unlikely to have ADHD, if the score is less than 40; ii) possible, but unconfirmed ADHD, if the score is between 40 and 54; and iii) highly likely but unconfirmed ADHD, if the score is above 55 (KAKUBO *et al.*, 2018).

ASRS is currently the most accepted and most widely used self-report questionnaire for screening for ADHD symptoms (KESSLER *et al.*, 2007). The questionnaire asks directly about the existence of inattention-hyperactivity-impulsivity symptoms. It consists of 18 questions, with scores for each question ranging from 0 to 4. Zero means that no symptoms were present within the last six months, while 4 indicates that all

symptoms were present within the last six months. The composite scores of this questionnaire, similarly to BADDS, classifies patients into categories depending on the risk of ADHD. Patients with scores between 0 and 16 are considered to be individuals with an unlikely risk of having ADHD; patients with scores between 17 and 23 are considered to be individuals with a likely chance of having ADHD; and finally, individuals with scores of 24 and over are considered to present a high likelihood of having ADHD (KAKUBO *et al.*, 2018). Only one patient in our case study presented score over 24 for ASRS and score 44 for BADDS, i.e. signs of ADHD. The author decides to work with only this data for feature extraction in this study.

To assess attention, visual stimuli related to the environment appear: fruits falling from the sky and landing in a place indicated by large colored circles. The patient is asked to look in its direction without moving the head. The difference between the second and third task is the apparition of a combination of right and wrong stimuli: in the selective attention task, the patient can only grab bananas, and he is instructed to do so. In the sustained attention, only one type of stimulus appears, *i.e.*, any grabbed fruit works. The time elapsed between the target apparition and the moment at which the participants take the target was not measured, it varies greatly and was not a good attention variable, as well as a button register made at each fruit catch. The signal from analog register spoiled some EEG data/added artifacts to it.

4.2 OGAMA MEASUREMENT

Eye-tracking data, using an *x,y* matrix followed by time information were the input data for OGAMA calculations. Some detections are specified as follows.

Fixation detection. The fixation calculation is done using the fixation detection algorithm published by LC technologies (www.eyegaze.com/doc/ FixationSourcecode.htm). It is a dispersion-type algorithm with a moving window (SALVUCCI; GOLDBERG, 2000). The source code is ported to C# and added a time estimation support, but the working principle is not changed (VOSSKÜHLER *et al.*, 2008). This is described in the source code documentation:

> *"The function detects fixations by looking for sequences of gaze-point measurements that remain relatively constant. If a new gaze point lies within a circular region around the running average of an on-going fixation, the fixation is extended to include the new gaze point. (The radius of the acceptance circle is the*

above user specified maximum distance.) To accommodate noisy measurements, a gaze point that exceeds the deviation threshold is included in an on-going fixation if the subsequent gaze point returns to a position within the threshold. If a gaze point is not found, during a blink for example, a fixation is extended if a) The next legitimate gaze point measurement falls within the acceptance circle, and b) There are less than the above minimum numbers of samples of successive missed gaze points. Otherwise, the previous fixation is considered to end at the last good gaze point measurement. (source code description, www.eyegaze.com /doc/FixationSourcecode.htm)"

Prior to the fixation calculation, the fixation detection algorithm applies a two-step filter. In the first step, empty values are ignored in the calculation. This is necessary because of the different sampling rates of the gaze and mouse data. The second step is to omit samples with both x- and y-coordinates equal to 0, which often marks the eye-tracker output during a blink, and to omit samples that lie out of the screen.

In the experimental settings, one must specify two parameters for this algorithm: (1) the maximum distance (in pixels) that a point may vary from the average fixation point that is still considered to be a part of the fixation, and (2) the minimum number of samples that defines a fixation. Depending on the experimental sampling rate and the research domain, these highly interdependent parameters must be chosen carefully (VOSSKÜHLER *et al.*, 2008).

The attention maps are calculated as aggregated Gaussian distributions of each fixation in a stimulus slide. The summed Gaussian distributions are then overlaid on the original stimulus slide. Doing this allows a quick visualization of a landscape of visited and unvisited locations on the stimulus slide. The attention map calculation uses a two-dimensional Gaussian kernel with an editable size to enable adjustable smoothing of fixation distribution landscapes. With a mean value of $\mu=0$, a standard deviation of σ, and an isotropic distribution, the Gaussian kernel is given by the following formula (VOSSKÜHLER *et al.*, 2008):

$$f(x,y) = \frac{e^{-\frac{x^2+y^2}{2\sigma^2}}}{2\pi\sigma^2} \quad x,y \in [-s,s] \qquad (1)$$

The standard deviation is internally set to σ= s/5. Each value of this template kernel is multiplied for each fixation with a factor that is given by the duration of the fixation.

This factor represents the weighting of this fixation. All multiplied kernels in a trial are then added to a stimulus-sized array at the positions of the respective fixations. Finally, the whole array is normalized. The result is a stimulus-sized height map or landscape. This landscape can be easily transformed into a color map by a predefined or custom gradient. The user can choose the subjects to include in the calculation along with whether the calculation should be based only on the first or on all fixations. Thus, one can easily answer questions like *"Where does the average subject have its first look?"* and *"What locations of the stimulus are not noticed by the average subject?"* (VOSSKÜHLER *et al.*, 2008).

4.3 SIGNAL PROCESSING

A study flowchart overview is seen in Fig. 4.3.1.

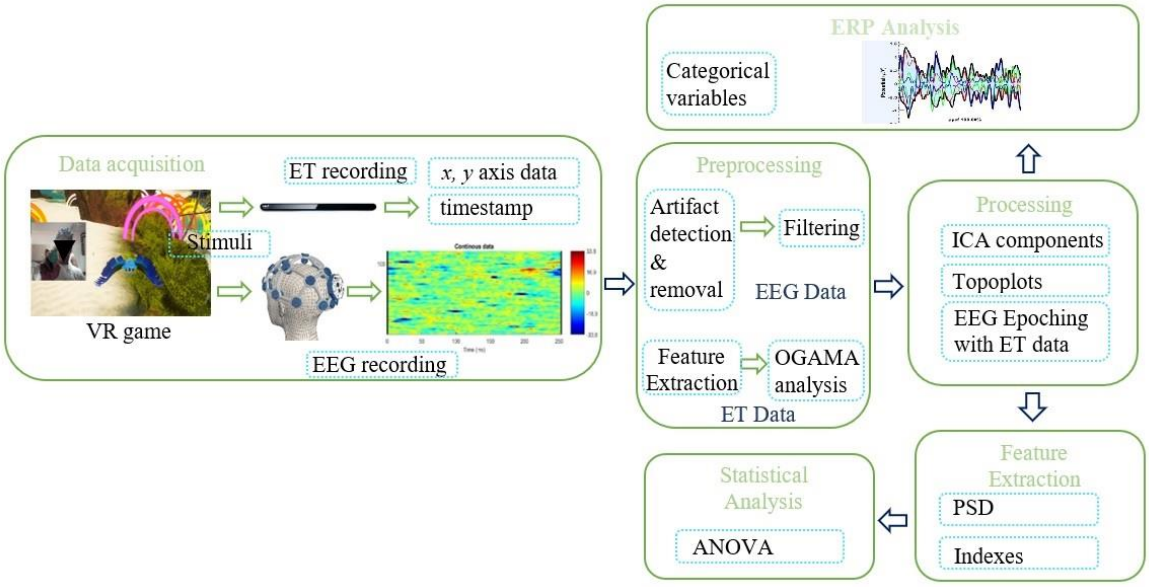

Fig. 4.3.1 Study flowchart

4.3.1 FILTERING THE DATA

The Fig. 4.3.1 shows graphical explanation of the meaning of cutoff frequencies, pass band, stop band, as well as transition bands.

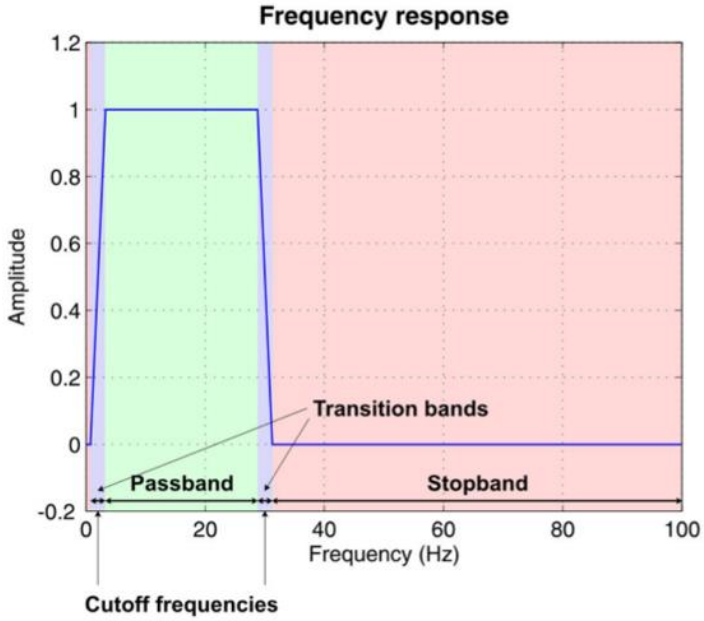

Fig. 4.3.1.1 Filter types and frequency response. [Source]: https://eeglab.org/tutorials/05_Preprocess/Filtering.html

In the default Windowed Sinc filter, EEGLAB® (DELORME; MAKEIG, 2004), used in this thesis, the start values there for the filter order: two times the cutoff frequency for *highpass* and *bandpass* (for cutoff < 2Hz). 20 to 40% of cutoff frequency for lowpass and 1 to 5 Hz for line noise *bandstop*. The basic rule is to have the transition band as wide (roll-off soft) as possible to avoid artifacts but separated from the signal of interest.

To remove linear trends, it is desirable to *highpass* filter the data. *Highpass* filtering the data at 1 Hz is recommended to obtain good quality ICA decompositions (KLUG; GRAMANN, 2021). *Lowpass* filtering high-frequency noise is also necessary in our EEG signal, limiting the *passband* from 1Hz to 30 Hz. EEG data were preprocessed offline in MATLAB (R2019a, Mathworks, Natick, MA, United States) using the EEGLAB toolbox (version March 3rd, 2023, Swartz Center for Computational Neuroscience, San Diego, CA, United States) and its extensions in combination with some custom MATLAB and Python (Jupyter Lab) scripts.

Data is fragmented into the sections indicated by each moment of the phase stimulation, in all 3 trials performed by the patient. Thus, artifacts and transition data between activity blocks were removed. The data were pre-processed in a few steps in EEGLAB®: (1) high-pass filter at 1 Hz (the standard EEGLAB *windowed sinc FIR filter* from the Firfilt plug-in (v2.6) with a cut-off frequency of 1 Hz was used and parameters: ripple 0.0022, transition band 30 Hz and sampling frequency 250 Hz, order: 414 (*onepass-zerophase, hamming-windowed sync FIR cutoff (- 6 dB) 1 Hz, transition width 2.0 Hz, stopband*

0-0.0 Hz, passband 2.0-125 Hz max. passband deviation 0.0022 (0.22%), stopband attenuation -53 dB); (2) The signal was low-pass filtered at 30 Hz by the *Short IIR filter*, EEGLAB®, with causal analysis marked (to aid in future connectivity analysis) - LPF has cutoff of 30.0 Hz, transition bandwidth of 1.0 Hz and its order is 11.0, removing the line noise; (3) Light cleaning the data – only 2nd option by *Clean RAWdata and ASR analysis* (ANDREAS EDGAR KOTHE, 2016), with removal of bad channels with many artifacts and reconstruction of continuous data, with minimum correlation of close channels adopted at 0.8. In the reconstruction of continuous data places, 'boundary' events are demarcated in place of the removed data; (4) The signal was re-referenced by averaging and interpolating the removed channels through spherical interpolation; (6) The data were then analyzed by independent components (ICA), *runica* method in the EEGLAB toolbox, with 'pca', -1 (due to component added by averaging the signal); (7) ICA was labelled, flagged and removed (8) The 2 final Steps of *Clean RAWdata and ASR* were performed; (9) Epochs extracted, [-1 2]ms interval, based on fixation events, with no baseline removal. See Fig. 4.3.1.2.

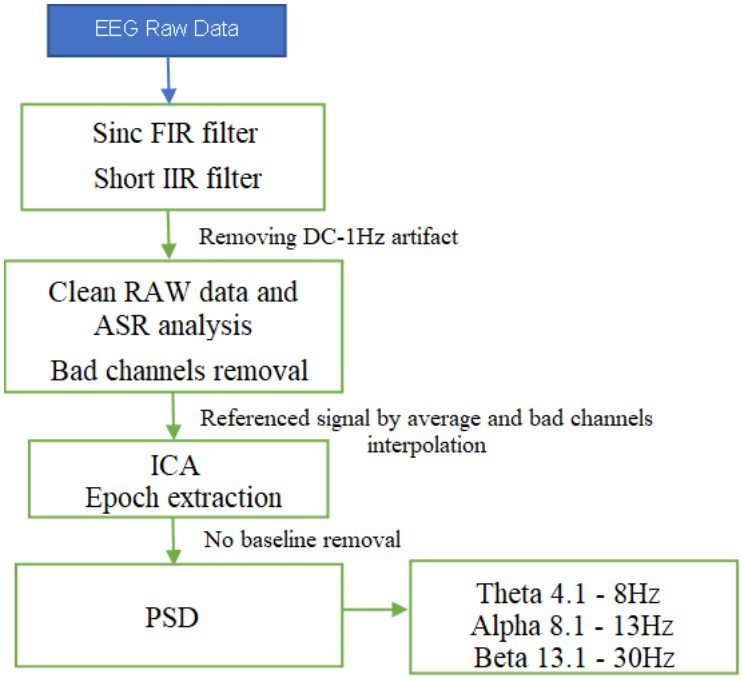

Fig. 4.3.1.2 Preprocessing and feature extraction flowchart

For EEG Epoching, Fixation-related potential (FRP) duration was defined as the duration post a gaze between saccades and EEG data was used as threshold for data extraction and the following classification. Epoch quantity varies among trials and states.

To assess the influence of different threshold on the classification, we have also used 200 ms to 500 ms as fixation interval with a step of 50 ms as threshold for the epoch extraction.

4.3.2 FEATURE EXTRACTION FROM EEG SIGNAL

The cleaned EEG signals are analyzed for spectral analysis using the fast Fourier transform (FFT). An epoch length of 3 s, equivalent to a 0.5-Hz resolution, is used for auto-spectral and cross-spectral analysis over the frequency range of 1–30 Hz for every epoch. The epoch length is then analyzed by advancing a 0.5-s sliding window, i.e. ~85% overlap between adjacent windows. The absolute power computed for all the frequency bands of interest (theta (4–8 Hz), alpha (8–13 Hz), beta (13–30 Hz)) is used to extract features such as relative power, relative power ratio, absolute power, and amplitude asymmetry. It is calculated as average power of a signal in a specific frequency range, using both Welch and the Multitaper spectral estimation methods.

To compute Power Spectral Density (PSD) Welch's periodogram, averaging consecutive Fourier transform of small windows of the signal, with overlapping is applied. The Welch's method improves the accuracy of the classic periodogram. The spectral content of the EEG changes over time, constantly modified by the neuronal activity at play under the scalp. To return a true spectral estimate, a classic periodogram requires the spectral content of the signal to be stationary (i.e. time-unvarying) over the time period considered. This does not happen in EEG, the periodogram is generally biased and contains too much variance. By averaging the periodograms obtained over short segments of the windows, the Welch's method allows to drastically reduce this variance (VALLAT, 2018). This comes at the cost, however, of a lower frequency resolution. Indeed, the frequency resolution is defined by:

$$F_{resolution} = \frac{F_S}{N} = \frac{F_S}{F_S t} = \frac{1}{t} \quad (2)$$

where *Fs* is the sampling frequency of the signal, *N* the total number of samples and *t* the duration, in seconds, of the signal. For example, to use the full hypothetical length of data (30 seconds), the final frequency resolution is 1/30=0.033 Hz, which is 30 frequency bins per Hertz. By using a 4-second sliding window in the code, the frequency resolution is reduced to 4 frequency bins per Hertz, i.e. each step represents 0.25 Hz (VALLAT, 2018).

For the calculations done in this work, the compound Simpson's rule was used – Midband power, computing Absolute power: the area is decomposed into several parabolas and then summed the area of these parabolas. This can also be done using a trapeze (trapezoidal rule) or a rectangle (as in Matlab's bandpower function), but the parabola usually gives better estimates.

Comparing the Multitaper Method and Welch's Method, the results are very similar with signals with a good signal-to-noise ratio, the case of this study. If the signal is too noisy, Multitaper always provides a more robust spectral analysis than the Welch method. As the presented signal is pre-processed in several steps, the results are quite alike between the two methods. The signal has an excellent signal to noise ratio. One advantage of the Multitaper method compared to the Welch method is that it is not necessary to specify a window duration as it will basically calculate the periodogram across the entire signal. See Fig. 4.3.2.1, as example of absolute power for theta band and two methods comparison, graphics help with (VALLAT, 2018) code. Welch's method Absolute Power (AP) is 6.156 uV² and Multitaper's method Absolute Power (AP) is 5.203 in this example.

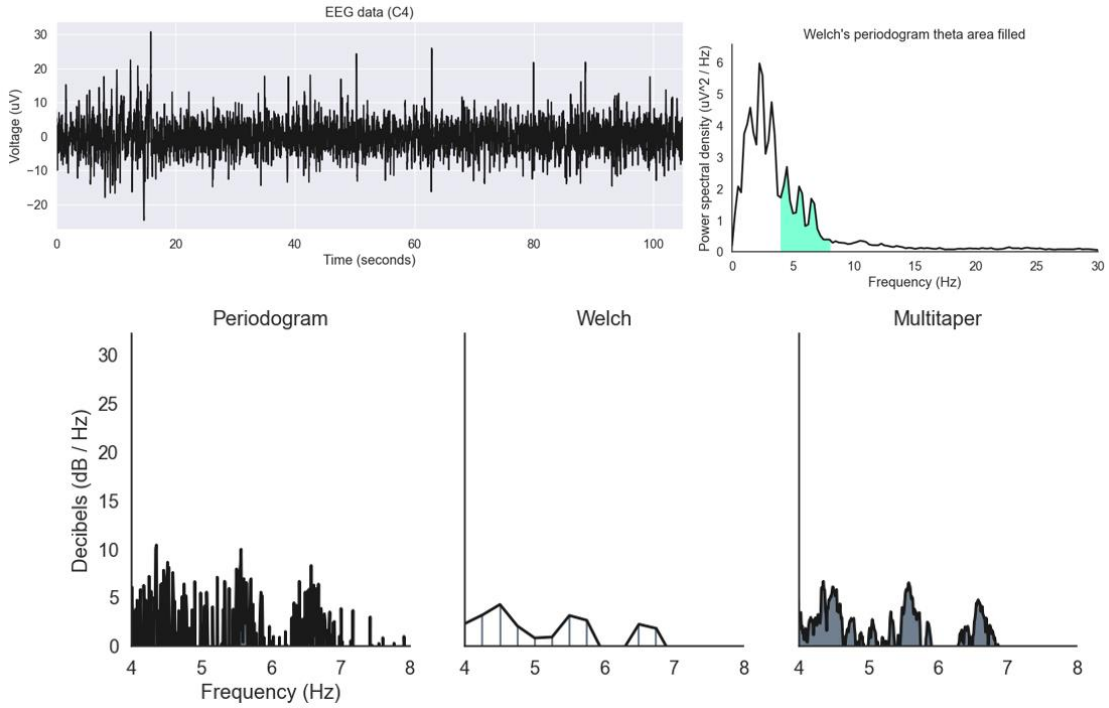

Fig. 4.3.2.1 Welch and Multitaper Methods comparison

The relative power (RP) is derived from the absolute power of the frequency bands, i.e. as the power in a specific frequency band divided by the total power as shown in Eq. (2). Relative power is computed for all five frequency bands across 8 electrodes, 6 electrodes removing bad channels, giving rise to a total of 18 features (three frequency

bands × 6 electrodes). These features are computed for the selected subject and at every level of the experiment.

$$RP = \frac{Power\ in\ Band}{Total\ Power} \quad (3)$$

The relative power ratio indicates the dominance of a frequency band over another. In this study, four ratios between the powers of three frequency bands, i.e. theta/alpha (immersion index), beta/theta, theta/beta, and (SMR + Mid-β)/T – concentration index – , being SMR (12-14.99 Hz), Mid-β (15-19.99 Hz), from (LIM; YEO; YOON, 2019) work, are calculated across every electrode. The ratios are restricted to the three most studied frequency bands. In this manner, a total of 24 ratios (four relative power ratios × 6 electrodes) for a patient at all phases/states of the experiment – *REST, SelAT* and *SusAT.*

The asymmetry is a connectivity measure that reflects the relative stimulation between two brain locations. The alpha asymmetry was addressed in this work, as FAA index – frontal alpha asymmetry –, it is a plugin from Michael's work (*https://zenodo.org/badge/latestdoi/64396201*). It is determined by considering the difference between the amplitude of the signals that are normalized to the sum of their amplitudes, as shown in Eq. (3), where *M* and *N* are the instantaneous amplitudes of the given signals.

$$Asymmetry = \frac{M-N}{M+N} \quad (4)$$

Frontal alpha asymmetry (FAA) refers to a difference in brain activity between the right and the left prefrontal cortices of the brain, and can be measured with a difference score between corresponding right and left electrode sites on an EEG device (KROGMEIER; COVENTRY; MOUSAS, 2022). FAA reflects the difference between the log alpha power density in the corresponding regions of the two hemispheres. Thus, the higher the FAA scores, the lower the amount of alpha activity and the relatively higher activity in the left hemispheres for a particular region. Although studied much less frequently in older adults, relatively greater left frontal activity in this age group has been linked to facets of well-being including life satisfaction, autonomy and engagement (ALLEN *et al.*, 2004). While, reduced FAA relates to current and remitted depression in adults, and is seen in offspring of mothers with depression as young as three months, suggesting a potentially transmittable mechanism of depression risk (HILL *et al.*, 2020).

4.3.3 STATISTICAL ANALYSIS

All ANOVAs tests were carried out in STATISTICA®, v. 7 (STATSOFT., 2004), after normality test confirmation. For post-hoc pairwise comparisons (t-tests, two-tailed) of the ANOVA all p-values were Bonferroni-Holm corrected for multiple comparisons. Tukey's test was taken too. Level of significance was set at α= .05 for all analyses and partial eta-square (η_p^2) is reported as a measure of effect size for the ANOVAs.

Chapter 5

RESULTS

5.1 FRP

The attention maps describing the number of fixation points – numbered in the image – and, consequently, heat map areas are shown in Figs. 5.1. All 1600 X 900 pixels screen is the area of interest (AOI) in this study.

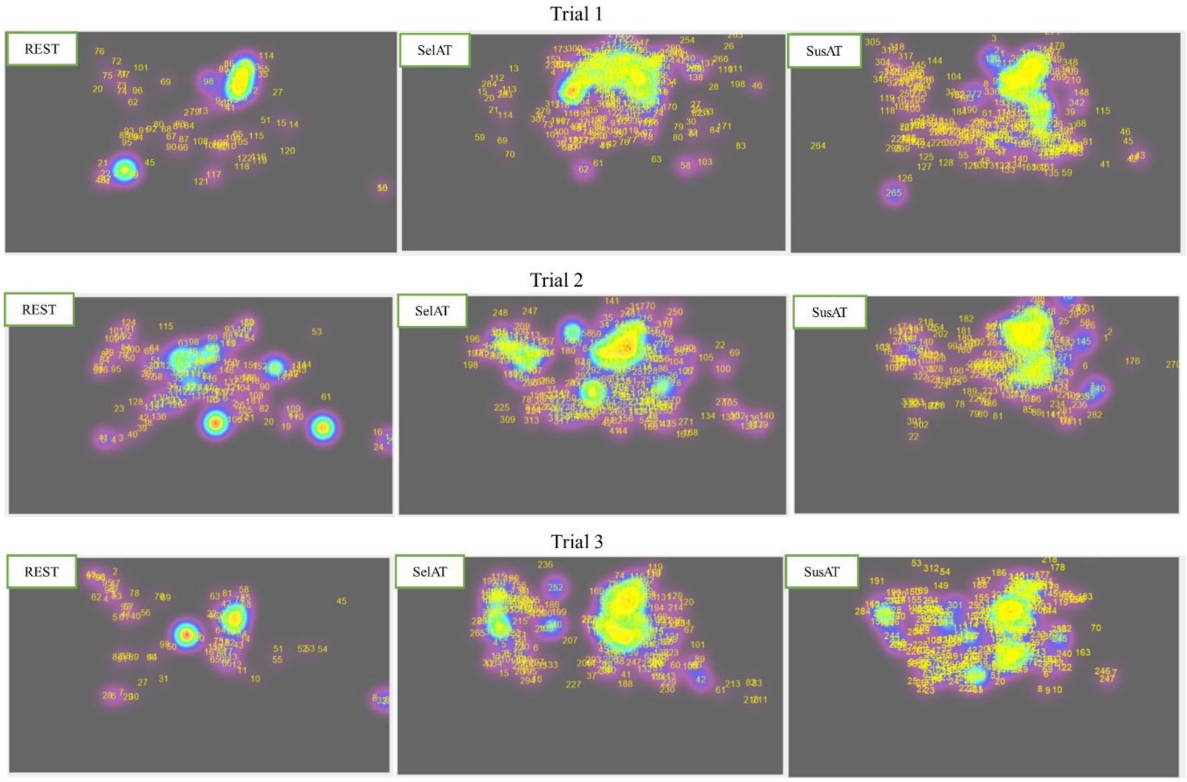

Fig. 5.1 Attention Maps of all states and trials

Fixation onsets served as contextual reference points when analyzing the EEG signal. Fixation-related potentials can be observed during any manipulation where eye movements occur. *OGAMA* measurements related to all these variables, indicating ET data, seen in Table 5.1:

- Trial (ID): trial number of the experiment, divided by state – *REST, SelAT, SusAT*;

- Duration (s): duration of the trial, it may vary in case of data loss;
- Gaze fixations (n): number of gaze fixations identified by *OGAMA*;
- Gaze fixations frequency (n/s): number of fixations per second in the trial;
- Fixations duration mean (ms): average time of fixations duration;
- Average Saccade Length (px): average path length, in pixels, between two fixation points;
- Average Saccade Velocity (px/s): average path length over time, in pixels per second, between two fixation points;
- Fixation/Saccade ratio: number of fixation vs saccade.

Table 5.1 – Eyetracking data from all trials

Trial ID	Duration (s)	Gaze Fixations (n)	Gaze Fixations freq. (n/s)	Fixations duration mean (ms)	Average Saccade Length (px)	Average Saccade Velocity (px/s)	Fixation/ Saccade ratio
REST – trial number							
1	65.549	122	1.861	438.279	175.116	2.109	815.726
2	65.980	153	2.319	320.333	185.227	2.041	742.816
3	41.605	99	2.379	309.737	215.810	2.012	737.027
Mean	**57.711 (±13.95)**	**125 (±27.09)**	**2.186 (±0.28)**	**356.116 (±71.35)**	**192.051 (±21.18)**	**2.054 (±0.05)**	**765.190 (±43.86)**
SelAT – trial number							
1	119.377	328	2.745	283.674	132.886	2.591	779.422
2	118.967	320	2.670	243.606	193.367	2.232	655.257
3	119.942	313	2.609	274.236	191.716	2.288	715.646
Mean	**119.429 (±0.49)**	**320 (±8)**	**2.675 (±0.07)**	**267.172 (±20.95)**	**172.656 (±34.45)**	**2.370 (±0.19)**	**716.775 (±62.09)**
SusAT – trial number							
1	120.952	352	2.910	262.721	151.955	2.323	764.584
2	120.933	334	2.762	265.629	160.180	2.089	733.629
3	119.956	312	2.600	273.589	177.598	2.139	711.594
Mean	**120.614 (±0.57)**	**333 (±20)**	**2.757 (±0.15)**	**267.313 (±5.62)**	**163.244 (±13.09)**	**2.184 (±0.12)**	**736.602 (±26.62)**

The hypotheses are as follows for the one-way ANOVA. All variables were tested among themselves.

H0: There is no difference between the variables for the states (*REST* and *SelAT/SusAT*).

H1: There is an increase in the analyzed variable in the states of attention when compared to the state of *REST*.

The obtained values reject the null hypothesis, accepting, only for the number of gaze fixations and gaze fixations frequency variables, the alternative hypothesis (there is a difference between the means). The alpha value chosen a priori informs that the

probability obtained in the comparison between the means by Tukey's test must be equal to or less than 0.01, so that the difference is statistically significant. The number of fixations and the gaze fixations frequency is smaller among the states of *REST* and both attention (selective and sustained), when comparing the states of attention between themselves, no significant difference occurs.

The two-factorial repeated-measures ANOVAs that were conducted on the gaze fixations (n) data, Fig. 5.2, revealed for the *REST* state a main effect of gaze fixations (n), F = 173.87, p = .0008. No main effect of the trial was observed, F = 3.073, p =.1558. Post-hoc pairwise comparisons of the main effect of states indicated a minor gaze fixations number for the *REST* as compared to both, the *SelAT* (p = .022), and the *SusAT* (p = .030) states.

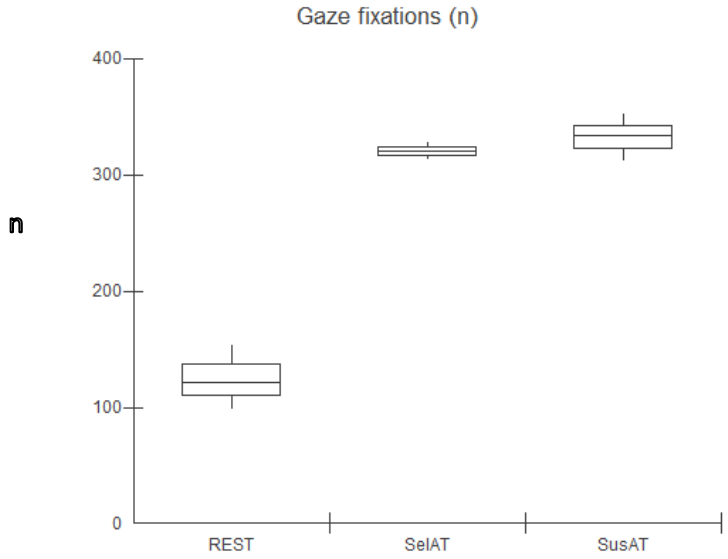

Fig. 5.2 Gaze fixations box plots for states

The two-factorial repeated-measures ANOVAs that were conducted on the gaze fixations frequency (n/s) data, Fig. 5.3, revealed that the F-test is significant between states (F = 7.32, p = 0.047), which did not occur with the trials (F = 0.05, p = 0.9507). The comparison between the means of the states shows significant differences between states *REST vs. SelAT and REST vs. SusAT*, which was not observed between states *SelAT vs. SusAT*. It can be concluded, therefore, that state *REST* referring to the 3 trials presented a smaller number of gaze fixation/s, consequently rejecting the null hypothesis between the states in pairs but accepting it regarding the trials.

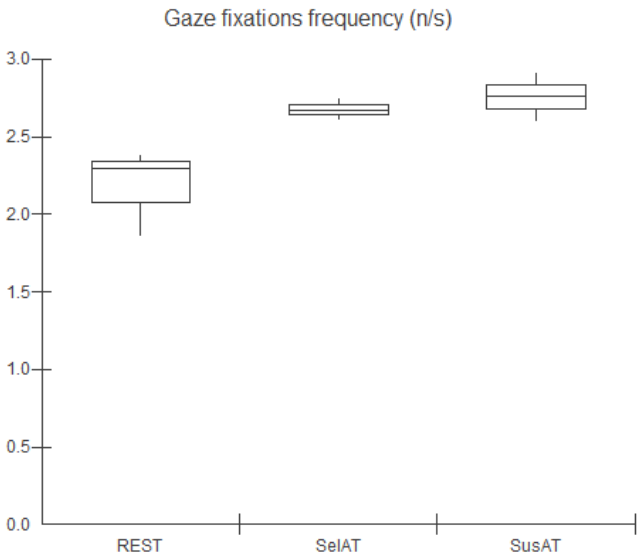

Fig. 5.3 Gaze fixation frequency box plots for states

The two-factorial repeated-measures ANOVAs that were conducted on the average saccade length (px) data, Fig. 5.4, revealed that the F-test is significant across trials ($F = 13.288$, $p = 0.018$), and across states ($F = 7.628$, $p = 0.044$). The comparison between the means of the states shows significant differences between states *REST vs. SelAT and REST vs. SusAT*, which was not observed between states *SelAT vs. SusAT*, as expected. The comparison between the means of the trials shows significant differences between trials 1 vs. 2 and 2 vs. 3, which was not observed between trials 1 vs. 3. The average saccade length decreases as states go on. It can therefore be concluded that the *REST* referring to the 3 trials presented a higher average saccade length, consequently rejecting the null hypothesis among the states and among the trials.

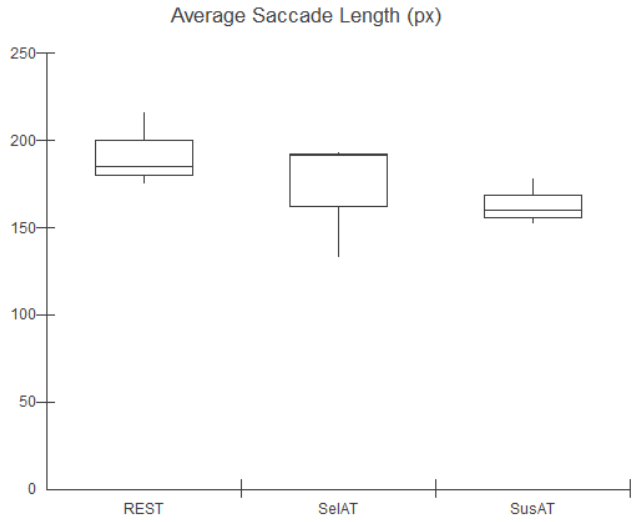

Fig. 5.4 Average saccade length box plots for states

The two-factorial repeated-measures ANOVAs that was conducted on the fixation/saccade ratio data, Fig. 5.5, revealed that the F-test is significant between states (F = 7.1545, p = 0.049), which did not occur with the trials (F = 2.5077, p = 0.1970). The comparison between the means of the states shows significant differences between the states *REST vs. SelAT and REST vs. SusAT*, which was not observed between states *SelAT vs. SusAT*, as expected. It can therefore be concluded that the *REST* state referring to the 3 trials presented a higher value, thus rejecting the null hypothesis among the states, but accepting to trials.

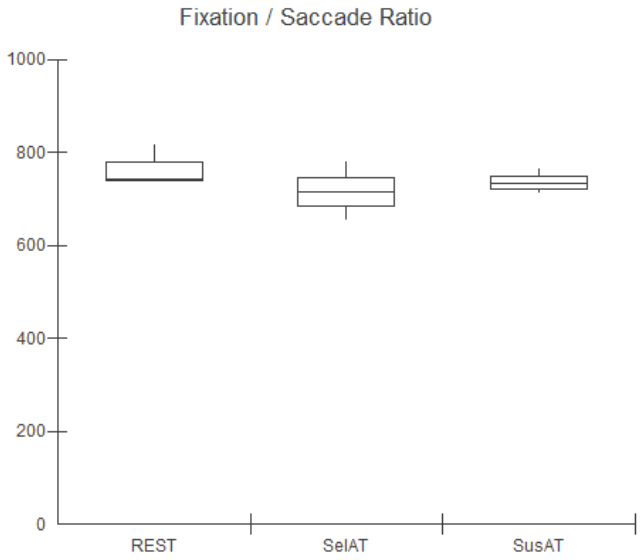

Fig. 5.5 Fixation/Saccade box plots for states

5.2 PSD AND INDEXES

Figures 5.6 and 5.7 show the Fourier transformation result for the mean absolute power of the Theta, Alpha, and Beta bands of the patient for each channel for the 3 trials, as descriptive analysis. It shows the values for the *REST*, *SelAT,* and *SusAT* states of each band. Figure 5.8 shows the relative powers of the Theta, Alpha, and Beta bands for the *REST*, *SelAT,* and *SusAT* states. Figure 5.9 shows the Concentration, T/A, and B/T ratios of the absolute powers for the *REST*, *SelAT,* and *SusAT* states. There are *REST*, *SelAT,* and *SusAT* states for each band, and the mean absolute power, mean relative power and mean ratios of the 3 trials in each channel are compared between the *SelAT* and *SusAT* states and the *REST* state. Channels 1-6 are, respectively, Fp1, Fp2, F3, Fz, C3 and C4. Pz and F4 were excluded due to artifacts and bad SNR ratio for many trials.

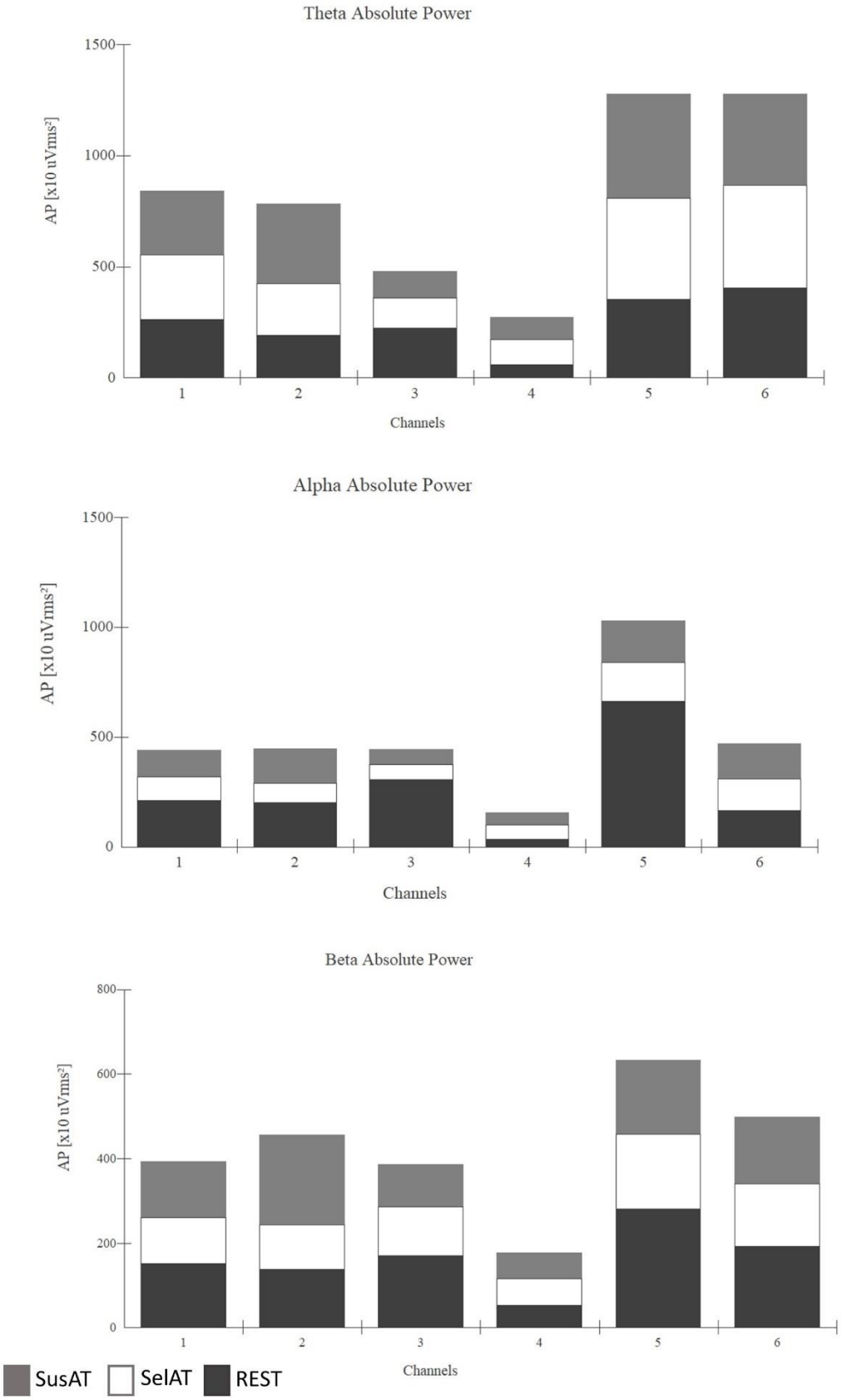

Fig. 5.6 Absolute mean power for 3 trials, at each band, for each channel

Fig.5.6 shows the Absolute Power for each EEG Frequency band. Alpha band demonstrates the narrowest variation, showing the lower amplitudes. The Alpha band decreases in the attention states compared to the rest state; however, the decrease in the SelAT state is a bit more pronounced. An increase of Theta in the frontal region can be seen for *SelAT* and *SusAT,* situations of mental load change, as described in (YIN; ZHANG, 2014)

The ANOVA one-way t-test was conducted for p=0.05 to test the difference among channels regarding only Absolute Power measures. All channels are statistically different among them, except 3 vs 4 and 5 vs 6, for Theta Absolute Power. For Alpha power, ANOVA did not work due to outliers. For Beta power, channels 1 vs 2, 1 vs 3, 2 vs 3 and 5 vs 6 did not present significant statistical difference.

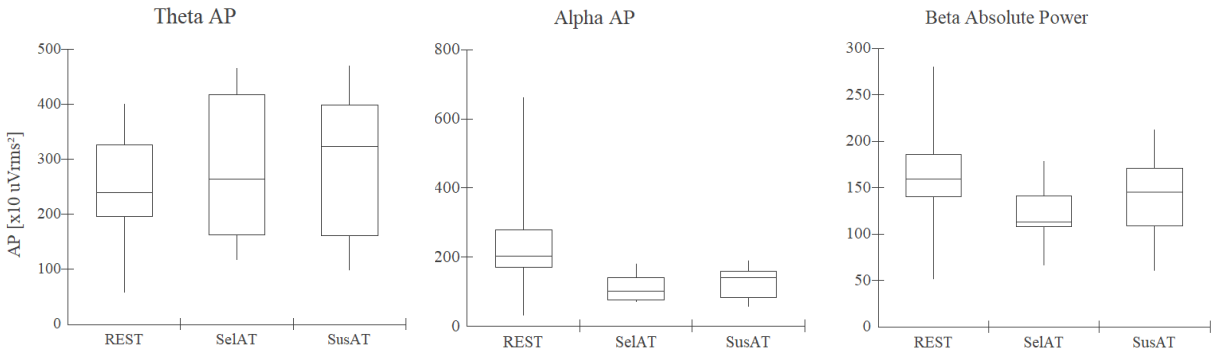

Fig. 5.7 Absolute mean power for 3 trials. Box plot variation for 6 channels

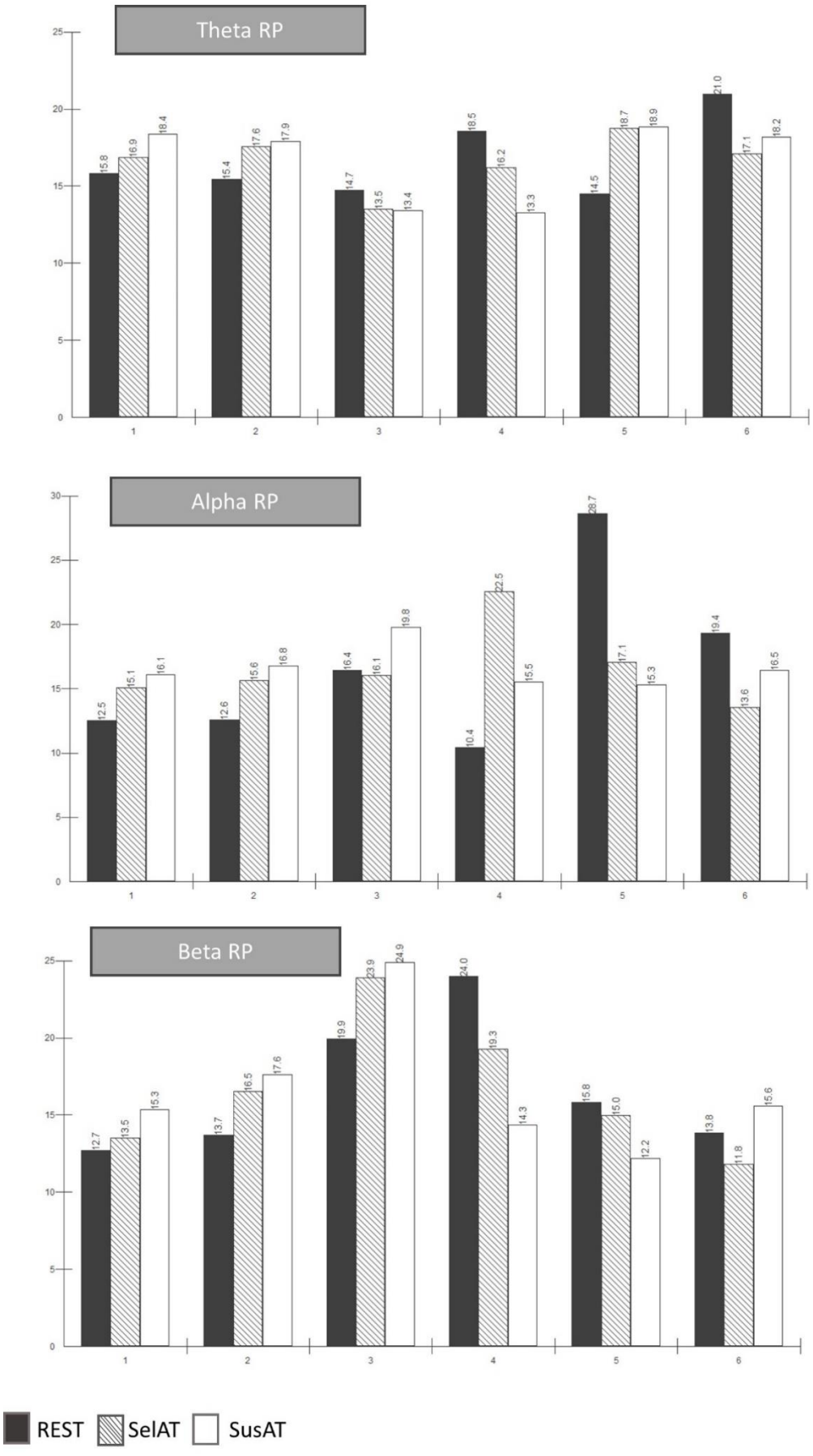

Fig. 5.8 Relative power (RP) for each band and each channel

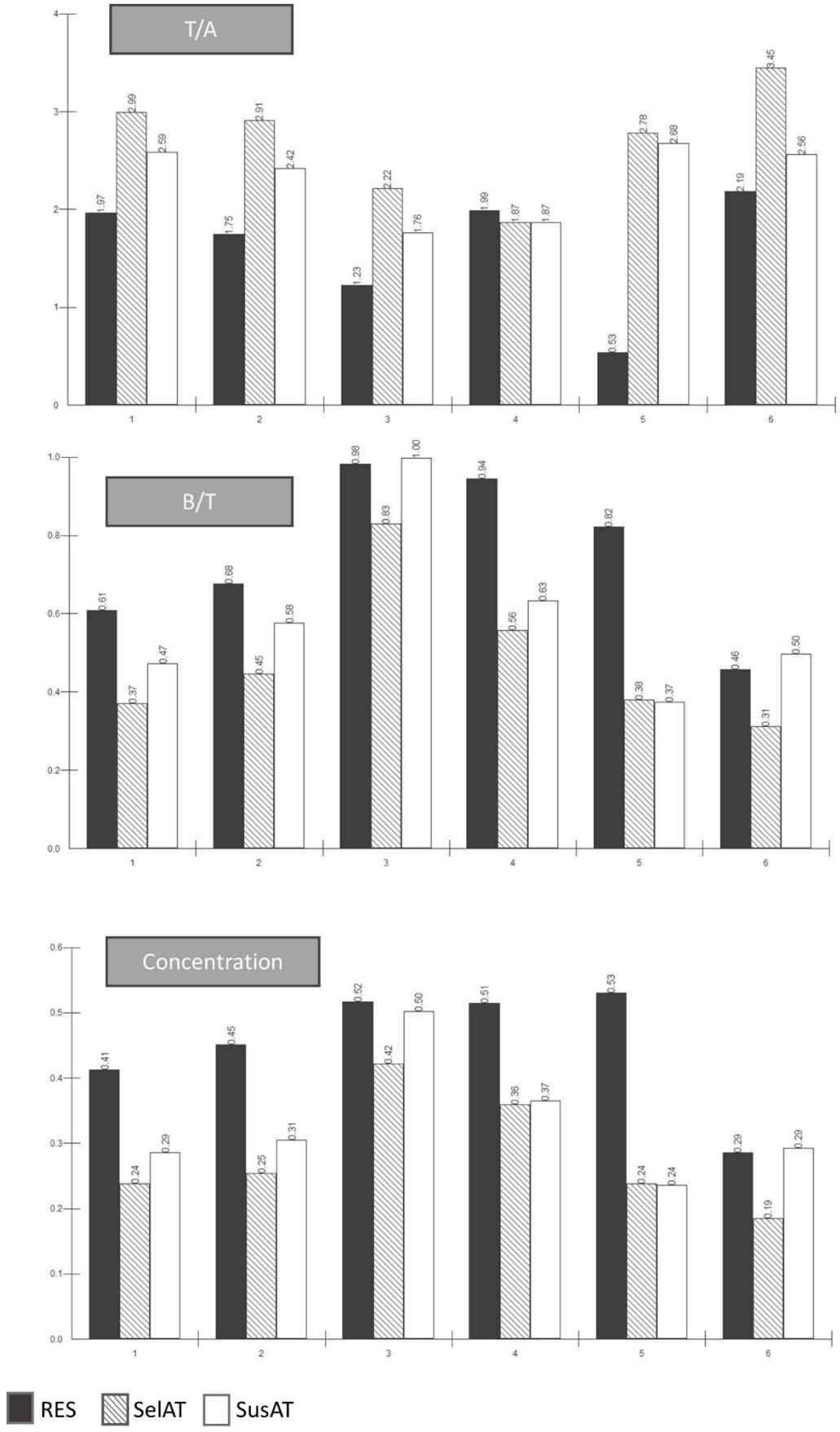

Fig. 5.9 T/A, B/T and Concentration indexes for each channel

One-way repeated measures ANOVA Repeated Measures ANOVA (RMA) is the extension of the paired t-test, used in the following analysis. RMA is also referred to as within-subjects ANOVA or ANOVA for paired-samples. Repeated measures design is a research design that involves multiple measures of the same variable taken on the same subject either under different conditions or more than two time periods. In paired samples t-test, compared the means between two dependent groups, whereas in RMA, compared the means between three dependent groups, the occurrence in this study.

The hypotheses are as follows:

H0: there is no difference between the analyzed index for the states (REST and SelAT/SusAT).

H1: there is a decrease in the analyzed index in the states of attention, when compared to the state of REST.

F(states) = 32.794 is highly significant (p = 0.0017), for 5 degrees of freedom in *SelAT*, just as F(states) = 7.396 is highly significant (p = 0.0246), 5 degrees of freedom in *SusAT*, rejecting the null hypothesis and accepting the alternative. The calculated **concentration index** is lower in attention states (*SelAT* and *SusAT*) compared to *REST*, Fig. 5.10. It is an inconsistent result, as seen in (GA; CHOI; YOON, 2015), mainly in frontal area.

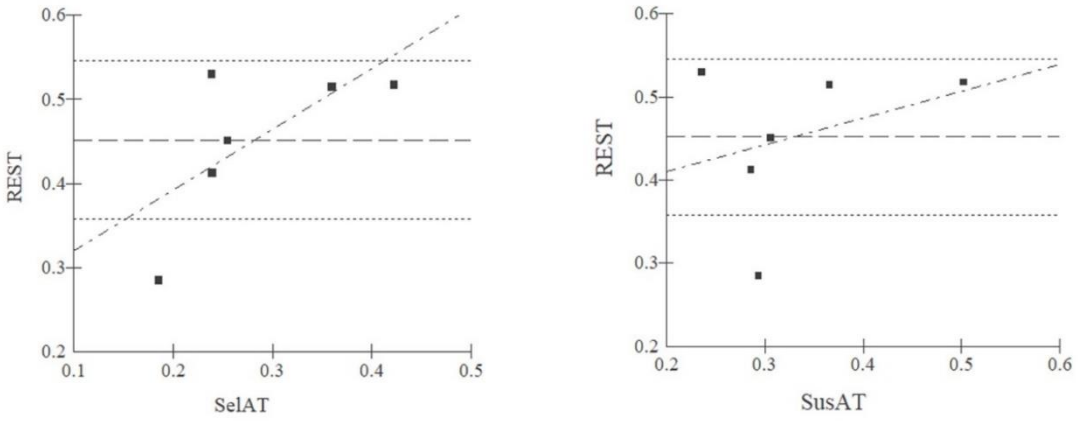

Fig. 5.10 Concentration index scatter plot for each state

F(states) = 28.394 is highly significant (p = 0.0021), for 5 degrees of freedom in *SelAT*, rejecting the null hypothesis and accepting the alternative. On the other hand, F(states) = 4.114 is not significant (p = 0.0741), for 5 degrees of freedom in *SusAT*, accepting the null hypothesis and rejecting the alternative. The calculated **B/T index** is

smaller in the *SelAT* attention state only, compared to *REST,* Fig. 5.11. As indicative of inhibitory processes, it is interesting to be smaller at attentional states (PICKEN *et al.*, 2020). This index is used as concentration index in (LIM; YEO; YOON, 2019), being smaller in *REST* states, contrary to this study.

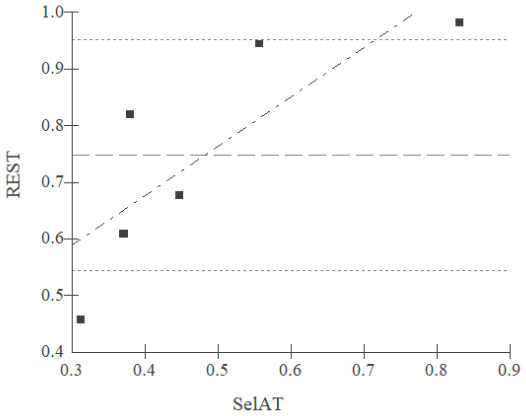

Fig. 5.11 B/T index scatter plot for significant states

F(states) = 12.5945 is highly significant (p = 0.0088), in SelAT, rejecting the null hypothesis and accepting the alternative. F(states) = 5.1067 is significant (p = 0.0367), in *SusAT*, rejecting the null hypothesis and accepting the alternative. The calculated **T/A index** is higher both in the *SelAT* and *SusAT* attention states, compared to *REST,* Fig. 5.12.

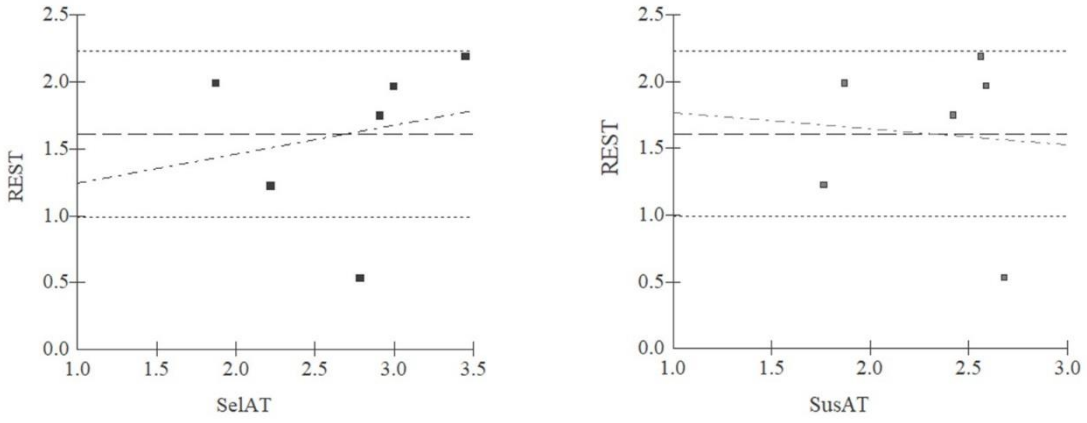

Fig. 5.12 T/A index scatter plot for significant states

T/A as immersion index, shows the significant increase in α and θ, as well as the significant decrease in β are indicative of fatigue (JAGANNATH; BALASUBRAMANIAN, 2014), or, in the case of this study, more attention allocation in states *SelAT* and *SusAT.* As a good indicative of immersion, it increases in attention states,

such as in (LIM; YEO; YOON, 2019) work. Change occurs in states SelAT and SusAT compared to the REST state in a general overview of indexes.

FAA index indicates that greater left relative to right prefrontal cortical activity is associated with increased approach motivation, defined as an organism's tendency to approach or expend energy in order to go toward stimuli rather than away (HARMON-JONES; GABLE, 2018). FAA was calculated within the state interval. No significant statistical differences were found in our data, comparing all Fp1-Fp2 FAA values in all states and trials, see Table 5.2. A state Eyes Closed (EC) was measured too, to understand the "Berger effect" - when observers open their eyes, the amplitude of EEG oscillations in the alpha band (8–13 Hz) decreases significantly – and compare with the open eyes' states.

Table 5.2: FAA index values calculated from trials and states

***n* IC components**	**Final channels**	**Channels FAA**	**FAA – 8-13Hz**
REST – T1			
5	***Fp1 Fp2 F3 Fz F4 C4***	Fp1 – Fp2	0.4192
		F3 – F4	2.1355
EC – T1			
5	***Fp1* Fp2 *F3 Fz F4 C4***	Fp1 – Fp2	1.1664
		F3 – F4	2.5342
SelAT – T1			
3	***Fp1 Fp2 F3 Fz C4***	Fp1 – Fp2	0.6934
		Fz – F3	1.5082
SusAT – T1			
2	***Fp1 Fp2 F3 Fz C4***	Fp1 – Fp2	0.3677
		Fz – F3	1.4187
REST – T2			
2	***Fp1 Fp2 Fz C4***	Fp1 – Fp2	0.4993
		Fz – Fp2	1.3580
EC – T2			
3	***Fp1 Fp2 F3 Fz C4***	Fp1 – Fp2	0.5731
		Fz – F3	1.5406
SelAT – T2			
3	***Fp1 Fp2 Fz C3 C4***	Fp1 – Fp2	0.7700
		Fz – Fp2/Fp1	0.9327/0.8097
		C3 – C4	1.5236
SusAT – T2			
4	***Fp1 Fp2 Fz C3 C4***	Fp1 – Fp2	1.8902
		Fz – Fp2/Fp1	1.7527/1.8042
		C3 – C4	1.3039
REST – T3			
4	***Fp1 Fp2 F3 F4 C3 C4***	Fp1 – Fp2	0.1547
		F3 – F4	1.2960
		C3 – C4	1.0965
EC – T3			
3	***Fp1 Fp2 F3 C3 C4***	Fp1 – Fp2	0.4143
		C3 – C4	1.4914

SelAT – T3			
3	***Fp1 Fp2 F3 C3 C4***	Fp1 – Fp2	0.5235
		C3 – C4	1.1662
SusAT – T3			
4	***Fp1 Fp2 F3 C3 C4***	Fp1 – Fp2	0.8513
		C3 – C4	0.7493

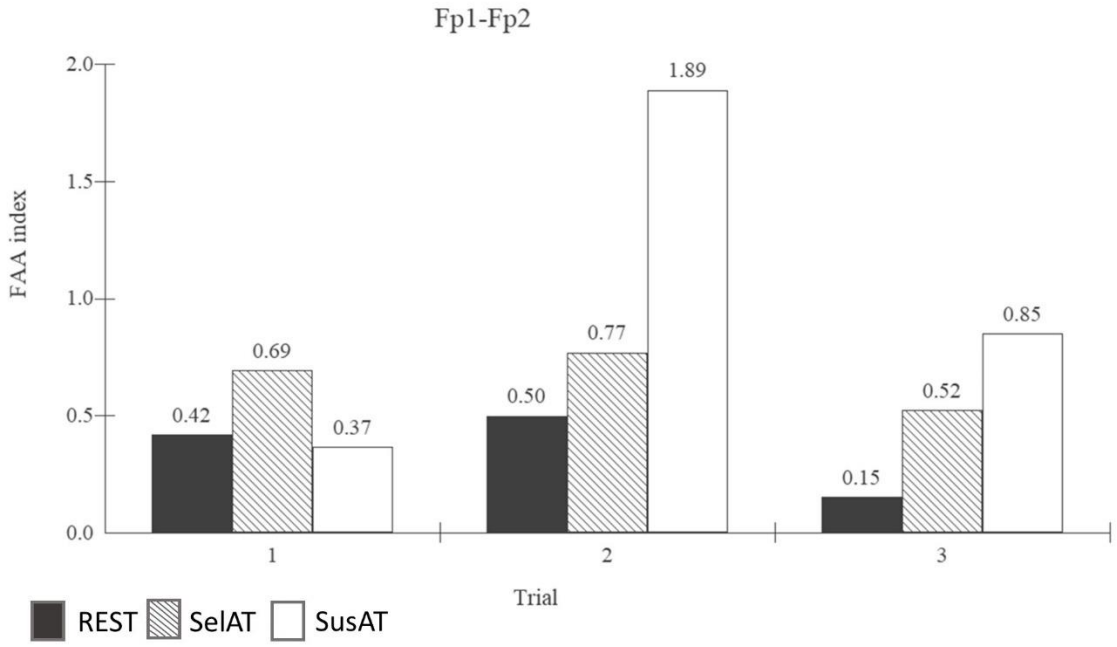

Fig. 5.13 FAA index all trials and states

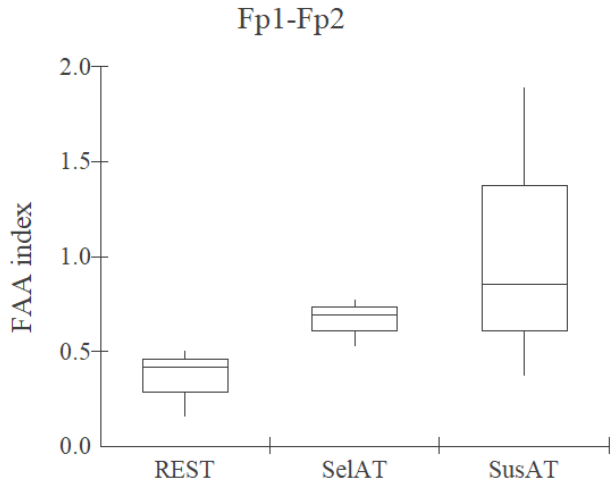

Fig. 5.14 FAA index box plots

Alpha power is inversely related to cortical activity (ALLEN *et al.*, 2004), a higher alpha power from the right electrode would indicate lower cortical activity from the right electrode. So, higher FAA indicates less alpha power activity, Fig. 5.13 and Fig. 5.14.

FAA index is in accordance with (KROGMEIER; COVENTRY; MOUSAS, 2022) work, the intra-subject observation resulted in FAA increase over more engaged/attention state situation. Although, no significant difference was found, and in the first trial *SusAT* did not show the higher FAA value, the last two trials showed FAA increase in situations that demand more attention allocation (*SelAT* and *SusAT*).

5.3 TOPOPLOTS

Fig. 5.15 shows averaged topography over time. Subtracted individual subject mean spectrum. There is no significant statistical difference among trials in each state, as detailed in Fig 5.16.

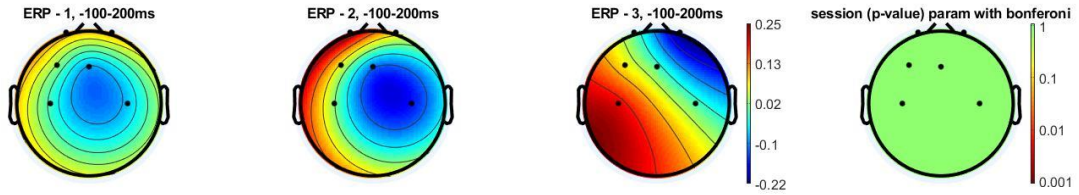

Fig. 5.15 Example of ERP comparison and Bonferroni correction among 3 trials for a state. All states compared among themselves through trials showed no significant differences

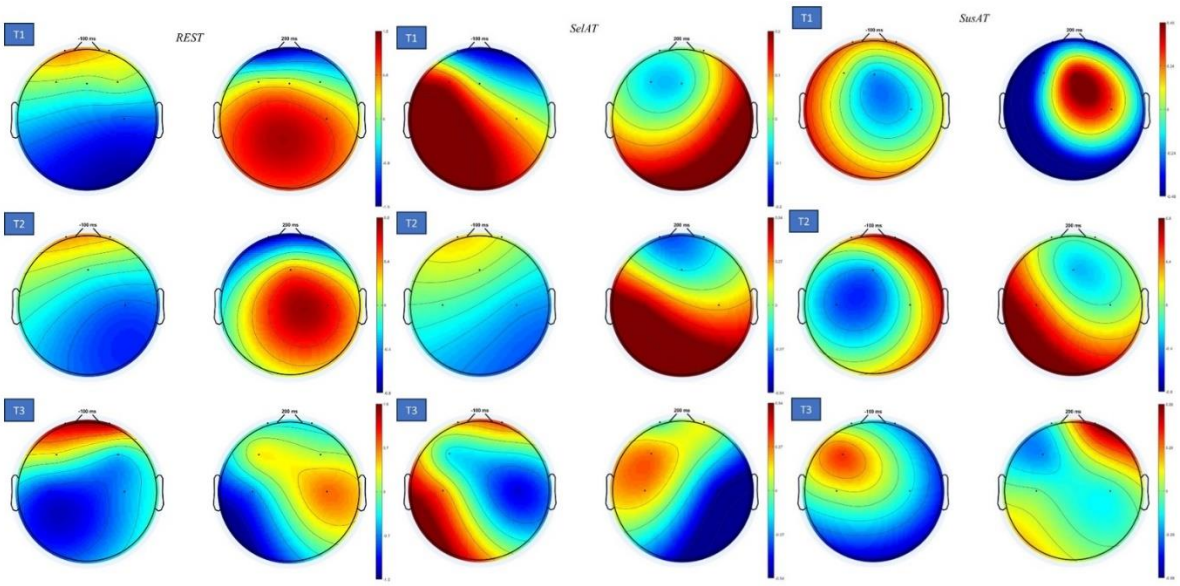

Fig. 5.16 Topoplots - All ERPs over time [-100 200]*ms*, in each state and trial. All spectrum [4 30]*Hz* is represented in this activation overview

5.3.1 *REST*

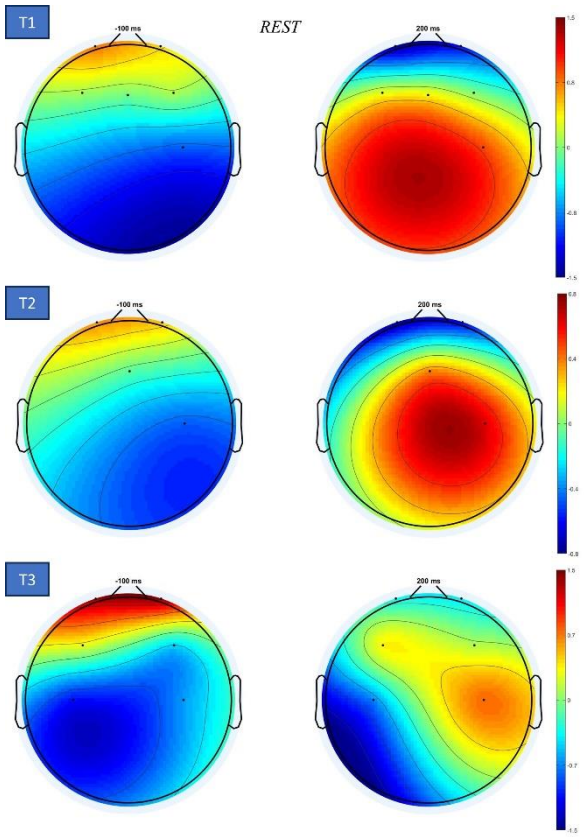

Fig. 5.17 Detailed REST state overtime for subtracted mean spectrum. The activation scale shows the average values for RMS μV potentials

At each ERP, shown in Fig. 5.17 over time, [-100 200]*ms* more activated areas are noticed at 200ms. It happens due to fixation event effects.

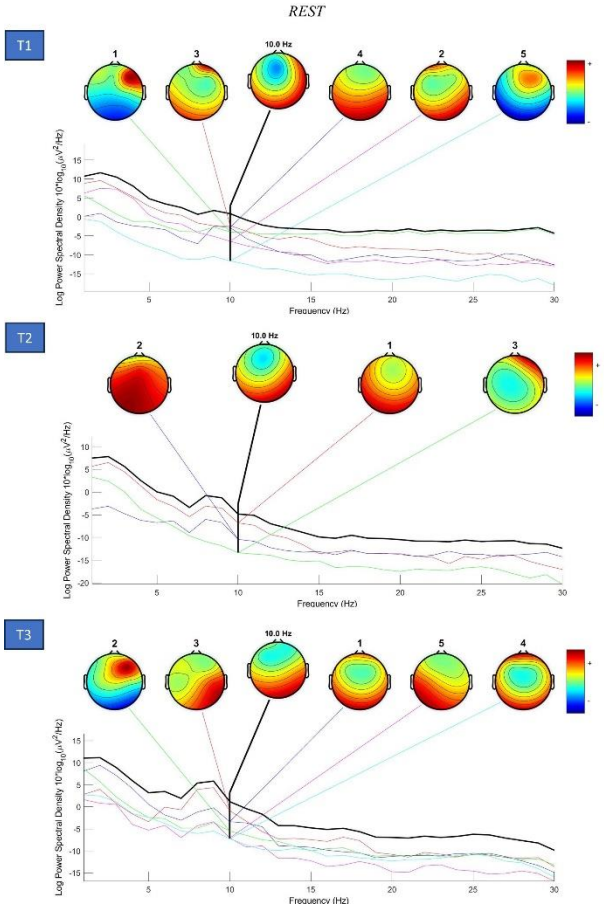

Fig. 5.18 Detailed REST IC components and main contributions over the spectrum. Each line is a channel

IC components were run with *pca* analysis, Fig. 5.18. All IC decomposition represented good visualization of the signal, seen to be originated from a single brain area, from a single equivalent dipole, where the scalp map is smoother. This guarantees good quality of input data, after also removing large erratic artifacts, removing bad channels, and filtering with high-pass slow drifts. Going through the *topoplots*, after bad IC components removed, seen in Fig. 5.18, it is possible to notice that IC components vary less between trials 1 and 3. The main activation is in the occipital area. Alpha activation is in the fronto-parietal and central areas. Fronto-parietal areas also show theta activation. 1 and 2 IC components in the trials refer mainly to saccade components, even after bad IC removal.

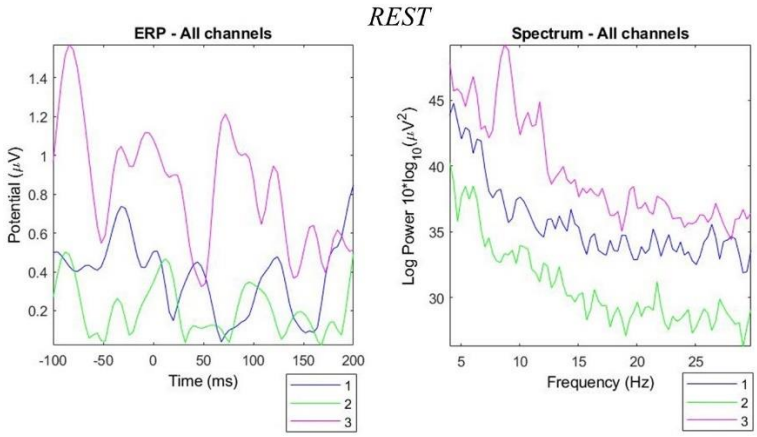

Fig. 5.19 *REST* - ERP and Spectrum average of all channels for trials 1, 2 and 3

Looking at averaged channels ERP, it is possible to notice that around 100 *ms*, P100 is shown, Fig. 5.19. Around 200ms a new rise is up to happen.

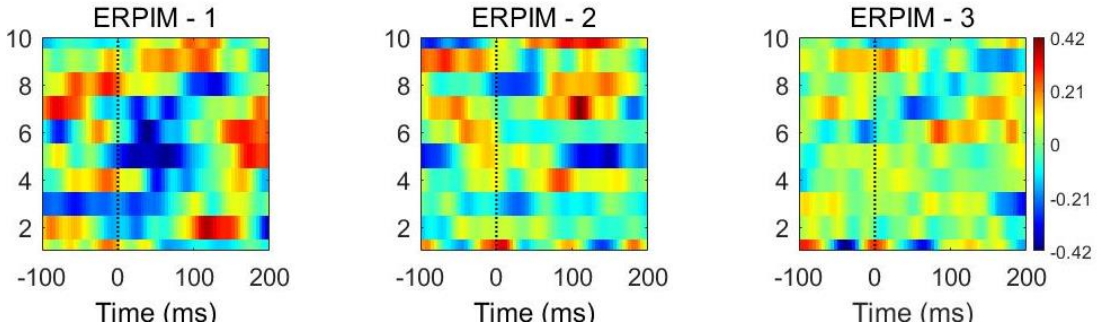

Fig. 5.20 image with each feature stacked on top of each other

ERP image shows immediately all the components and have an idea of activity of each component, Fig. 5.20.

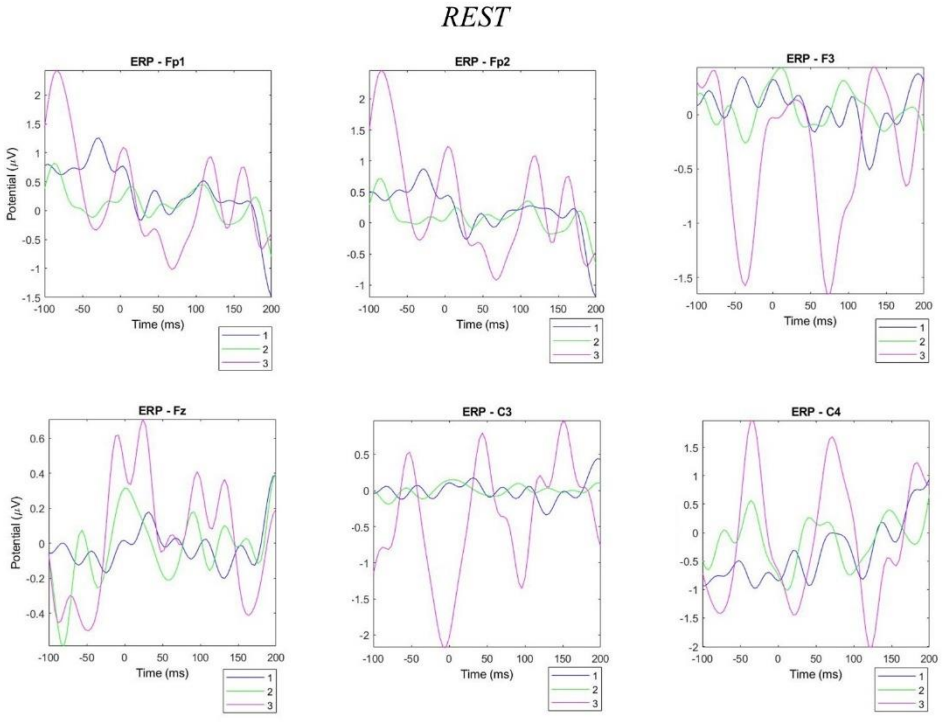

Fig. 5.21 ERP of individual channels, *REST* state and numbered trials

Pronounced negative peaks can be seen in F3 and C3 channels only in *REST* state, Fig. 5.21.

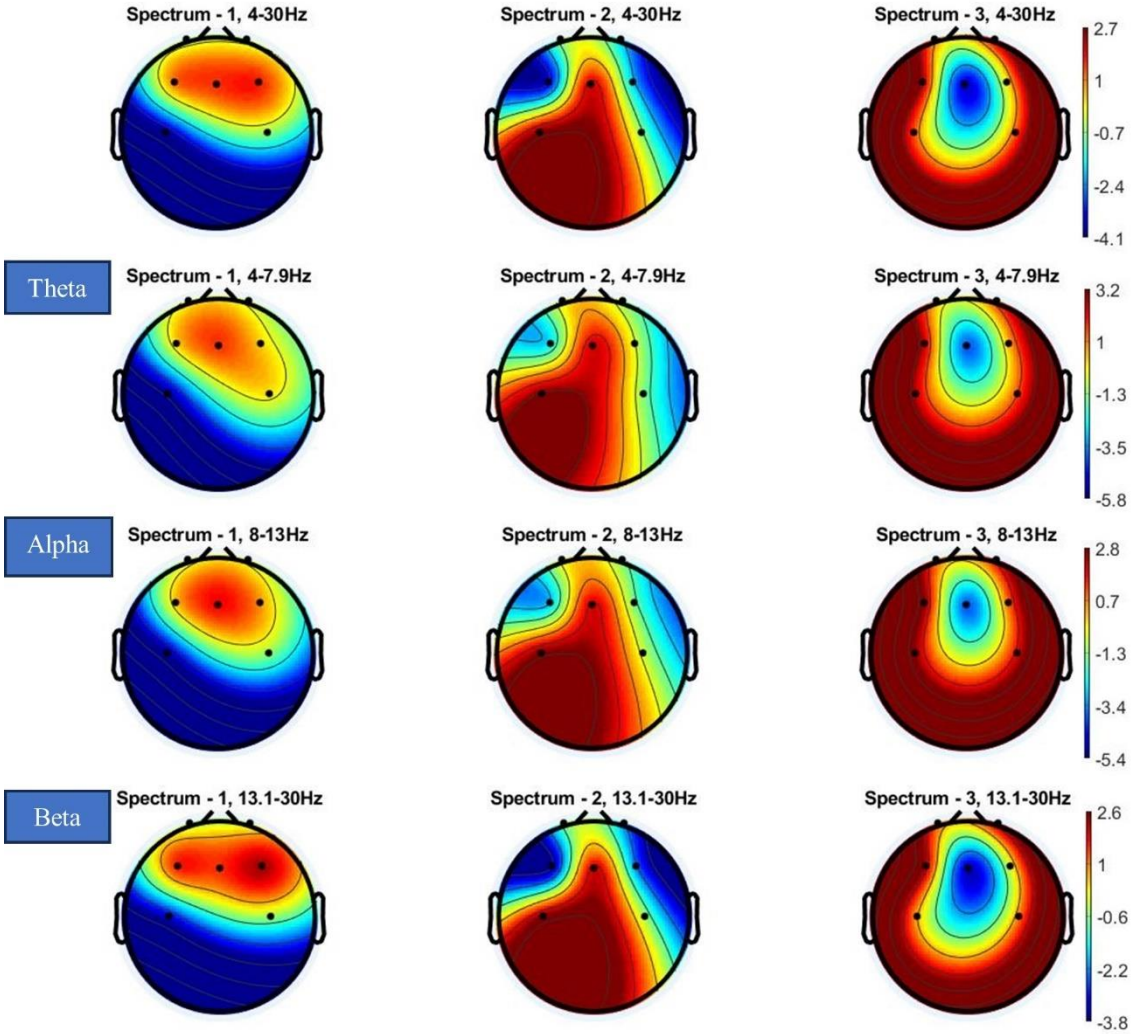

Fig. 5.22 *REST* - Spectrum average of all channels for trials 1, 2 and 3. Topoplots of each EEG band showing location of channels and related activation. No relevant difference can be seen over the spectrum, among trials for each EEG band. ERPs of each trial are similar among themselves

From Fig. 5.22, bilateral occipital alpha – mainly trial 1 –, frontal midline theta – mainly trial 3 – and occipital central theta – mainly trial 2, can be notice in each distinct trial. No similar occurrence happens in the trials.

5.3.2 *SELAT*

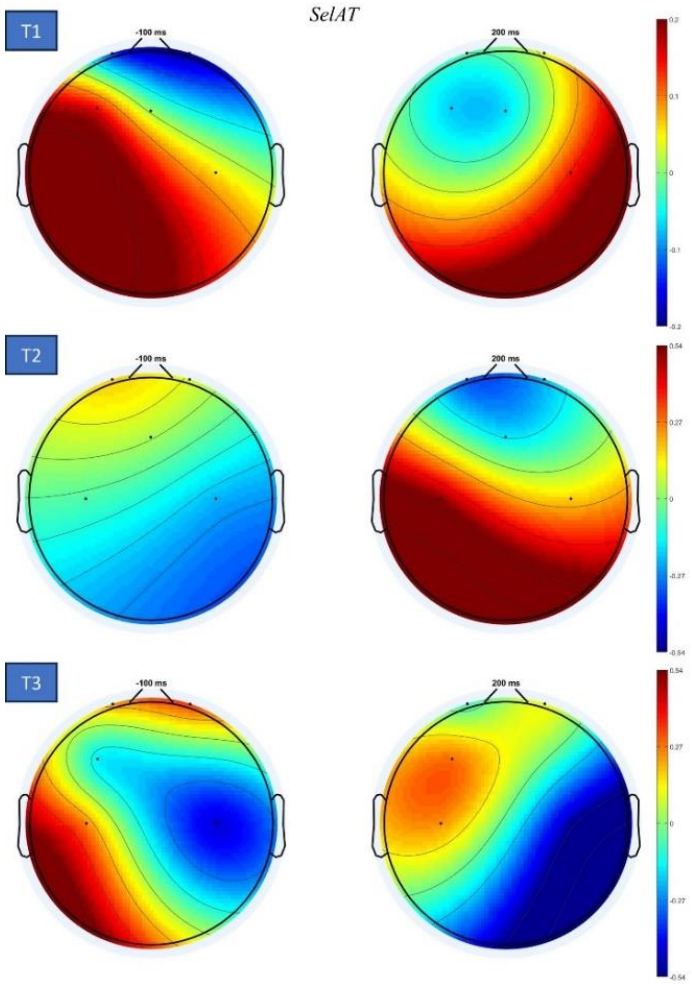

Fig 5.23. Detailed *SelAT* state overtime for subtracted mean spectrum. The activation scale shows the average values for RMS μV potentials

At each two points of epochs, shown in Fig. 5.23 over time, [-100 200]*ms* more activated areas are noticed at 200ms. It happens due to fixation event effects.

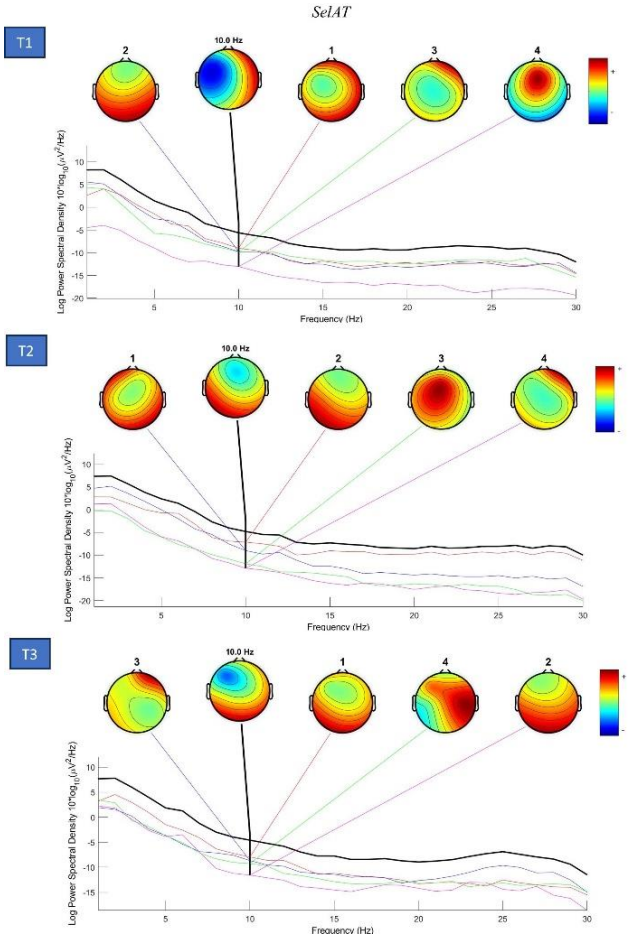

Fig. 5.24 Detailed SelAT IC components and main contributions over the spectrum. Each line is a channel

Going through the *topoplots*, after bad IC components removed, seen in Fig. 5.24, it is possible to notice that IC components vary less between trials 2 and 3. The main activation is in the occipital area. Alpha activation is in the fronto-parietal area. Fronto-parietal areas also show theta activation.

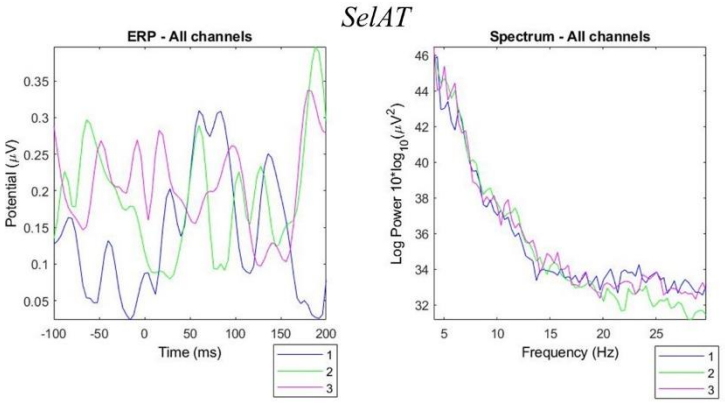

Fig. 5.25 *SelAT* - ERP and Spectrum average of all channels for trials 1, 2 and 3

Looking at averaged channels ERP, it is possible to notice that around 200 *ms*, a peak is pronounced, although very smaller than *REST* state, Fig. 5.25.

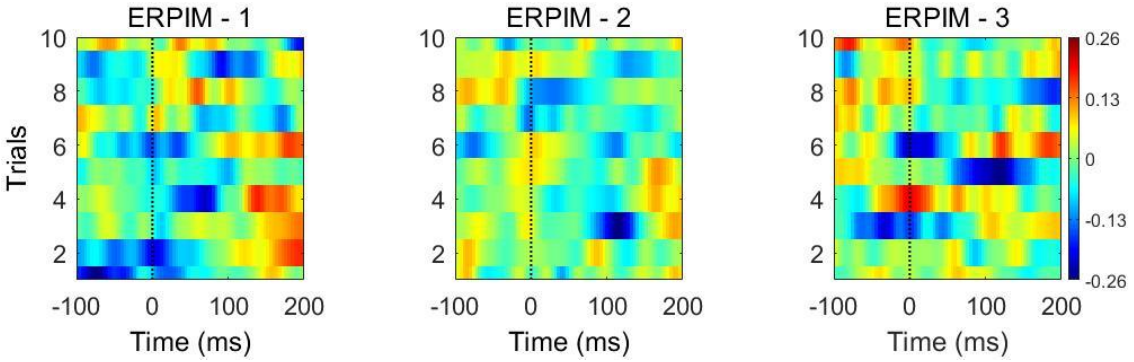

Fig. 5.26. *SelAT* - ERP image with each feature stacked on top of each other

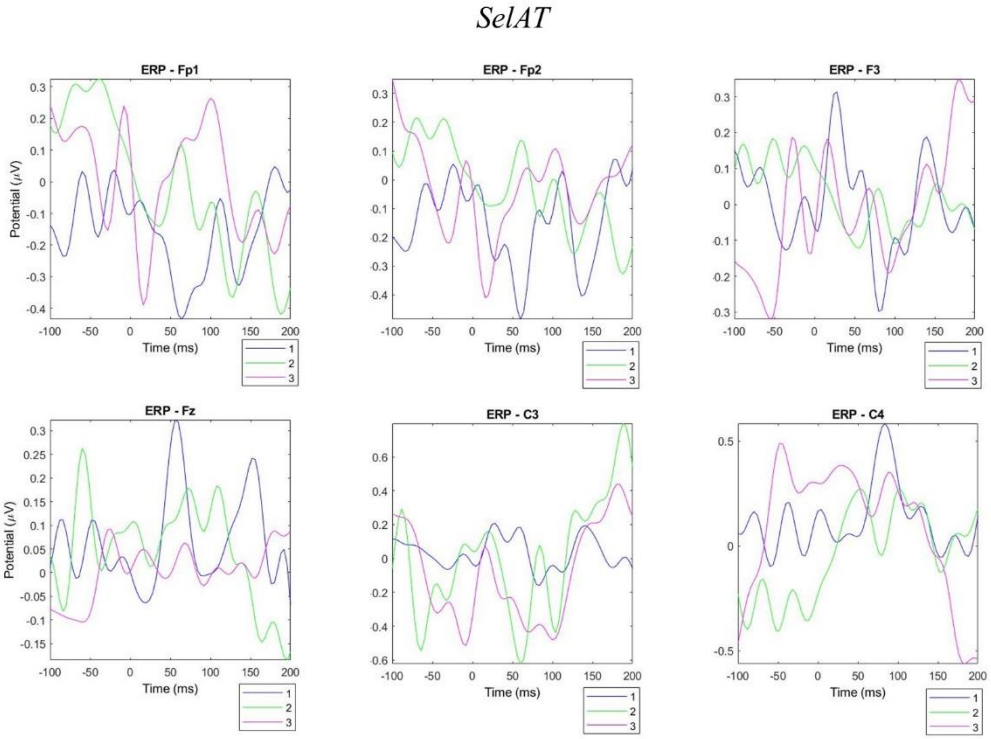

Fig. 5.27 of individual channels, *SelAT* state and numbered trials

No relevant peaks can be seen in any channels or any state, Fig. 5.27.

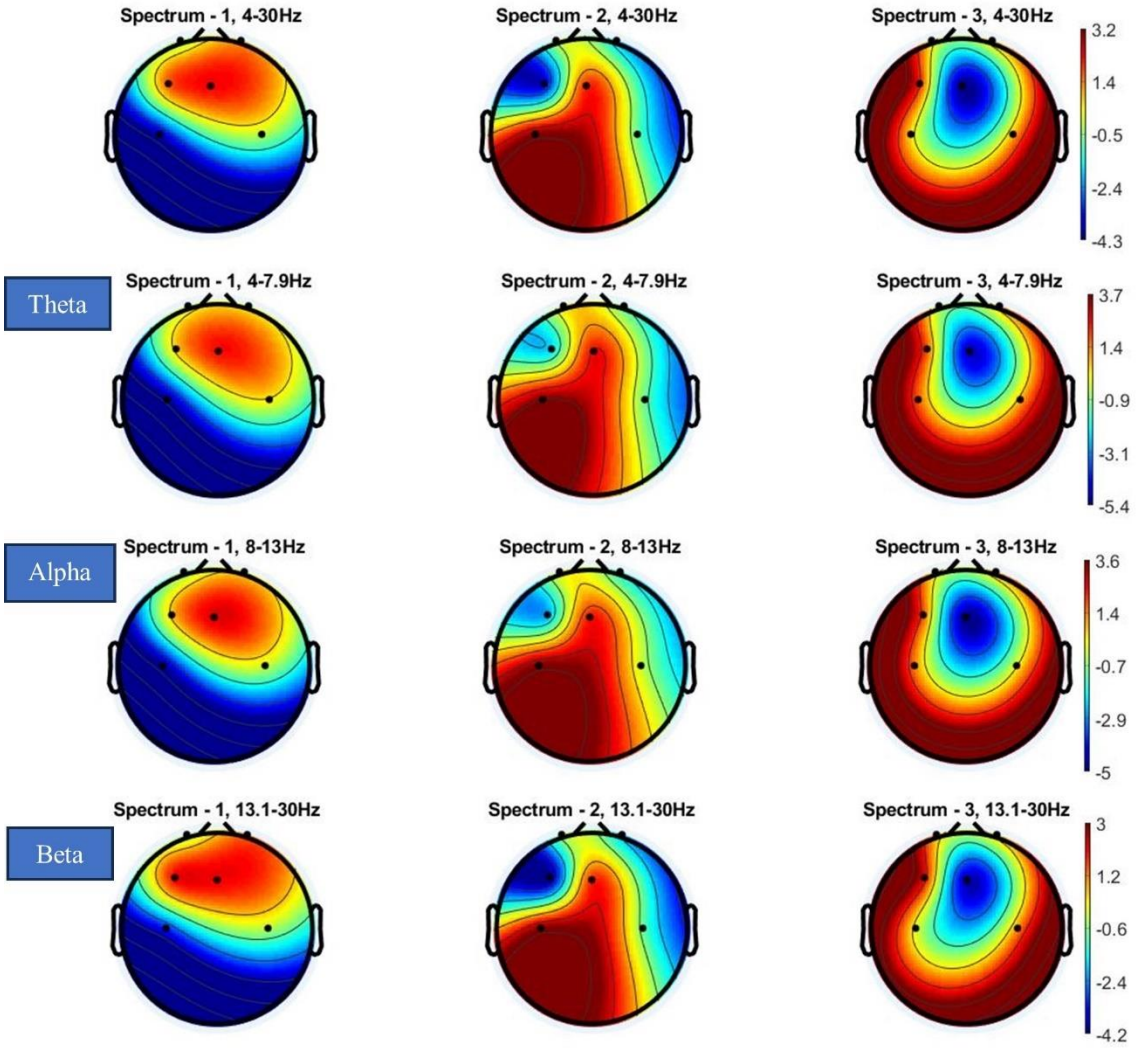

Fig. 5.28 *SelAT* - Spectrum average of all channels for trials 1, 2 and 3. Topoplots of each EEG band showing location of channels and related activation. No relevant difference can be seen over the spectrum, among trials for each EEG band. ERPs of each trial are similar among themselves

From Fig. 5.28, bilateral occipital alpha – mainly trial 1 –, frontal midline theta – mainly trial 3 – and occipital central theta – mainly trial 2, can be notice in each distinct trial. No similar occurrence happens in the trials. The brain activation areas are very similar between states *REST* and *SelAT*, also the amplitude of activation.

5.3.3 *SUSAT*

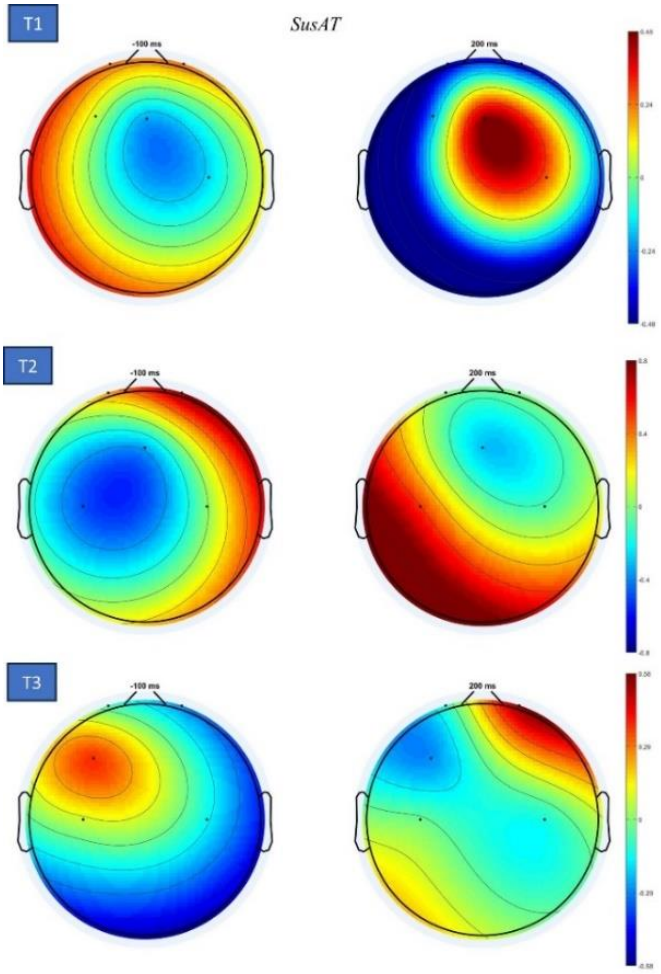

Fig. 5.29. Detailed *SusAT* state overtime for subtracted mean spectrum. The activation scale shows the average values for RMS μV potentials

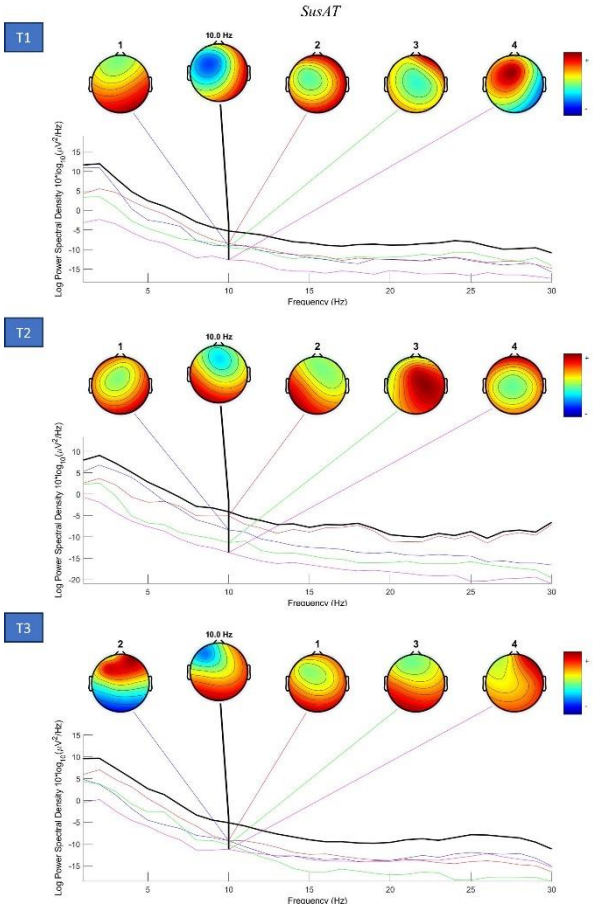

Fig. 5.30 Detailed *SusAT* IC components and main contributions over the spectrum. Each line is a channel

Going through the *topoplots*, after bad IC components removed, seen in Fig. 5.30, it is possible to notice that IC components vary a little bit among all 3 trials. The main activation is in the occipital area. Alpha activation is in the fronto-parietal areas. Fronto-parietal areas also show theta activation, mainly seen in occipital area.

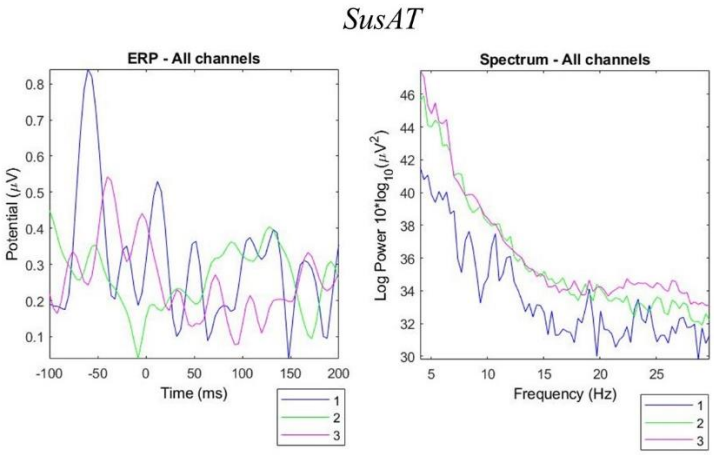

Fig. 5.31 *SusAT* - ERP and Spectrum average of all channels for trials 1, 2 and 3

Looking at averaged channels ERP, no peak around 100 or 200 *ms* is pronounced, although more like *SelAT* state than *REST* state, Fig. 5.31.

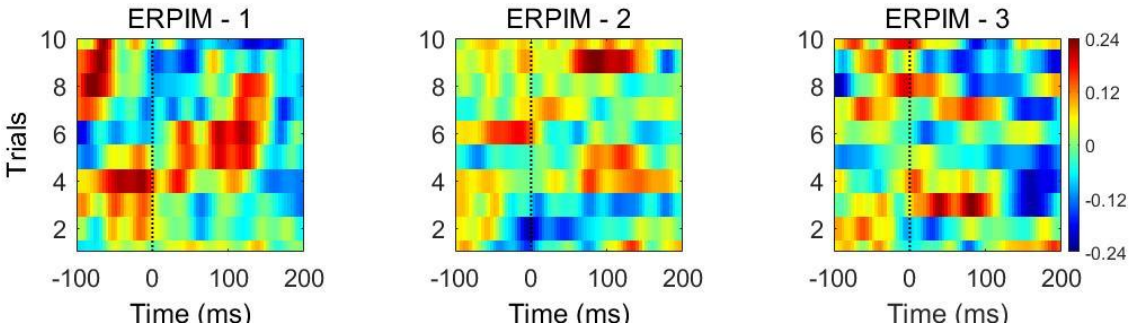

Fig. 5.32 *SusAT* - ERP image with each feature stacked on top of each other

ERP image shows more features, variations, in *SusAT*, than the other states, Fig. 5.32.

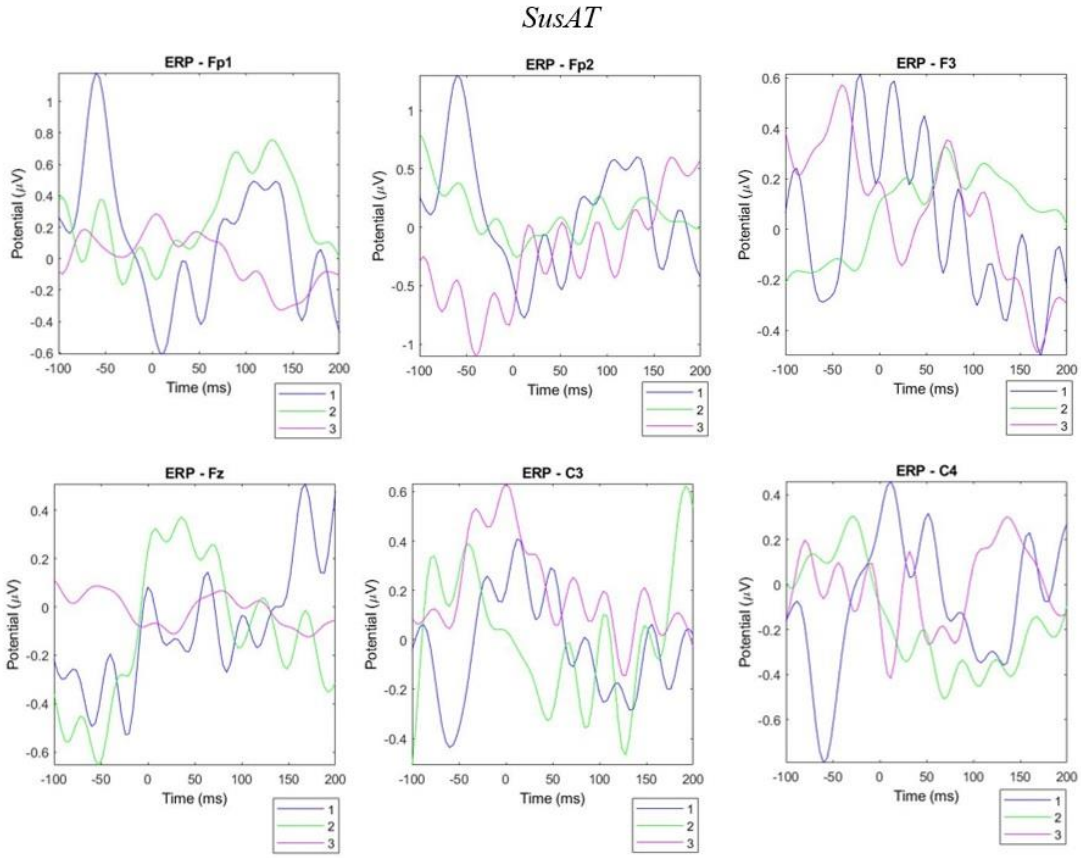

Fig. 5.33 ERP of individual channels, *SusAT* state and numbered trials

Looking at averaged channels ERP, a peak around 200 *ms* is pronounced, both in *SelAT* and *SusAT* states, Fig. 5.33.

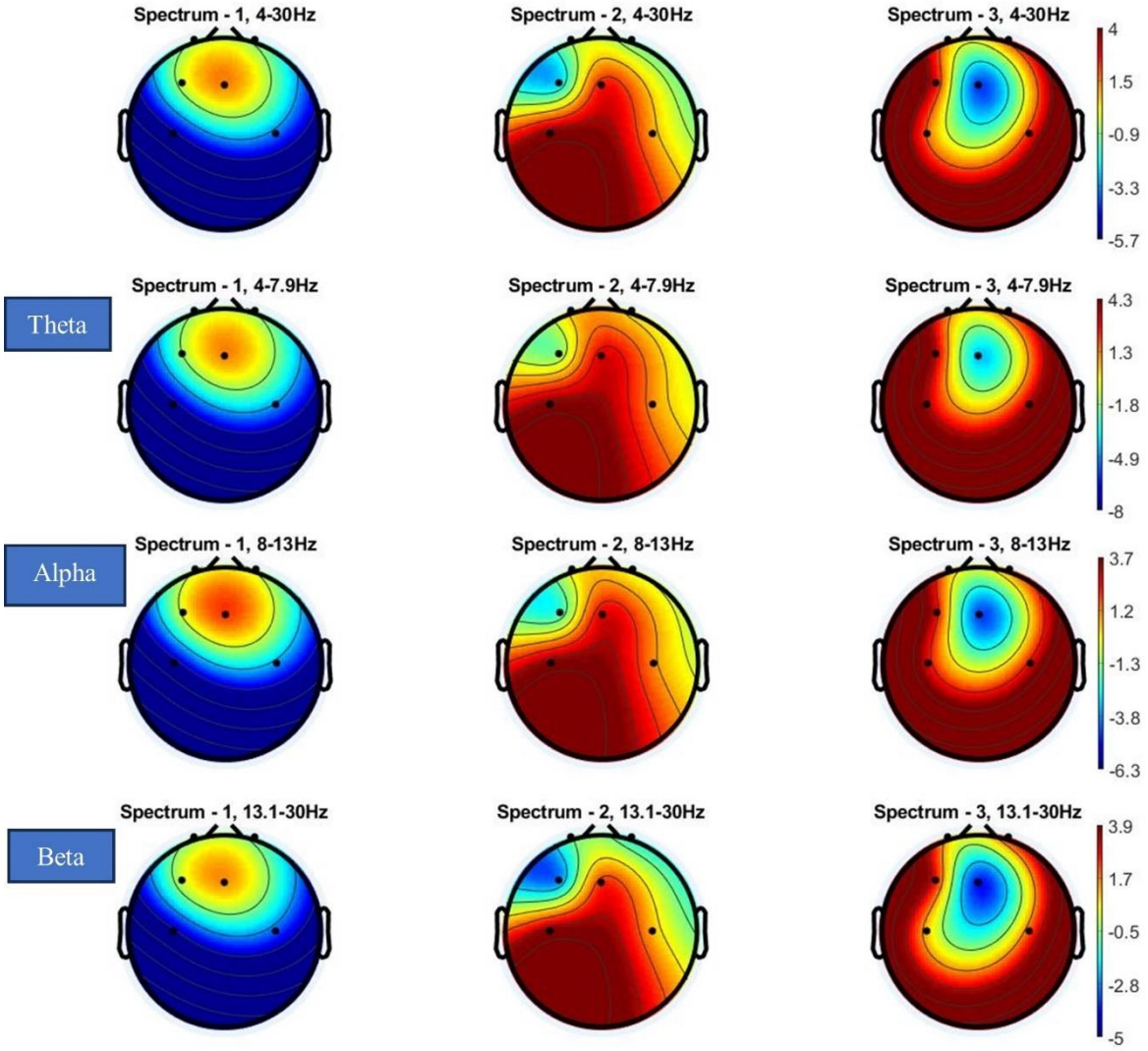

Fig. 5.34 *SusAT* - Spectrum average of all channels for trials 1, 2 and 3. Topoplots of each EEG band showing location of channels and related activation. No relevant difference can be seen over the spectrum, among trials for each EEG band. ERPs of each trial are similar among themselves

From Fig. 5.34, bilateral occipital alpha – mainly trial 1 –, frontal midline theta – mainly trial 3 – and occipital central theta – mainly trial 2, can be notice in each distinct trial. No similar occurrence happens in the trials. The brain activation areas are very similar between states *REST* and *SelAT*, also the amplitude of activation.

Chapter 6

DISCUSSION, CONCLUSION, AND FUTURE WORK

Performing cognitive tasks proposing new methodologies of attention evaluation, with selecting or sustained attention requires more brain resources, leading to higher attention allocation. On this premise, many studies have been dedicated to the assessment of mental workload, especially in the field of Neuroscience. To that end, a variety of tasks have been proposed to assess user attention, in the context of VR systems, as seen in (SOUZA; NAVES, 2021).

Brain activity recording modalities provide evidence of the complex neurophysiological mechanisms governing attention allocation/engagement and subsequently, mental exhaustion/fatigue. Electroencephalography (EEG) is the most common method employed, allowing the monitoring of the brain's electrical activity with high-temporal resolution in a non-invasive manner. In this regard, researchers have examined the brain properties in different mental-load conditions/tasks, utilizing EEG-based features both in the time and in the frequency domain, such as ERPs and power spectral density (PSD).

Furthermore, the recent development of mobile dry electrode EEG devices allows monitoring of real-time activities leading to evaluations outside laboratory conditions. The usually smaller number of dry EEG sensors, in a few scalp areas, used in this kind of solution, sets out to infer an overview of the underlying mechanisms involved in mental workload management by the brain, such as we see in this study.

Some assumptions can be made about this study, in accordance with the derivative published paper (SOUZA; NAVES, 2021):

- Attention can be investigated by means of ERP components to identify attention allocation through N100, N200, P100, and P300 in fronto-central-occipital brain areas. In this case with the help of FRP events.
- Attention can be investigated by means of brain waves increase, decrease and beta (12–31.25 Hz)/theta (3–8 Hz) ratio in fronto-parietal brain areas, θ band in occipital area, θ in frontal area, and other ratios.

- θ/ α, or T/A, ratio is a good indicative of immersion, it increases in attention states, such as in (LIM; YEO; YOON, 2019) work. Change occurs significantly in states SelAT and SusAT compared to the REST state.
- Regarding the frequency bands related to mental effort/attention allocation, in an EEG study, frontal areas were activated in δ, θ, α, and β bands, while parietal-occipital areas were activated in θ, α, and β bands (DIMITRAKOPOULOS *et al.*, 2023). Delta band was not evaluated in this study.
- In an EEG experiment, evaluating brain networks, it was found to affect functional connections between Fz and parietal areas in the high alpha band, while frontal theta activity was found to be highly associated with mental workload (DIMITRAKOPOULOS *et al.*, 2023). It goes in agreement with this study, for the alpha band in Fz, but also C3 channels. About frontal theta, it increases in the frontal area through the attentional states in this study too.
- Avoid overprocessing EEG signals, avoiding inputting new biases.
- Improvement of actual free-viewing approaches through EEG band analysis and ET data.
- Vary methodologies to study attention allocation in immersion and concentration states, besides different cognitive load conditions may obtain more results of attention allocation in brain signals out of different triggers.

A positive, effortlessly relaxed mental state may be best for neurofeedback interaction in BCIs as a biomarker (FRIEDRICH *et al.*, 2014). This approach is accomplished using the exergame like in this study.

Considering that the participant's motivation, locus of control as well as empathy levels can play a role in BCI performance (FRIEDRICH *et al.*, 2014), a greater focus on participant characteristics would inform both neurofeedback success rates with experimental BCIs, and design techniques for future BCI experiences as we have shown in this study.

In future work, it is important to explore BCI usage in an environment outside the university or departmental setting, with the goal of investigating a more diverse group of stroke patients. A replication of this study using a medical-grade EEG device may also allow learning more about patients' engagement/attention allocation success during VR interaction. Other suggestions can be made:

- Inter-subject FAA correlations analysis can be made to evaluate better FAA index, as shown in (KROGMEIER; COVENTRY; MOUSAS, 2022).
- A follow-up study could examine experimental components individually, to understand the influence of each component, in a more robust scenario.
- Test in 3D environments. (BERGER; DAVELAAR, 2018) examined attentional control in their BCI system and determined that participants had a higher learning rate for increasing attention in their 3D environment than in their 2D environment.
- The role of some topographic evaluations, as well as indexes, are not robust in the present study and should be investigated in future work. Our study contributes to the goal of presenting a new methodology, in a concise manner (few channels, few patients) in an enjoyable, and motivating way, applied to a VR system for rehabilitation, while investigating experimental techniques which engage participants during a VR interaction, capturing data to evaluate attention allocation.
- Connectivity evaluations, as well as merged time-frequency analysis may allow new outcomes to apply in this context.

REFERENCES

ALLEN, J. J. B.; URRY, H. L.; HITT, S. K.; COAN, J. A. The stability of resting frontal electroencephalographic asymmetry in depression. **Psychophysiology**, vol. 41, no. 2, 2004. https://doi.org/10.1111/j.1469-8986.2003.00149.x.

ANDREAS EDGAR KOTHE, C. **Artifact removal techniques with signal reconstruction**. **Google Patents**. [*S. l.*: *s. n.*], 2016.

BERGER, A. M.; DAVELAAR, E. J. Frontal Alpha Oscillations and Attentional Control: A Virtual Reality Neurofeedback Study. **Neuroscience**, vol. 378, 2018. https://doi.org/10.1016/j.neuroscience.2017.06.007.

BIOULAC, S.; PURPER-OUAKIL, D.; ROS, T.; BLASCO-FONTECILLA, H.; PRATS, M.; MAYAUD, L.; BRANDEIS, D. Personalized at-home neurofeedback compared with long acting methylphenidate in an european non-inferiority randomized trial in children with ADHD. **BMC Psychiatry**, vol. 19, no. 1, 2019. https://doi.org/10.1186/s12888-019-2218-0.

COENEN, F.; SCHEEPERS, F. E.; PALMEN, S. J. M.; DE JONGE, M. V.; ORANJE, B. Serious Games as Potential Therapies: A Validation Study of a Neurofeedback Game. **Clinical EEG and Neuroscience**, vol. 51, no. 2, 2020. https://doi.org/10.1177/1550059419869471.

COHEN, M. X. Analyzing Neural Time Series Data: Theory and Practice. **MIT Press**, 2014. https://doi.org/10.7551/mitpress/9609.001.0001

CORNELISSEN, T.; SASSENHAGEN, J.; VÕ, M. L. H. Improving free-viewing fixation-related EEG potentials with continuous-time regression. **Journal of Neuroscience Methods**, 2019. https://doi.org/10.1016/j.jneumeth.2018.12.010.

COWLEY, B.; RAVAJA, N. Learning in balance: Using oscillatory EEG biomarkers of attention, motivation and vigilance to interpret game-based learning. **Cogent Education**, vol. 1, no. 1, 2014. https://doi.org/10.1080/2331186X.2014.962236.

DEGNO, F.; LIVERSEDGE, S. P. Eye movements and fixation-related potentials in reading: A review. **Vision (Switzerland)**, vol. 4, no. 1, 2020. https://doi.org/10.3390/vision4010011.

DELORME, A.; MAKEIG, S. EEGLAB: An open source toolbox for analysis of single-trial EEG dynamics including independent component analysis. **Journal of Neuroscience Methods**, 2004. https://doi.org/10.1016/j.jneumeth.2003.10.009.

DELVIGNE, V.; WANNOUS, H.; VANDEBORRE, J. P.; RIS, L.; DUTOIT, T. Attention Estimation in Virtual Reality with EEG based Image Regression. 2020. **Proceedings - 2020 IEEE International Conference on Artificial Intelligence and Virtual Reality, AIVR 2020** [...]. [*S. l.*: *s. n.*], 2020. https://doi.org/10.1109/AIVR50618.2020.00012.

DEMECO, A.; ZOLA, L.; FRIZZIERO, A.; MARTINI, C.; PALUMBO, A.; FORESTI, R.; BUCCINO, G.; COSTANTINO, C. Immersive Virtual Reality in Post-Stroke Rehabilitation: A Systematic Review. **Sensors**, vol. 23, no. 3, 2023. https://doi.org/10.3390/s23031712.

DIMITRAKOPOULOS, G. N.; KAKKOS, I.; ANASTASIOU, A.; BEZERIANOS, A.; SUN, Y.; MATSOPOULOS, G. K. Cognitive Reorganization Due to Mental Workload: A Functional Connectivity Analysis Based on Working Memory Paradigms. **Applied Sciences (Switzerland)**, vol. 13, no. 4, 2023. https://doi.org/10.3390/app13042129.

DOUSSOULIN, A.; RIVAS, C.; BACCO, J.; SEPÚLVEDA, P.; CARVALLO, G.; GAJARDO, C.; SOTO, A.; RIVAS, R. Prevalence of Spasticity and Postural Patterns in the Upper Extremity Post Stroke. **Journal of Stroke and Cerebrovascular Diseases**, vol. 29, no. 11, 2020. https://doi.org/10.1016/j.jstrokecerebrovasdis.2020.105253.

FRIEDRICH, E. V. C.; WOOD, G.; SCHERER, R.; NEUPER, C. Mind over brain, brain over mind: Cognitive causes and consequences of controlling brain activity. **Frontiers in Human Neuroscience**, vol. 8, no. MAY, 2014. https://doi.org/10.3389/fnhum.2014.00348.

GAZZALEY, A.; ROSEN, L. D. The distracted mind : ancient brains in a high-tech world. **Professional Safety**, 2016.

GRASSINI, S.; REVONSUO, A.; CASTELLOTTI, S.; PETRIZZO, I.; BENEDETTI, V.; KOIVISTO, M. Processing of natural scenery is associated with lower attentional and cognitive load compared with urban ones. **Journal of Environmental Psychology**, 2019. https://doi.org/10.1016/j.jenvp.2019.01.007.

GA, Y.; CHOI, T.; YOON, G. Analysis of Game Immersion using EEG signal for Computer Smart Interface. **Journal of Sensor Science and Technology**, vol. 24, no. 6, 2015. https://doi.org/10.5369/jsst.2015.24.6.392.

HAIDER, H.; FRENSCH, P. A. Eye Movement during Skill Acquisition: More Evidence for the Information-Reduction Hypothesis. **Journal of Experimental Psychology: Learning Memory and Cognition**, vol. 25, no. 1, 1999. https://doi.org/10.1037/0278-7393.25.1.172.

HARMON-JONES, E.; GABLE, P. A. On the role of asymmetric frontal cortical activity in approach and withdrawal motivation: An updated review of the evidence. **Psychophysiology**, vol. 55, no. 1, 2018. https://doi.org/10.1111/psyp.12879.

HARTEIS, C.; KOK, E.; JARODZKA, H. Editorial The journey to proficiency: Exploring new objective methodologies to capture the process of learning and professional development. frontline Learning Research, 2018. https://doi.org/10.14786/flr.v6i3.435.

HILL, K. E.; NEO, W. S.; HERNANDEZ, A.; HAMRICK, L. R.; KELLEHER, B. L.; FOTI, D. Intergenerational Transmission of Frontal Alpha Asymmetry Among Mother–Infant Dyads. **Biological Psychiatry: Cognitive Neuroscience and Neuroimaging**, vol. 5, no. 4, 2020. https://doi.org/10.1016/j.bpsc.2019.12.003.

JAGANNATH, M.; BALASUBRAMANIAN, V. Assessment of early onset of driver fatigue using multimodal fatigue measures in a static simulator. **Applied Ergonomics**, vol. 45, no. 4, 2014. https://doi.org/10.1016/j.apergo.2014.02.001.

KAKUBO, S. M.; MENDEZ, M.; SILVEIRA, J. D.; MARINGOLO, L.; NITTA, C.; DA SILVEIRA, D. X.; FIDALGO, T. M. Translation and validation of the brown attention-deficit disorder scale for use in Brazil: Identifying cases of attention-deficit/hyperactivity disorder among samples of substance users and non-users. cross-cultural validation study. **Sao Paulo Medical Journal**, 2018. https://doi.org/10.1590/1516-3180.2017.0227121217.

KESSLER, R. C.; ADLER, L. A.; GRUBER, M. J.; SARAWATE, C. A.; SPENCER, T.; VAN BRUNT, D. L. Validity of the World Health Organization Adult ADHD Self-Report Scale (ASRS) Screener in a representative sample og health plan members. **International Journal of Methods in Psychiatric Research**, vol. 16, no. 2, 2007. https://doi.org/10.1002/mpr.208.

KHOKALE, R.; S. MATHEW, G.; AHMED, S.; MAHEEN, S.; FAWAD, M.; BANDARU, P.; ZERIN, A.; NAZIR, Z.; KHAWAJA, I.; SHARIF, I.; ABDIN, Z. U.; AKBAR, A. Virtual and Augmented Reality in Post-stroke Rehabilitation: A Narrative Review. **Cureus**, 2023. https://doi.org/10.7759/cureus.37559.

KLUG, M.; GRAMANN, K. Identifying key factors for improving ICA-based decomposition of EEG data in mobile and stationary experiments. **European Journal of Neuroscience**, vol. 54, no. 12, 2021. https://doi.org/10.1111/ejn.14992.

KROGMEIER, C.; COVENTRY, B. S.; MOUSAS, C. Frontal alpha asymmetry interaction with an experimental story EEG brain-computer interface. **Frontiers in Human Neuroscience**, vol. 16, 2022. https://doi.org/10.3389/fnhum.2022.883467.

LEE, F. J.; ANDERSON, J. R. Does Learning a Complex Task Have to Be Complex?: A Study in Learning Decomposition. **Cognitive Psychology**, vol. 42, no. 3, 2001. https://doi.org/10.1006/cogp.2000.0747.

LEE, K. Evaluation of Attention and Relaxation Levels of Archers in Shooting Process using Brain Wave Signal Analysis Algorithms. **감성과학**, vol. 12, no. 3, 2009. .

LI, G.; HUANG, S.; XU, W.; JIAO, W.; JIANG, Y.; GAO, Z.; ZHANG, J. The impact of mental fatigue on brain activity: A comparative study both in resting state and task state using EEG. **BMC Neuroscience**, vol. 21, no. 1, 2020. https://doi.org/10.1186/s12868-020-00569-1.

LI, G.; ZHOU, S.; KONG, Z.; GUO, M. Closed-loop attention restoration theory for virtual reality-based attentional engagement enhancement. **Sensors (Switzerland)**, 2020. https://doi.org/10.3390/s20082208.

LI, Z.; GUO, P.; SONG, C. A Review of Main Eye Movement Tracking Methods. 1802., 2021. **IOP Conference Series: Earth and Environmental Science** [...]. [*S. l.*: *s. n.*], 2021. vol. 1802, . https://doi.org/10.1088/1742-6596/1802/4/042066.

LIM, S.; YEO, M.; YOON, G. Comparison between concentration and immersion based on EEG analysis. **Sensors (Switzerland)**, vol. 19, no. 7, 2019. https://doi.org/10.3390/s19071669.

LIN, C. W.; KUO, L. C.; LIN, Y. C.; SU, F. C.; LIN, Y. A.; HSU, H. Y. Development and Testing of a Virtual Reality Mirror Therapy System for the Sensorimotor Performance of Upper Extremity: A Pilot Randomized Controlled Trial. **IEEE Access**, vol. 9, 2021. https://doi.org/10.1109/ACCESS.2021.3050656.

LINDSAY, G. W. Attention in Psychology, Neuroscience, and Machine Learning. **Frontiers in Computational Neuroscience**, vol. 14, 2020. https://doi.org/10.3389/fncom.2020.00029.

MAGOSSO, E.; DE CRESCENZIO, F.; RICCI, G.; PIASTRA, S.; URSINO, M. EEG alpha power is modulated by attentional changes during cognitive tasks and virtual reality immersion. **Computational Intelligence and Neuroscience**, vol. 2019, 2019. https://doi.org/10.1155/2019/7051079.

MATHEWSON, K. E.; BASAK, C.; MACLIN, E. L.; LOW, K. A.; BOOT, W. R.; KRAMER, A. F.; FABIANI, M.; GRATTON, G. Different slopes for different folks: Alpha and delta EEG power predict subsequent video game learning rate and improvements in cognitive control tasks. **Psychophysiology**, 2012. https://doi.org/10.1111/j.1469-8986.2012.01474.x.

MATTHEWS, G.; REINERMAN-JONES, L. E.; BARBER, D. J.; ABICH, J. The psychometrics of mental workload: Multiple measures are sensitive but divergent. **Human Factors**, vol. 57, no. 1, 2015.

https://doi.org/10.1177/0018720814539505.

Computational Intelligence and Neuroscience, vol. 2019, 2019. https://doi.org/10.1155/2019/7051079.

NEUPER, C.; PFURTSCHELLER, G. Event-related dynamics of cortical rhythms: Frequency-specific features and functional correlates. 43., 2001. **International Journal of Psychophysiology** [...]. [*S. l.*: *s. n.*], 2001. vol. 43, . https://doi.org/10.1016/S0167-8760(01)00178-7.

ÖGÜN, M. N.; KURUL, R.; YAŞAR, M. F.; TURKOGLU, S. A.; AVCI, Ş.; YILDIZ, N. Effect of leap motion-based 3D immersive virtual reality usage on upper extremity function in ischemic stroke patients. **Arquivos de Neuro-Psiquiatria**, vol. 77, no. 10, 2019. https://doi.org/10.1590/0004-282X20190129.

PFURTSCHELLER, G.; LOPES DA SILVA, F. H. Event-related EEG/MEG synchronization and desynchronization: Basic principles. **Clinical Neurophysiology**, vol. 110, no. 11, 1999. https://doi.org/10.1016/S1388-2457(99)00141-8.

PICKEN, C.; CLARKE, A. R.; BARRY, R. J.; MCCARTHY, R.; SELIKOWITZ, M. The Theta/Beta Ratio as an Index of Cognitive Processing in Adults With the Combined Type of Attention Deficit Hyperactivity Disorder. **Clinical EEG and Neuroscience**, vol. 51, no. 3, 2020. https://doi.org/10.1177/1550059419895142.

RAY, W. J.; COLE, H. W. EEG alpha activity reflects attentional demands, and beta activity reflects emotional and cognitive processes. **Science**, vol. 228, no. 4700, 1985. https://doi.org/10.1126/science.3992243.

SALVUCCI, D. D.; GOLDBERG, J. H. Identifying fixations and saccades in eye-tracking protocols. 2000. **Proceedings of the Eye Tracking Research and Applications Symposium 2000** [...]. [*S. l.*: *s. n.*], 2000. https://doi.org/10.1145/355017.355028.

SCHARINGER, C.; SCHÜLER, A.; GERJETS, P. Using eye-tracking and EEG to study the mental processing demands during learning of text-picture combinations. **International Journal of Psychophysiology**, vol. 158, 2020. https://doi.org/10.1016/j.ijpsycho.2020.09.014.

SOUZA, R. H. C. e.; NAVES, E. L. M. Attention Detection in Virtual Environments Using EEG Signals: A Scoping Review. **Frontiers in Physiology**, vol. 12, 2021. https://doi.org/10.3389/fphys.2021.727840.

StatSoft, Inc. (2011) STATISTICA (Data Analysis Software System), Version 10. http://www.statsoft.com

STRATTON, G. M. Symmetry, linear illusion, and the movements of the eye. **Psychological Review**, vol. 13, no. 2, 1906. https://doi.org/10.1037/h0072441.

SUBRAMANIAN, S. K. Influence of cognitive deficits on the ability to use feedback for arm motor recovery in chronic stroke. **Stroke**, vol. 44 (12), 2013. https://doi.org/10.1109/ICVR.2013.6662124

TANNUS DE SOUZA, J.; VALENTINI, C.; NAVES, E. L. M.; LAMOUNIER, E. A. A Virtual Reality Exergame with a Low-cost 3D Motion Tracking for At-Home Post-Stroke Rehabilitation. 2021. **ACM International Conference Proceeding Series** [...]. [*S. l.*: *s. n.*], 2021. https://doi.org/10.1145/3488162.3488223.

TREJO, L. J.; KUBITZ, K.; ROSIPAL, R.; KOCHAVI, R. L.; MONTGOMERY, L. D. EEG-Based

Estimation and Classification of Mental Fatigue. **Psychology**, vol. 06, no. 05, p. 572–589, 2015. DOI 10.4236/psych.2015.65055. Available at: http://www.scirp.org/journal/doi.aspx?DOI=10.4236/psych.2015.65055.

VARELA CASAL, P.; LORENA ESPOSITO, F.; MORATA MARTÍNEZ, I.; CAPDEVILA, A.; SOLÉ PUIG, M.; DE LA OSA, N.; EZPELETA, L.; PERERA I LLUNA, A.; FARAONE, S. V.; RAMOS-QUIROGA, J. A.; SUPÈR, H.; CAÑETE, J. Clinical Validation of Eye Vergence as an Objective Marker for Diagnosis of ADHD in Children. **Journal of Attention Disorders**, vol. 23, no. 6, 2019. https://doi.org/10.1177/1087054717749931.

VALLAT, R. Pingouin: statistics in Python. **Journal of Open Source Software**, vol. 3, no. 31, 2018. https://doi.org/10.21105/joss.01026.

VORTMANN, L. M.; KROLL, F.; PUTZE, F. EEG-Based Classification of Internally- and Externally-Directed Attention in an Augmented Reality Paradigm. **Frontiers in Human Neuroscience**, 2019. https://doi.org/10.3389/fnhum.2019.00348.

VOSSKÜHLER, A.; NORDMEIER, V.; KUCHINKE, L.; JACOBS, A. M. OGAMA (Open Gaze and Mouse Analyzer): Open-source software designed to analyze eye and mouse movements in slideshow study designs. **Behavior Research Methods**, vol. 40, no. 4, 2008. https://doi.org/10.3758/BRM.40.4.1150.

WALTEMATE, T.; GALL, D.; ROTH, D.; BOTSCH, M.; LATOSCHIK, M. E. The impact of avatar personalization and immersion on virtual body ownership, presence, and emotional response. **IEEE Transactions on Visualization and Computer Graphics**, vol. 24, no. 4, 2018. https://doi.org/10.1109/TVCG.2018.2794629.

WOBROCK, D.; FINKE, A.; SCHACK, T.; RITTER, H. Using Fixation-Related Potentials for Inspecting Natural Interactions. **Frontiers in Human Neuroscience**, vol. 14, 2020. https://doi.org/10.3389/fnhum.2020.579505.

YIN, Z.; ZHANG, J. Identification of temporal variations in mental workload using locally-linear-embedding-based EEG feature reduction and support-vector-machine-based clustering and classification techniques. **Computer Methods and Programs in Biomedicine**, vol. 115, no. 3, 2014. https://doi.org/10.1016/j.cmpb.2014.04.011.

YU, K.; PRASAD, I.; MIR, H.; THAKOR, N.; AL-NASHASH, H. Cognitive workload modulation through degraded visual stimuli: A single-trial EEG study. **Journal of Neural Engineering**, vol. 12, no. 4, 2015. https://doi.org/10.1088/1741-2560/12/4/046020.